

GENETIC STRUCTURE AND GENE EXPRESSION PROFILE OF  
*PLASMODIUM VIVAX* IN EAST AFRICA

by

Daniel Kepple

A dissertation submitted to the faculty of  
The University of North Carolina at Charlotte  
in partial fulfillment of the requirements  
for the degree of Doctor of Philosophy in  
Biological Sciences

Charlotte

2022

Approved by:

---

Dr. Eugenia Lo

---

Dr. Ian Marriott

---

Dr. Todd Steck

---

Dr. Kausik Chakrabarti

---

Dr. Daniel Janies



## ABSTRACT

DANIEL KEPPLER. Genetic Structure and Gene Expression Profile of *Plasmodium vivax* in East Africa. (Under the direction of DR. EUGENIA LO)

*Plasmodium vivax* malaria is a neglected tropical disease, despite being more geographically widespread than any other form of malaria. *P. vivax* was previously thought to be rare or absent in Africa because people of African descent often lack the Duffy blood group antigen, known as the Duffy antigen-chemokine receptor (DARC). DARC is a glycoprotein on the surface of red blood cells (RBCs) that allows *P. vivax* to bind and invade human erythrocytes. The documentation of *P. vivax* infections in different parts of Africa where Duffy-negative individuals are predominant suggested that there are alternative pathways for *P. vivax* to invade human erythrocytes that remain elusive. Duffy-negative individuals may be just as fit as Duffy-positive individuals and are no longer resistant to *P. vivax* malaria.

The genetic characteristics and erythrocyte invasion mechanisms of *P. vivax* in Duffy-negative infections are largely unknown due to the less frequent occurrence in Africa and the complicated biology of *P. vivax*. There is evidence of alternative Duffy-independent pathways through utilization of reticulocyte binding proteins (RBPs), merozoite surface proteins (MSPs), and tryptophan rich antigens (TRAg). However, these pathways remain poorly characterized. This dissertation research aims to examine the genetic, transcriptomic, and transmission features of East African *P. vivax* and identify candidate ligands for erythrocyte invasion through comparative transcriptomics of major surface protein genes. Our group has shown no clear genetic differentiation in *P. vivax* between the two Duffy groups, indicating between-host transmission. Furthermore, we found *P. vivax* from Ethiopia and Sudan showed similar genetic

clusters, except samples from Khartoum, possibly due to distance and road density that inhibited parasite gene flow.

Lastly, our group was able to characterize the expression levels of 4,404 gene transcripts belonging to 12 functional groups. We closely examined 43 erythrocyte binding gene candidates in the Ethiopia isolates and compared with four Cambodian and two Brazilian *P. vivax* published transcriptomes. Overall, there were 10-26% differences in the gene expression profile amongst the continental isolates, with the Ethiopian and Cambodian *P. vivax* being most similar. Majority of the gene transcripts involved in protein transportation, host interaction, and resistance were upregulated in the Ethiopian isolates. Transcripts involved in host-interactions were differentially expressed across the three continental isolates. For instance, *PvDBP1* and *PvEBP/DBP2* were highly expressed in the Cambodian but not the Brazilian and Ethiopian isolates. *PvRBP2a* and *PvRBP2b* showed higher expression in the Ethiopian and Cambodian isolates than the Brazilian ones. In the Ethiopian schizonts, *PvRBP2a* and *PvRBP3* expressed six-fold higher than *PvDBP1* and 60-fold higher than *PvEBP/DBP2* highlighting their importance. Other invasion genes including *PvRBP1a*, *PvMSP3.8*, *PvMSP3.9*, *PvTRAG2*, *PvTRAG14*, and *PvTRAG22* also showed relatively high expression. We also found that PVP01\_1403000 from female and PVP01\_1208000 from male gametocytes were highly expressed consistently across all isolates compared to *Pvs25*, the current industry standard for gametocyte detection. Together, these data indicate the Duffy negative *P. vivax* originated from Duffy positive individuals and transmission may occur between both phenotypes. We also provide evidence of a Duffy-independent invasion mechanism by select *PvRBP*, *PvRBP*, and *PvTRAG* genes. Lastly, our data provide a reliable method for detecting sub-microscopic *P. vivax* gametocytes through male and female gametocyte detection. The data presented is critical

for understanding *P. vivax* infection, transmission, and provide the first evidence for alternative invasion ligands that may be ideal targets for pharmaceutical intervention.

## Acknowledgements

I would like to offer a special thank you to my advisor, Dr. Eugenia Lo, for her years of guidance encouragement, and patience through my graduate studies. I'd also like to thank Dr. Kausik Chakrabarti and Dr. Daniel Janies for their continued support with development and troubleshooting of various procedures. I am grateful to Dr. Todd Steck and Dr. Ian Marriott for their guidance and encouragement through both my undergraduate and graduate studies.

I am thankful for Dr. Sharon Bullock and Dr. Tuan Cao for their letters of recommendation and friendly encouragement. I am grateful to the graduate school at UNC-Charlotte and the NIH for their financial support and allowing me this wonderful opportunity. I am grateful for the many undergraduates and friends I have made along the way; I couldn't have made it through without the emotional support of Cheikh Dieng, Kareen Pestana, Colton Cantley, Greyson Cantley, Haylee Wheeler, Gabrielle Kolesar, and the many undergraduates who assisted in the many experiments.

Lastly, I'd like to offer a huge thank you to my family for their unwavering emotional and financial support during tough times. Without their dedication to aid my pursuits I wouldn't be the scholar I am today. I'd also like to thank my wife, Abigail Kepple, for her hard work to provide and offer loving support the whole way through. Thank you.

## Table of Contents

List of Tables .....	ix
List of Figures .....	x
Chapter 1: Introduction.....	1
1.1 Introduction.....	1
1.2. Pathogenesis of <i>P. vivax</i> .....	3
1.3 Erythrocyte Invasion Mechanisms in Non- <i>Plasmodium vivax</i> .....	5
1.4 <i>Plasmodium vivax</i> Ligand Proteins and Host Receptors for Erythrocyte Invasion .....	9
1.5 Humoral Immune Response against <i>P. vivax</i> and Vaccine Targets .....	14
1.6 Conclusions .....	18
1.7 Tables.....	20
Chapter 2: Materials and Methods.....	21
2.1. Ethic's Statement .....	21
2.2 Study area and genotyping .....	21
2.3 Linkage disequilibrium and multiplicity of infections .....	22
2.4 Genetic diversity and population structure .....	22
2.5 Identification of source-sink dynamics and direction of transmission .....	23
2.6 Analyses of geographic and landscape factors .....	23
2.7 Sample preparation of the 10 Ethiopian <i>P. vivax</i> transcriptomes.....	24
2.8 Data analyses of the 10 Ethiopian <i>P. vivax</i> transcriptomes.....	26
2.9 Continental comparison of <i>P. vivax</i> transcriptomes .....	27
3.1 Rationale .....	28
3.2 Results.....	29
3.2.1 Linkage disequilibrium and multiplicity of infections.....	29
3.2.2 Genetic diversity and population structure .....	30
3.2.3 Source-sink dynamics and direction of transmission.....	31
3.2.4 Influence of geographic and landscape factors .....	32
3.3 Discussion.....	33
3.4 Tables.....	37
3.5 Figures .....	41
Chapter 4: East African <i>Plasmodium vivax</i> transcriptomes reveal differences in gene expression profiles related to erythrocyte invasion and gametocyte detection from other geographical isolates .....	48
4.1 Rationale .....	48
4.2 Results.....	50
4.2.1 Overview of the Ethiopian <i>P. vivax</i> transcriptomes .....	50
4.2.2 Top 30 transcripts of Ethiopian <i>P. vivax</i> .....	51
4.2.3 Differentially expressed genes among continental <i>P. vivax</i> .....	52

4.2.4 Expression of genes related to erythrocyte invasion.....	53
4.3 Discussion.....	55
4.4 Figures .....	59
Chapter 5: From Genes to Biomarkers: Understanding The Biology of Malaria Gametocytes and their Detection .....	67
5.1 Rationale .....	67
5.2 Results.....	68
5.2.1 Sub-microscopic gametocyte densities .....	68
5.2.2 Expression of female and male <i>P. vivax</i> gametocyte genes .....	69
5.3 Discussion.....	70
5.4 Figures .....	72
Chapter 6: Summary Conclusions .....	74
6.1 <i>Plasmodium vivax</i> from Duffy-Negative and Duffy-Positive Individuals Shares Similar Gene Pool Indicative of Between-Host Transmission.....	74
6.2 East African <i>Plasmodium vivax</i> transcriptomes are different in gene expression profiles related to erythrocyte invasion.....	75
6.3 Alternative biomarkers for male and female <i>P. vivax</i> detection show higher expression compared to <i>Pvs25</i> and <i>Pvs16</i> .....	76
References.....	77
Appendix: Publications.....	94



## List of Tables

Table 1. Currently known <i>P. vivax</i> genes and amino acid regions responsible for binding human erythrocytes	20
Table 2. Host Duffy status, linkage disequilibrium, and complexity of infection among <i>P. vivax</i> samples by study site	37
Table 3. Comparison of genetic diversity based on microsatellite markers in Duffy-negative and Duffy-positive <i>P. vivax</i> infections	38
Table 4. Average genetic relatedness among individuals by site and host Duffy status using the identical-by-descent (IBD) method	39
Table 5. Fit criteria used to rank the resistance surfaces, and the slope and significance of the relationship between resistance and genetic distance for each surface.	40

## List of Figures

Figure 1. Study sites with <i>P. vivax</i> incidence heatmap for reference	41
Figure 2. Bayesian inferences of the <i>K</i> cluster estimated by STRUCTURE for the <i>P. vivax</i> samples, according to host Duffy status and location	42
Figure 3. Results of DAPC analyses showing the first two principal components of the data grouped by site and host Duffy status	43
Figure 4. Bayesian inferences of the <i>K</i> cluster estimated by STRUCTURE for the <i>P. vivax</i> samples, according to host Duffy status and country	44
Figure 5. (A) Genetic relatedness among <i>P. vivax</i> populations with a large sample size; (B) Two-dimensional MDS of genetic distance between the same populations (i.e., <i>P. vivax</i> from Duffy-negatives at sites GJ, NH, and KH was excluded).	45
Figure 6. Source Hub Ratio (SHR) networks generated from (A) samples grouped by country and host Duffy status and (B) samples grouped by site.	46
Figure 7. Resistance surfaces fit to genetic distances based on (A) land cover alone and (B) a combination of road density and elevation	47

Figure 8. Categorization of (A) all detectable transcripts and (B) Highly transcribed (TPM > 20) transcripts for the Ethiopian <i>P. vivax</i> by gene function	59
Figure 9. CIBERSORTx deconvolution of (A) the 10 Ethiopian <i>P. vivax</i> transcriptomes; (B) the four Cambodian <i>P. vivax</i> transcriptomes; (C) the two Brazilian transcriptomes using a <i>P. berghei</i> homologue matrix	60
Figure 10. Microscopy analysis of five Ethiopian <i>P. vivax</i> samples	61
Figure 11. Heat map showing the top 30 highly transcribed genes based on $\log(2)\text{CPM}+1$	62
Figure 12. (A) Comparisons of the entire transcriptomes with genes sorted by functionality among the Ethiopian, Cambodian, and Brazilian <i>P. vivax</i> ; (B) Ethiopian and Cambodian; (C) Ethiopian and Brazilian; (D) Cambodian and Brazilian isolates	64
Figure 13. Heatmap showing 43 genes associated with erythrocyte binding function in the Ethiopian <i>P. vivax</i> based on $\log(2)\text{TPM}+1$ values	65
Figure 14. Comparisons of 43 genes associated with erythrocyte binding function based on $\log(2)\text{TPM}+1$ values across the Ethiopian,	66

Cambodian, and Brazilian *P. vivax* for (A) *PvDBP1*, *PvEBP*, and *PvRBP* genes; (B) *PvMSP* genes; (C) *PvTRAg* genes; (D) other putatively functional ligands

Figure 15. (A) Comparison of asexual parasitemia and gametocytemia among *P. vivax* infections from Ethiopia. (B) Significant correlation was observed between asexual parasitemia and gametocytemia

Figure 16. Heatmap comparing 26 *P. vivax* gametocyte biomarker candidates across the Ethiopian, Cambodian, and Brazilian *P. vivax*

## Chapter 1: Introduction

### 1.1 Introduction

*Plasmodium vivax* malaria is a neglected tropical disease, despite being more geographically widespread than any other form of malaria (1) and causes 132–391 million clinical infections each year (2). Compared to *P. falciparum*, *P. vivax* has a broader temperature tolerance and an earlier onset of gametocyte development, enabling the parasites to spread through diverse climates (3) and making them more difficult to control and eliminate (4). Currently, there is no vaccine available for *P. vivax*, though several preventative medications have been shown to be effective (5, 6). The epidemiology of *P. vivax* malaria is further complicated by the pathogen's unique ability to form dormant-stage hypnozoites in the host liver cells, giving rise to recurrent relapse infections from weeks/months to years later (7, 8). Relapse infections have substantially impacted progress in malaria control, especially in countries that are approaching elimination (9-11).

*Plasmodium vivax* was previously thought to be rare or absent in Africa because people of African descent often lack the expression of a Duffy blood group antigen, known as the Duffy antigen–chemokine receptor (DARC). It is believed that the fixation of the Duffy negativity trait, and the rarity of *P. vivax* infection in Africa supports that Duffy-negative individuals are refractory to *P. vivax*. Unlike *P. falciparum*, which utilizes multiple erythrocyte receptors for invasion and has merozoite proteins with overlapping and redundant receptor-binding functions, invasion of erythrocyte by *P. vivax* merozoites exclusively relies on the interaction between PvDBP and DARC expressed on the surface of erythrocytes and reticulocytes. DARC is a glycoprotein on the surface of red blood cells (RBCs) that allows *P. vivax* to bind and invade

human erythrocytes at the cysteine-rich region II of Duffy Binding Protein 1 (DBP1) (12-14). However, recent studies have reported several cases of *P. vivax* in Duffy-negative people in different parts of Africa where Duffy-negative populations are predominant (15-17). It is apparent that Duffy-negative individuals are no longer resistant to *P. vivax* malaria (15, 16). This phenomenon raises important questions of how *P. vivax* invades erythrocytes of Duffy-negative individuals. To date, only a single *P. vivax* ligand protein PvDBP1 has been studied in great detail (15). It has been hypothesized that either mutations in *PvDBP1* provided a new pathway of entry, or a low expression of DARC in Duffy-negative individuals binds readily with parasites that contain high copies of *PvDBP1* (18, 19). Recent studies have shown that, despite several mutational differences observed in *PvDBP1* between Duffy-positive and Duffy-negative infections, none of them bind to Duffy-negative erythrocytes (15), implying that an alternative parasite ligand is being used.

The investigation of erythrocyte invasion mechanisms in *P. vivax* could be complicated by the genetic characteristics and epidemiology of *P. vivax* in Duffy-negative individuals. *P. vivax* has a significantly higher nucleotide diversity at the genome level, compared to *P. falciparum* (20). Such a contrast could be attributed to frequent gene flow via human movement, intense transmission, and variation in host susceptibility (21-23). Genes associated with erythrocyte binding, such as Duffy binding protein (*PvDBP*), erythrocyte binding protein (*PvEBP*), reticulocyte binding protein (*PvRBP*), merozoite surface protein (*PvMSP*), apical membrane antigen 1 (*PvAMA1*), and tryptophan-rich antigen genes (*PvTRAg*) families, are highly diverse in *P. vivax* from Africa and Southeast Asia (24-28). These genes have been shown to play a role in reticulocyte invasion (24, 28) and patient antigenicity (29, 30) and provide explanations to high levels of selection detected at the genome levels in *P. vivax* from South Korea (31), Kyrgyz

Republic (32), New Guinea (33), and Thailand (34). Proteins such as RBP, TRAg, anchored micronemal antigen (GAMA), and Rhoptry neck protein (RON) have been suggested to play a role in red cell invasion, especially in low-density infections (35-39). Unfortunately, studies that investigated erythrocyte invasion pathways are scattered with no definitive evidence and systematic approaches to clarify the exact role of these target genes. Due to a lack of reliable and logistical long-term in vitro methods (40), *P. vivax* remains a parasite for which it is difficult to effectively study the molecular mechanisms and biology in detail, beyond genetic characterizations.

## 1.2. Pathogenesis of *P. vivax*

Recent findings of *P. vivax* cases in Duffy-negative individuals suggest that some lineages may have evolved to use ligands other than Duffy for erythrocyte invasion (15). This significantly increases the risk of *P. vivax* infection in the African populations and may eventually become a new cause of epidemics and severe disease across Africa. To establish how the phenomenon of *P. vivax* infection of Duffy-negative individuals has evolved and identify potential vaccine candidates to target it, it is important to understand how this parasite invades Duffy-negative erythrocytes and, hence, causes malaria. The investigations of *P. vivax* at the cellular and molecular levels have been restricted by the lack of a continuous in vitro culturing of live parasites. With the advancement in *P. vivax* genome sequencing technology, coupled with the ability to mature ex vivo isolates, it is now possible to obtain high-quality transcriptomes of the blood stages. However, there is still a lack of viable methods to indefinitely culture *P. vivax*, due to the need for young reticulocytes to sustain long-term culture. Strategies to overcoming this problem have been proposed but remain impractical due to a large initial and continuous

investment of labor and infrastructure (41). The successes of short-term culture utilizing young reticulocytes from placental blood (40, 42) and indefinite culture in *Saimiri boliviensis* and *Aotus nancymae* monkeys (43, 44) shed light on pathogenesis in humans and potential ligands for invasion (37, 44); however, several unanswered questions remain.

While mature asexual *P. vivax* and its transmissive gametocytes occur in peripheral blood, histological analyses of *P. vivax* in *Aotus* and *Saimiri* monkeys have shown immature gametocytes and few asexual schizonts present in the parenchyma of bone marrow (45). Asexual schizonts appear to be more concentrated in the sinusoids of the liver (45), suggesting that bone marrow could be a critical reservoir for *P. vivax* gametocyte development and proliferation. Indeed, the bone marrow reservoirs may suggest that microscopic detection is not ideal for active case detection and treatment of *P. vivax* until bone marrow samples are accessible. As *P. vivax* requires reticulocytes for growth (46-49), the general low proportion of reticulocytes (that make up only 1% of the total number of host erythrocytes) may explain low parasite loads in symptomatic patients (50-52) and a lack of observable schizonts in blood circulation (52, 53). Additionally, pathological analyses of *S. boliviensis* tissues showed that *P. vivax* infections also affect the lungs and kidneys, both of which had mononuclear infiltrates, higher macrophage levels, alveolar wall thickening, collagen deposition, and type II pneumocyte hyperplasia (44). The level of tissue damage is parasite-load dependent and determined by the amount of by-product, namely hemozoin, being produced (44). These findings may imply a large number of asymptomatic *P. vivax* carriers in the general populations. It is well-known that *P. vivax* has the ability to relapse from dormant liver-stage hypnozoites, from weeks to years after the clearance of the primary blood-stage infection, and this is a major obstacle to its control and elimination (20, 54). The liver and bone marrow have been shown to be major parasite reservoirs for *P. vivax*



hypnozoites in *Saimiri* monkey models (45, 55), but mechanisms of hypnozoite development remain largely unknown and are difficult to study due to a lack of long-term in vitro culture. Moreover, relapse varies systemically by geographic region and/or seasonal changes in the environment (54). In regions where *P. vivax* transmission is intense and stable, relapse is common and enhances local transmission (20, 54), whereas, in Africa, *P. vivax* transmission is relatively low and usually seasonal and unstable (56-58). The rate of relapse is largely unknown. There is, as of yet, no information on the frequency and clinical impacts of relapse in Duffy-negative *P. vivax* infections, nor reliable biomarkers for relapse detection, due to limited technologies and substantial knowledge gaps in the biology of *P. vivax* hypnozoites and relapse. Future investigations employing a longitudinal study design that monitors the dynamics and consequences of relapse infections in both Duffy-positive and Duffy-negative individuals will offer deep insights into the epidemiology and biology of *P. vivax* infections.

### 1.3 Erythrocyte Invasion Mechanisms in Non-*Plasmodium vivax*

Our current knowledge of the molecular mechanisms of erythrocyte invasion in several *Plasmodium* species offers a reference model on candidate invasion ligands in *P. vivax*. *Plasmodium falciparum* invades a wide range of red blood cells, from young reticulocytes to mature normocytes. One of the main binding protein ligands is the erythrocyte binding ligand (EBL) family, which includes multiple members, such as EBA-175, EBA-140, EBL-1, and EBA-181. EBA-175 binds to the sialic acid-containing structure on human erythrocyte receptor glycoporphin A (GpA) during invasion (59). The role of the EBA-175 protein has been shown to be critical for erythrocyte invasion, as antibodies raised against EBA-175 prevent binding to GpA in vitro (60, 61). EBA-175 triggers changes in the erythrocyte membrane (62, 63), and the

shedding of EBA-175 causes uninfected red blood cells to cluster or form rosette, which allows for immune evasion (64). The host immune responses may explain the polymorphisms and diversifying selection observed in EBA-175 (65). Other ligands, such as EBA-140 and EBL-1, are known to bind to glycophorin C (GpC) (66) and glycophorin B (GpB), respectively, on the erythrocytes. Unlike GpA and GpC, the GpB exhibits high levels of polymorphisms, particularly in people of African ancestry, suggesting that a strong selective pressure may have provided an evolutionary advantage to parasite invasion (67). For example, the S-s-U- and Dantu GpB phenotypes both showed moderate protection against invasion; however, this does not hold true for all GpB phenotypes (67-70). To the best of our knowledge, the specific receptor for EBA-181 is chymotrypsin-sensitive, trypsin-resistant, and neuraminidase-sensitive to erythrocytic treatment (71, 72), although it remains to be identified. Another important binding protein family of *P. falciparum* is the reticulocyte-binding homologue (PfRh) that includes PfRh1, PfRh2a, PfRh2b, PfRh4, and PfRh5. PfRh1 binds to an unidentified receptor “Y”, which has been characterized to be trypsin- and chymotrypsin-resistant and neuraminidase-sensitive (73, 74). PfRh1 is necessary for sialic acid-dependent invasion of human red blood cells (74). Antibodies raised against PfRh1 have been shown to block invasion by inhibiting calcium signaling in the merozoite (75). PfRh2a and PfRh2b are identical for much of the N-terminus region, but each has a unique 500 C-terminus region (76) and differential expressions in various *P. falciparum* lines, including deletions, such as a deletion of PfRh2b in *P. falciparum* D10 (76, 77). The loss of PfRh2b does not appear to impact invasion or growth of the parasites and suggests compensatory mechanisms for the loss of PfRh2b (78). PfRh2a binds to more than one receptor on erythrocytes, but these receptors have yet to be identified (79, 80). PfRh2b has been shown to be involved in merozoite calcium signaling (79). It binds to an unknown receptor “Z” on

erythrocytes, which is neuraminidase- and trypsin-resistant and chymotrypsin-sensitive (81). PfRh4 has been shown to have sialic acid-independent binding activity with the complement receptor type I (CR1) on erythrocytes (82, 83). The PfRh5 complex is composed of PfRh5, Ripr, CyRPA, and Pf113, which collectively promote successful merozoite invasion of erythrocytes by binding to basigin (BSG, CD147) (84, 85). A BSG variant on erythrocytes, known as Ok<sup>a</sup>, has been shown to reduce merozoite binding affinities and invasion efficiencies (86). This variant was reported so far only from people of Japanese ancestry (87). Previous knockout or double-knockout experiments have indicated that the *EBL* and *PfRh* gene families work cooperatively or can functionally compensate for the loss of each other (88, 89). For example, a loss of *EBA-175* can activate *PfRh4* (88, 89). When *EBA-181* expression was disrupted, *PfRH2b* was no longer functional (88). When *EBA-181* and *EBA-140* genes were disrupted, the parasite deleted the *PfRh2b* gene (88). Further study is needed to gain a deeper understanding of how they may work synergistically to promote invasion and immune evasion.

Until recently, *P. knowlesi* was considered primarily a simian malaria that infects *Macaca fascicularis*, *Macaca nemestrina*, and *Presbytis melalophos* (90). *P. knowlesi* is now confirmed to cause malarial infections in humans (91). *P. knowlesi* has been shown to use different ligands to invade macaques and human erythrocytes (90). Two gene families, *DBL* and *RBP*, are responsible for erythrocyte binding. The *DBL* gene family comprises *PkDBP-α*, *PkDBP-β*, and *PkDBP-γ*. In humans, the parasite ligand responsible for erythrocyte invasion is *PkDBP-α*, which binds to the DARC receptor. The other two Duffy-binding proteins, *PkDBP-β* and *PkDBP-γ*, bind only to macaque but not human erythrocytes (12). The normocyte-binding protein Xa (NBPXa) is required for binding in human erythrocytes, but it is not necessary for invasion of *Macaca mulatta* erythrocytes (92). Variation in *PkNBPXa* has been shown to be linked with

parasite virulence and severity of disease (93). The receptors for NBPXa and NBPXb necessary for invasion for either human or *M. mulatta* erythrocytes have yet to be identified [90]. Unlike *P. vivax*, both *P. falciparum* and *P. knowlesi* can be maintained in long-term culture, making them ideal systems for studying invasion mechanisms (94, 95).

*P. cynomolgi* is a vivax-like simian malaria that shares many genomic and phenotypic characteristics with *P. vivax* and has been often used as a reference model of *P. vivax* (96). Two gene families, erythrocyte binding-like (*EBL*) and reticulocyte binding-like (*RBL*), are responsible for erythrocyte binding and invasion in *P. cynomolgi* (97-99). The *EBL* gene family encodes *PcyDBP-1* and *PcyDBP-2*, similar to *PkDBP*, which binds to the complementary DARC receptor on Duffy-positive erythrocytes. *PcyDBP-1* is an ortholog for *PkDBP- $\alpha$* , while *PcyDBP-2* has no known orthologs with other *Plasmodium* DBPs (100). Previous studies have shown no variation in gene copy number of either *PcyDBP-1* or *PcyDBP-2* among *P. cynomolgi* laboratory strains (101). Studies of field isolates of both *P. cynomolgi* and *P. knowlesi* have shown that *PcyDBP-1* exhibits high levels of nucleotide diversity, as compared to *PcyDBP2* or *PkDBPs* (102). The *RBL* gene family is composed of *PcyRBP1*, *PcyRBP1a*, *PcyRBP1b*, *PcyRBP2a*, *PcyRBP2b*, *PcyRBP2c*, *PcyRBP2d*, *PcyRBP2e*, *PcyRBP2f*, and *PcyRBP3*, most of which are responsible for mediating parasite invasion into reticulocytes (101). Functional studies of *PcyRBPs* are further complicated, as different strains of *P. cynomolgi* have a different set of *RBL* genes. For example, *PcyRBP2a* is present in the *P. cynomolgi* B and *P. cynomolgi* Cambodian strains but absent in the *P. cynomolgi* Berok strain. Similarly, *PcyRBP1b* is present in the *P. cynomolgi* Berok and Gombak strain but absent in the *P. cynomolgi* B, Cambodian and Rossan strain (96). While it is possible that the loss of *PcyRBP1b* can be compensated by the presence of

*PcyRBP2a* (101), the relative role of *PcyRBP1b* and *PcyRBP2a* in RBC invasion requires further investigations (103).

#### 1.4 *Plasmodium vivax* Ligand Proteins and Host Receptors for Erythrocyte Invasion

The Duffy-binding protein of *P. vivax* (PvDBP) and *P. knowlesi* (PkDBP- $\alpha$ ) interact with DARC on erythrocytes (104). A 140 kD region II of PvDBP (amino acids at site 198–522; Table 1) was identified as the key binding site to human erythrocytes (12). In humans, there are two major codominant alleles for DARC, Fy<sup>a</sup> and Fy<sup>b</sup>, which differ by a single nucleotide substitution at amino acid position 42 with glycine and aspartic acid, respectively. Individuals who are Fy<sup>a+b-</sup> have been shown to be at reduced risk for clinical *P. vivax* in comparison to Fy<sup>a-b+</sup> individuals (105, 106). Individuals with a single point mutation c.1-67T>C (rs2814778) in the GATA-1 box of the *DARC* gene are considered Duffy-negative (Fy<sup>-</sup>), as erythrocytic expression of DARC is abolished. Duffy-negative (Fy<sup>-</sup>Fy<sup>-</sup>) individuals were previously thought to be resistant to infection by *P. vivax* and *P. knowlesi* due to the parasites' inability to infect erythrocytes (107), but several recent studies have shown that *P. vivax* can infect Duffy-negative individuals, potentially utilizing another invasion ligand(s) (108). The *P. vivax* erythrocyte binding protein (PvEBP), which is similar to PcyM DBP2 sequences in *P. cynomolgi* and contains a Duffy-binding like domain, was discovered in 2013 by de novo genome assembly of field isolates from Cambodia (109). Binding assay of PvEBP region II (amino acids at site 171–484; Table 1) showed that, unlike PvDBP region II, PvEBP is able to moderately bind to Duffy-negative erythrocytes (15), lending support to the hypothesis of an alternative invasion pathway in *P. vivax*.

The comparisons of genomic sequences between *P. vivax* and other *Plasmodium* species have identified several members of the *P. vivax* reticulocyte binding protein (RBP) gene family (46, 110, 111). The *P. vivax* RBP gene family comprises several full-length genes, including *PvRBP1a*, *PvRBP1b*, *PvRBP2a*, *PvRBP2b*, and *PvRBP2c*; partial genes, including *PvRBP1p1*, *PvRBP2p1*, and *PvRBP2p2*; and pseudogenes, including *PvRBP2d*, *PvRBP2e*, and *PvRBP3*. *PvRBP1* comprises *PvRBP1a* and *PvRBP1b* and shares homologous regions with *P. falciparum* *PfRh4* (112). The binding regions of *PvRBP1a* and *PvRBP1b* are homologous to that of *PfRh4*, and the amino acids at site ~339–599 were confirmed to interact with human reticulocytes (82, 113) (Table 1). *PvRBP1a* is orthologous to the pseudogene of *PkNBP1*, but no orthologous region of *PvRBP1b* was detected in *P. knowlesi* (96). While the host receptors of both *PvRBP1a* and *PvRBP1b* proteins are unclear, it has been shown that the receptors are neuraminidase resistant (82). *PvRBP1p1* contains a fragment which has 95% similarity to a C-terminal sequence in *PvRBP1b* (114). Several members of *PvRBP2* (*PvRBP2a*, *PvRBP2b*, *PvRBP2c*, *PvRBP2d*, *PvRBP2e*, *PvRBP2p1*, and *PvRBP2p2*) are orthologous to *PfRH2a* and *PfRH2b* (82, 111), as well as *PcyRBP2* (96). Some of them, such as *PvRBP2a* and *PfRh5*, also share high structural similarity (115). *PvRBP2b* and *PvRBP2c* are orthologous to *PcyRBP2b* and *PcyRBP2c*, respectively (96). Recently, the receptor for *PvRBP2b* has been identified as transferrin receptor 1 (TfR1) and the *PvRBP2b*–TfR1 interaction plays a critical role in reticulocyte invasion in Duffy-positive infections (116). While *PvRBP2p1* has been identified in all human *P. vivax* infections, *PvRBP2p2* was only present in certain lineages of *P. vivax* (117). *PvRBP2d*, *PvRBP2e*, and *PvRBP3* are pseudogenes that share homology with other *PvRBPs* but encode for nonfunctional proteins (117). In addition, *PvRBP2e* is present in the Cambodian field isolates but

not in the *P. vivax* Salvador I (109). The role of these *PvRBP* genes in erythrocyte invasion remains unclear.

Tryptophan-rich antigens (TRAgS) are a family of antigens found on human and rodent malaria parasites. In *P. vivax*, the number of encoded tryptophan-rich proteins is much higher than that of *P. falciparum*. In the latter case, some of these proteins have been shown to play important role in red-cell invasion and thus are proposed as potential vaccine candidates against *P. falciparum* malaria (18, 19). Although the reason as to why such a large number of tryptophan-rich proteins are being expressed by *P. vivax* is unknown, the stage-specific expression of these genes is indicative of their different roles in the parasite's life cycle (20, 118). The PvTRAg family contains 36 members, each with a positionally conserved tryptophan-rich domain in the C-terminus region (119, 120). Of the 36 PvTRAgS, 33 transcribe differently during the ring, trophozoite, and schizont stages of *P. vivax*, indicating their involvement in blood-stage development (39). A majority of transcription take place during the schizont-ring transition (121), suggesting their role in erythrocyte invasion. The proportion of non-synonymous SNPs in *PvTRAg* genes was shown to be significantly high, suggesting the effect of diversifying selection related to antigenic function (122). Nine PvTRAgS have been shown to bind to human erythrocytes, including PvTRAg33.5, PvTRAg35.2, PvTRAg69.4, PvTRAg34, PvTRAg38, PvTRAg36, PvTRAg74, PvTRAg26.3, and PvTRAg36.6. These proteins possess erythrocyte-binding activity with predicted protein localization to be during the schizont stage (123, 124), and each protein recognizes multiple erythrocyte receptors (124). A comparison of *P. vivax* transcriptomes between *Aotus* and *Saimiri* monkeys indicated the expression of six *PvTRAg* genes in *Saimiri P. vivax* was 37-fold higher than in the *Aotus* monkey strains (37). Five of these highly expressed *PvTRAg* genes were previously shown to bind to human erythrocytes

(38, 123). Although most TRAg receptors remain poorly characterized and unnamed, the receptor of PvTRAg38 has been identified as Band 3 that binds to amino acid positions 197–214 (125) (Table 1). The 10 PvTRAg ligands cross-compete with one other and each receptor is shared by more than one TRAg ligand, e.g., PvTRAg38 and PvTRAg74 share a common chymotrypsin-sensitive erythrocyte receptor (123, 124). In addition, the expression of the 10 PvTRAGs varies and is stage-specific, suggesting their differential roles in parasite growth and development. For example, PvTRAg, PvTRAg26.3, PvTRAg36.6, and PvTRAg69.4 are all expressed at the ring and early trophozoite stages of the parasites, indicative of an important role in rosetting; PvTRAg35.2, PvTRAg38, PvTRAg36, and PvTRAg34 are expressed during the schizont and merozoite stages, indicative of invasion properties (124). Further, PvTRAg36.6 interacts with early transcribed membrane protein (PvETRAMP) to form a protein complex that is apically localized in merozoites, suggesting that this protein is critical for development or maintenance of the parasitophorous vacuole membrane (38). Recent studies have shown that the PvTRAg35.2 gene sequences were highly conserved in the parasites, and amino acid residues 155–190 and 263–283 were involved in erythrocyte binding (126) (Table 1). PvTRAg35.2 competes with PvTRAg 33.5 and PvTRAg28 and may play a redundant role in erythrocyte invasion (126). Orthologs of *Pv-fam-a* are present in *P. knowlesi*, *P. falciparum*, and *P. yoelii*, suggesting that these genes may play a critical role for invasion throughout *Plasmodium* evolution (110). Other PvTRAGs, such as PvTRAg56.6 and PvTRAg56.2, interact with PvMSP1 and PvMSP7, to stabilize surface protein complexes on merozoites, and are likely not involved in erythrocyte binding (38). Additionally, PvTRAGs elicit a strong IgG antibody immune response in *P. vivax*-infected individuals, with memory lasting up to 5–12 years after being infected (39). Nine TRAGs (PvTRAg3, PvTRAg7, PvTRAg13, PvTRAg14, PvTRAg15, PvTRAg18,



PvTRAg20, PvTRAg26, and PvTRAg35) showed high IgG positivity and conserved IgG reactivity in three Asian countries with low malaria endemicity (39), demonstrating the universal antigenicity of these TRAg proteins.

Merozoite Surface Proteins (MSPs) are a large family of genes found on the surface of merozoites, and a few members are suggested to be involved in non-DBP1 erythrocyte invasion pathways (59). MSP1 is a 200 kDa highly conserved antigen that undergoes several cleavage events as invasion occurs (78, 87). MSP1 shows a strong binding affinity between 20 and 150 nM at the 42 and 19 kDa fragment cleavage sites, with high-activity binding peptides (HABPs) clustered close to these two fragments at positions 280–719 and 1060–1599, respectively (59), suggesting its critical role in erythrocyte invasion. MSP1 has the potential to be a vaccine target due to its strong immunogenicity (127), but further research is needed (128, 129). MSP3 transcribes during the trophozoite and schizont stages of *P. vivax* (130) and is highly expressed in *Saimiri* infections (37). Although it is yet unclear whether MSP3 binds to human erythrocytes, MSP3.3 and MSP3.5 were expressed on the surface of mature schizonts and interact with MSP1, MSP7, and MSP9 (37). The MSP3 gene family contained RNA expression of 11 members during the trophozoite and schizont stages, hinting at the MSP3 family playing an important role in both maturation and binding (130). Interestingly, MSP3.7 was detected at the apical end of merozoites, which differentiates probable roles from other MSP3 family members (130). Additionally, MSP3.11 transcripts were present, but with no corresponding protein being detected, questioning the exact role of this protein (130). Although the *MSP7* gene family has not been shown to bind to erythrocytes, it forms a complex with PvTRAg36.6 and PvTRAg56.2 and localizes on the surface, likely assisting in stabilization of the protein complex at the merozoite surface (38). Several *MSP7* genes, including *MSP7C*, *MSP7H*, and *MSP7I*, are strong antibody

targets and contain high genetic diversity due to frequent positive selection (131). The MSP9 family also undergoes frequent selection and recombination and forms a co-ligand complex with the 19 kDa fragment of MSP1, but no erythrocytic binding activity was observed (132). It is possible that MSP9 assists MSP1 in binding to erythrocytes. MSP9 is highly immunogenic at conserved regions 795–808, making it a good vaccine candidate (133, 134).

### 1.5 Humoral Immune Response against *P. vivax* and Vaccine Targets

The severity of malaria infection during the erythrocyte stage of *Plasmodium* depends on various factors, including the following: the location of parasitized red blood cells in the target organs; the local and systemic action of the parasite's bioactive products; pro-inflammatory cytokine production, as well as innate and adaptive immune system at the cellular levels that involves cytokine and chemokine regulators; and the activation, recruiting, and infiltration of inflammatory cells (135). During *P. vivax* infection, some individuals can acquire immunity naturally. Such immunity consists of humoral IgG antibodies, cellular cytokines, and proteolytic enzymes production as part of the host response to *the* pathogen (136, 137). Apart from the invasion capability of *P. vivax*, host immune response to the pathogen is also a key factor for determining parasitemia and pathology. For example, patients with moderate parasitemia in endemic regions of Colombia were shown with cellular immune responses including high IFN- $\gamma$  and TNF- $\alpha$  levels and a pro-inflammatory cytokine profile in unstable transmission regions (138). The balance in interleukin (IL)-10/TNF- $\alpha$  rate could prevent increased parasitemia and host pathology (139). To date, DBP is the primary target antigen for *P. vivax* vaccine development. Serological studies have shown that region II of PvDBP, which *P. vivax* uses to bind to human erythrocytes, induces antibodies against DBP and is naturally immunogenic in

people residing in endemic regions, through repeated exposure to the infection (140, 141). However, the naturally acquired neutralizing antibodies against DBP are short-lived, increasing with acute infection, and are strain specific (142, 143). Antibodies from plasma from naturally exposed people and from animals immunized with recombinant Duffy binding protein (rDBP) have blocked the specific interaction between the PvDBP ligand domain in vitro and its receptor on erythrocyte surface (142, 143). Such inhibitory activity was correlated with antibody titers. The DBP1 binding domain is polymorphic, tending to compromise the efficacy of any vaccine associated with strain-specific immunity (144). While almost all mutations in polymorphic residues did not alter RBC binding (145, 146), such polymorphism has a synergic effect on the antigenic nature of DBP (146). However, polymorphic SNP variants in the binding domain of PvDBP1 had no effect on the degree of inhibition by anti-DBP monoclonal antibodies. On the contrary, a higher *PvDBP* gene copy number was shown to reduce susceptibility to anti-PvDBP antibody response (147), but not for better invasion of FyA/FyA and FyA/FyB reticulocytes.

Apart from DBP, the MSP family is responsible of the interaction between merozoites and reticulocytes during the erythrocyte phase. PvMSP1, PvMSP3, and PvMSP9 are potential vaccine candidates, since they are exposed to the immune system and are recognized by antibodies from naturally infected individuals (148). Cytoadherence assays demonstrated that MSP1<sub>19</sub> is an essential adhesion molecule used in *P. vivax* invasion to erythrocytes (149) and is immunogenic in people living in areas of unstable malaria transmission in Southeast Asia, Papua New Guinea, and Brazil (150). Two recombinant polypeptides, rPvMSP<sub>114</sub> and rPvMSP<sub>120</sub>, from the MSP1 C-terminal region show high binding activity to reticulocytes, but no antibodies against these peptides were detected in immunized *Aotus* monkeys (87). MSP3 is an abundant ligand on the merozoite surface that is essential for reticulocyte invasion. PvMSP3 $\alpha$  block II and

the C-terminal region were shown to be highly immunogenic. Individuals living in an endemic region with a high number of previous episodes of malaria were shown to have increased IgG1 and IgG3 anti-PvMSP3 $\alpha$  (148, 151, 152). Likewise, the PvMSP9 C-terminal and NT domains have also been shown to induce memory T-cell response (higher IFN- $\gamma$  and IL-4 cytokine production) in individuals living in *P. vivax*-endemic regions of the Brazilian Amazon and Papua New Guinea (152, 153) and are specific targets of *P. vivax* vaccine. It is unclear if Duffy-negative individuals acquire high levels of antibodies against the 19-kDa C-terminal region of the *P. vivax* PvMSP1, PvMSP3, and PvMSP9, resulting in a low susceptibility to *P. vivax* infection (105).

PvRBP2b was recently shown to bind transferrin receptor 1 of the reticulocytes, through the apical domain and the protease-like domain of TfR1 and the N-terminal region of Tf (115). RBP2P1 protein was found to be expressed in schizonts and localized at the apical end of the merozoite, and it preferentially binds reticulocytes over normocytes. Monoclonal antibodies raised against PvRBP2b prevent reticulocyte binding and reduce *P. vivax* invasion (115). *P. vivax* malaria patients had higher IgG levels against rRBP2P1 than did naive individuals. Human antibodies to this protein also exhibit erythrocyte binding inhibition and are associated with lower parasitemia (154). PvRBP1a and PvRBP1b are highly transcribed during the parasite schizont stage (118). PvRBP1a-34 and PvRBP1b-32 proteins bounded specifically to reticulocytes and showed significantly higher reticulocyte binding activity than normocyte-binding activity (82). Clinical assays have indicated that PvRBP1<sub>435-777</sub> is poorly immunogenic, likely because PvRBP1 had multiple promiscuous T-cell epitopes, which did not induce specific genetic restriction (155). IgG prevalence against the NT region (including the most polymorphic region) of the PvRBP1a and b was intermediate in a population from Thailand (117), but IgG

prevalence against the PvRBP1a-34 and PvRBP1b-32 proteins was significantly higher in *P. vivax* patients than healthy individuals in the Republic of Korea (82). Moreover, the highly conserved region III (between amino acids 1941–2229), with the greatest amount of high-affinity reticulocyte-binding peptides and high binding affinity, was shown to induce high antibody titers in *Aotus* monkeys and be able to recognize the full PvRBP1 in parasite lysate (156). The expression of PvRBPs in the African *P. vivax* and the antibody response against PvRBP in Duffy-negatives will provide important implications to the usefulness of a future vaccine in *vivax* malaria control in Africa.

While the circumsporozoite protein (CSP) is one of the most important proteins described in hepatocyte invasion by *Plasmodium* sporozoites, previous studies involving individuals residing in *P. vivax* malaria-endemic regions in Brazil showed low responses for antibodies directed against the repeat and C-terminal regions (157). On the other hand, members of the *TRAg* gene family that were highly expressed in non-DARC *Saimiri*-infected *P. vivax* have also shown to induce antibody response in people from *vivax*-endemic regions. A recent study of 383 children in Papua New Guinea showed that antibodies against PvFAM-D2 were significantly more common in children with active *P. vivax* infections (158). The coexpression of PvFAM-A2 and PvFAM-D2 proteins in infected reticulocytes is spleen-dependent, based on the *Aotus* monkey model (159). These proteins were recognized by a high percentage of sera and are highly immunogenic targets of naturally acquired immune responses (159). These results are in agreement with members of these families being highly expressed in transcriptional analysis of parasite isolates (37, 160). Moreover, PVX\_108770 (VIR14) of the multi-gene VIR family largely located at the subtelomeric regions also presented high sero-positivity, despite the role of its conserved globular domains in eliciting cross-reacting antibodies being unclear (161, 162).

Other proteins, such as HYP, which is 100% conserved among *P. vivax* isolates from Mauritania, North Korea, India, and Brazil, and had antibodies significantly associated with protection against clinical *P. vivax* episodes in children (158), are a potential target of blood-stage vaccine. Taken together, it is possible that individuals with low-to-no DARC expression have lower susceptibility to infection than individuals having high DARC expression by eliciting high frequency and magnitude of anti-DBP, anti-MSP, anti-RBP, and anti-FAM antibody response against *P. vivax* during the blood stage. This may imply that one of *P. vivax*'s primary mechanisms for evading host immunity works through indirect, negative regulation of DARC, influencing the humoral response against erythrocyte invasion and parasite development.

## 1.6 Conclusions

The documentation of *P. vivax* infections in different parts of Africa where Duffy-negative individuals are predominant (163-169) suggested that there are alternative pathways for erythrocyte invasion. It is apparent that Duffy-negative individuals are no longer resistant to *P. vivax* malaria. The increased risk of *P. vivax* infection and the growing clinical burden across Africa, as well as in Duffy-negative individuals, certainly highlight the public health concern of *P. vivax* malaria. Future studies should clarify the function and immunogenicity of various candidate parasite ligand proteins and identify their corresponding receptors involved in alternative Duffy-independent erythrocyte invasion, critically examine the host antibody response with respect to *P. vivax* proteins across wide ethnic groups, provide a rigid comparison and analysis of asymptomatic reservoirs and transmission mechanisms of *P. vivax* in Duffy-negative populations, and unveil the biological features of relapse infections in Africa. Furthermore, future studies should investigate the biology of relapse infections, including the

development and characteristics of hypnozoites in *P. vivax*, which remain largely unclear, despite the overwhelming importance with regard to the impact of relapses on genetic variation of the parasites, transmission, and antimalarial treatment of *P. vivax* cases.

## 1.7 Tables

Table 1. Currently known *P. vivax* genes and amino acid regions responsible for binding human erythrocytes.

Gene Name	Amino Acid Binding Region	Target Cell(s)
PvDBP1	198–522 (12)	Duffy-positive Erythrocytes
<u>PvEBP/DBP2</u>	171–484 (15)	Erythrocytes
PvRBP1a	352–599 (113)	Reticulocytes
PvRBP1b	339–587 (82)	Reticulocytes
PvRBP2a	160–1000 (115)	Mature RBCs and Reticulocytes
PvRBP2b	161–1454 (116)	Reticulocytes
PvRBP2c	Native protein (46)	Reticulocytes
-	168–524 (170)	10% reticulocytes
	464–876 (170)	34% reticulocytes
PvTRAg38	197–214 (125)	Erythrocytes
PvTRAg35.2	155–190 (126)	Erythrocytes
	263–283 (126)	Erythrocytes
PvMSP1	280–719 (59)	Erythrocytes
	1060–1599 (59)	Erythrocytes



## Chapter 2: Materials and Methods

### 2.1. Ethic's Statement

Scientific and ethical clearance was obtained from the institutional scientific and ethical review boards of Jimma University, Ethiopia and University of North Carolina, Charlotte, USA. Written informed consent/assent for study participation was obtained from all consenting heads of households, parents/guardians (for minors under 18 years old), and each individual who was willing to participate in the study.

### 2.2 Study area and genotyping

Clinical samples were obtained from six different study sites, three from Ethiopia and three from Sudan. Study sites in Ethiopia included Jimma (JM), Gojeb (GJ), and Arjo (AJ); and study sites in Sudan included Khartoum (KH), River Nile (RN), and New Halfa (NH). These sites are located around the Ethiopia-Sudan border area (Figure 1) and experience low to moderate transmission (171). Samples were processed and screened for *P. vivax* following the published protocol (172). A total of 305 and 107 *P. vivax* samples from Duffy-positive and Duffy-negative individuals, respectively, were included in microsatellite analyses. These included 150 samples from Duffy-positive and 83 samples from Duffy-negative individuals in Ethiopia, and 155 and 24 samples, respectively, in Sudan. Eight microsatellites with tri- or tetranucleotide repeats, which mapped to 6 chromosomes, were typed for *P. vivax* following the published protocol (4).

### 2.3 Linkage disequilibrium and multiplicity of infections

To examine whether the microsatellite loci are in linkage disequilibrium (LD), multilocus LD was assessed among the parasite samples for each study site using LIAN version 3.7 (173). The standardized index of association ( $I_A^S$ ), which measures the strength of linkage disequilibrium and views as a function of the rate of recombination among samples, was calculated. Due to small samples from Duffy-negatives in New Halfa, Sudan ( $N=2$ ), this population was excluded from LD analyses. The percentage of polyclonal infections, as well as average multiplicity of infection (MOI), were estimated for each of the study sites and Duffy groups. MOI was scored as the maximum number of alleles observed in each sample, when all loci were considered.

### 2.4 Genetic diversity and population structure

Genotypic variation was calculated in GenoDive, version 2.0b27 based on the mean of individual markers (174) and tested for significance by two-tailed T-tests. A model-based Bayesian method implemented in STRUCTURE v2.3.4 (175) was performed separately at the site and country levels to examine the partitioning of individuals to genetic clusters. The partitioning of clusters was visualized with DISTRUCT (176). In addition, Discriminant Analysis of Principle Components (DAPC) was performed to identify the optimal number of components that best separate samples into pre-defined clusters (177). Phylogenetic analyses were conducted at the population level to examine the relatedness of *P. vivax* from Duffy-positive and Duffy-negative individuals.

## 2.5 Identification of source-sink dynamics and direction of transmission

The StrainHub software (178) v0.2.0 was used to generate a transmission network from the phylogeny of our samples. The squared Euclidean distances based on the number of times a certain allele is found in two individuals were computed between each pair of individuals using GenoDive and an unrooted neighbor-joining tree was constructed using the ape R package v5.4\_1 (179). StrainHub used the genetic relationships from the tree and the associated metadata states to reconstruct an estimate of ancestral states. Samples were grouped by country, site, and Duffy status to illustrate the directions of transmission. Values near 1 indicate a source, values near 0 indicate a sink, and values in the middle suggest the node is a hub. It is worth noting that StrainHub is a phylogenetic method that does not account for recombination among lineages. To validate the results of StrainHub, relatedness among groups were also computed using the identical-by-descent (IBD) method described in Taylor *et al.* (180).

## 2.6 Analyses of geographic and landscape factors

To test for isolation-by-distance, the Mantel test was performed on the matrix of pairwise  $F_{ST}$ -values. This test was conducted with the ade4 R package, version 1.7\_15, with 10,000 permutations performed to estimate significance (181). For this analysis, the geographical coordinates of the six study sites were used for estimating physical distances between sites, and *P. vivax* samples from Duffy-positives and Duffy-negatives were combined for each study site.

To determine whether the observed patterns of genetic differentiation are explained by landscape factors, resistance surfaces were fit to the genetic data for a variety of gridded,

environmental datasets. Specifically, these were: road density, as estimated by Meijer *et al.* (182); elevation, as measured by the Shuttle Radar Topography Mission; and land cover, obtained from the MCD12Q1 dataset (183). Road density was selected as a proxy for human movement, whereas elevation and land cover were chosen to be representative of mosquito habitat. The malaria samples were gathered between 2017 and 2019, so land cover data for 2018 was chosen as representative. The other two datasets are static and all three were projected to a consistent coordinate system. Resistance surfaces based on these three environmental datasets that best explain the observed genetic distances (pairwise  $F_{ST}$ -values) were modeled using the ResistanceGA R package, version 4.0-14 (184). Resistance surfaces were fit for each individual environmental variable, and composite resistance surfaces were fit for each possible combination of multiple environmental variables.

## 2.7 Sample preparation of the 10 Ethiopian *P. vivax* transcriptomes

For 10 Duffy positive *P. vivax* samples from Ethiopia, 10mL whole blood was preserved into sodium heparin from microscopy-confirmed *P. vivax* patients at hospitals in Jimma, Ethiopia area who had 4,000 parasites/ $\mu$ L parasitemia and had not received prior antimalarial treatment. Blood samples were cryo-preserved with two times glycerolyte 57 and stored in liquid nitrogen. Prior to culture, samples were thawed by adding 0.2V of 12% NaCl solution drop-by-drop followed by a 5-minute room temperature incubation. Ten-times volume of 1.6% NaCl solution was then added drop-by-drop to the mixture and the samples were centrifuged at 1000 rcf for 10 minutes to isolate the red blood cell pellet. This process was repeated with a 10x volume of 0.9% NaCl. Following centrifugation, the supernatant was removed via aspiration, and 18mL of sterile IMDM (added 2.5% human AB plasma, 2.5% HEPES buffer, 2% hypoxanthine, 0.25% albumax,

and 0.2% Gentamycin) per 1mL cryo mixture was added to each sample for a final hematocrit of 2%. 10% Giemsa thick microscopy slides were made to determine the majority life stage and duration of incubation required, averaging 20-22 hours for the majority trophozoites and 40-44 hours for the majority ring. Samples were incubated at 37°C in a 5% O<sub>2</sub>, 5% CO<sub>2</sub> atmosphere to allow growth to the schizont stage. *In vitro* maturation was validated through microscopic smears 20-40 hours after the initial starting time, dependent on the majority stage, and subsequently checked every one to two hours if immature.

Cultured pellets were isolated via centrifugation and placed in 10x volume trizol for RNA extraction. RNA extraction was performed using Zymo direct-zol RNA prep kit according to the manufacturer's protocol, followed by two rounds of DNA digestion using the DNA-free kit (Zymo). Samples were analyzed with a nanodrop 2000 and RNA Qubit to ensure sample concentrations were above 150 ng total for library construction. For samples with no significant amount of DNA or protein contaminants, RNA libraries were constructed using Illumina rRNA depletion library kits according to the manufacturer's protocol. Completed libraries were quality checked using a bioanalyzer to ensure adequate cDNA was produced before sequencing. Sample reads were obtained using Illumina HiSeq 2x150bp configuration to obtain at least 35 million reads per sample. Sequence reads were aligned with HISAT2 (185), using the Rhisat2 R package (186) to the P01 *P. vivax* reference genome and all human reads were filtered out using SAMtools (187) (implemented in the R package (188)). The alignment was mapped to the P01 reference annotation using the Rsubread package (189). Sequences for the 10 Ethiopian transcriptomes are available on the National Center for Biotechnology Information Short Read Archive under BioProject: PRJNA784582. All code is available on GitHub at [https://github.com/colbyford/vivax\\_transcriptome\\_comparisons](https://github.com/colbyford/vivax_transcriptome_comparisons).

## 2.8 Data analyses of the 10 Ethiopian *P. vivax* transcriptomes

To further confirm samples were majority schizont stage, sequence reads of each sample were deconvoluted in CIBERSORTx (190) based on *P. berghei* homologs as previously described in Tebben et al (191). We used the established matrix to determine the frequency of expression for each gene calculated for rings, trophozoites, and schizonts, respectively. Samples that were expressed 30% or more were sorted into their respective stage(s). All reads were annotated using the Rsubread package and classified into 12 different categories by function. We then examined the top 30 transcribed genes using the counts per million (CPM) metric.

Our previously published whole genome sequence data identified several mutations and structural polymorphisms in genes from the *PvEBP*, *PvRBP*, *PvMSP*, and *PvTRAg* gene families that are likely to involve in reticulocyte invasion (24). Specific binding regions in some of *PvDBP1*, *PvEBP*, *PvRBP*, and *PvMSP* genes have been identified (192). To further explore the putative function, we compared relative expression levels of these genes in the 10 Ethiopian *P. vivax* samples with other geographical isolates of majority schizont stage. We used the CPM and TPM metric in R package edgeR (193). The CPM metric was used to obtain the top 30 transcripts overall and does not consider gene length, while TPM considers gene length for normalization and allows an unbiased conclusion to be made relative between and to other transcriptomes (194). We then transformed the data using  $\log(2)TPM+1$  to illustrate relative expression levels via a heat map with an average abundance. We also selected 26 gametocyte gene candidates from the literature (195) to assess their continental expression levels relative to the standard *Pvs25*.

## 2.9 Continental comparison of *P. vivax* transcriptomes

RNA-seq data of four *in vitro* Cambodian (52) and two Brazilian (194) *P. vivax in vitro* samples were downloaded from the GitHub repository and analyzed with the same bioinformatic methods described above to minimize potential batch effects. Samples were deconvoluted using the same matrix and found to have a non-significant difference in troph or schizont concentrations (P values: 0.14 and 0.41 respectively). The Ethiopian *P. vivax* samples were cultured and sequenced using similar protocol as the Cambodian (52) and Brazilian (194) ones except with slight modification in media and library preparation. We obtained the average expression and standard deviation in TPM for each gene target and determined potential difference in transcription levels by conducting pairwise differential expression (DE) analysis among the Cambodian, Brazilian, and Ethiopian samples. The expression level of 6,829 genes were examined for DE by edgeR dream (193, 196) and variancePartition (197), with adjusted  $p$ -value  $> 1.0 \times 10^{-6}$  for DE gene concordance. A linear mixed effects models was used to ensure accuracy in triplicated Brazilian samples, and the Kenward-Roger method was used to estimate the effective degree of freedom for hypothesis testing due to small sample sizes.

## Chapter 3: *Plasmodium vivax* from Duffy-Negative and Duffy-Positive Individuals Shares

### Similar Gene Pool in East Africa

#### 3.1 Rationale

Ethiopia and Sudan are two of the few African countries where *P. vivax* malaria is prevalent (198), and Duffy-negative and Duffy-positive individuals coexist (14). *P. vivax* prevalence is lower in Duffy-negative than Duffy-positive individuals (172, 199). In Central and West Africa, more than 97% of the population is Duffy-negative (14). By contrast, in Ethiopia and Sudan, about 35% and 50% of the general population, as well as 20% and 18% of the hospitalized malaria patients, respectively, are Duffy-negatives (4, 14, 200). Other East African countries such as Eritrea and Madagascar have also reported significant *P. vivax* infections in Duffy-positive and Duffy-negative individuals who live side-by-side (1, 14), suggesting the potential of between-host transmission. The genetic diversity and population structure of *P. vivax* have been shown to be substantially different from *P. falciparum* (21, 201). *P. vivax* has a higher nucleotide diversity than *P. falciparum* (201), likely due to frequent gene flow via human movement, higher transmission intensity and recombination, as well as variation in host susceptibility (21). In Papua New Guinea, *P. vivax* had a 3.5-fold higher rate of polyclonality and nearly double the multiplicity of infection (MOI) than *P. falciparum* infections (202). Similarly, in Cambodia (203), the Indo-West Pacific (204, 205), and the Brazilian Amazon (206), *P. vivax* had a higher microsatellite diversity than its sympatric *P. falciparum*. These findings highlight the potential for *P. vivax* to adapt to a wide range of landscapes and climates.

The questions of whether *P. vivax* infecting Duffy-negatives is genetically similar to that from Duffy-positives in the same region, and how landscape or environmental factors influence



*P. vivax* gene flow in Africa, remain unclear. This study has two objectives: 1) to examine genetic variation and source-sink dynamics of *P. vivax* between Duffy-negative and Duffy-positive populations in Ethiopia and Sudan; 2) to estimated how landscape and environmental factors influence parasite gene flow. Findings provide critical insights into whether and how *P. vivax* evolves and spreads in Duffy-negative individuals and highlight the need for *P. vivax* diagnosis, tracking, and control in Africa.

### 3.2 Results

#### 3.2.1 Linkage disequilibrium and multiplicity of infections

Clinical samples were obtained from six different study sites, three from Ethiopia and three from Sudan. Study sites in Ethiopia included Jimma (JM), Gojeb (GJ), and Arjo (AJ); and study sites in Sudan included Khartoum (KH), River Nile (RN), and New Halfa (NH). These sites are located around the Ethiopia-Sudan border area (Figure 1) and experience low to moderate transmission. Significant linkage disequilibrium (LD) was detected for all pairwise combinations of microsatellite loci (Bonferroni-corrected  $P < 0.05$ ). When all loci were pooled together, *P. vivax* from Duffy-negatives in both countries showed a slightly higher level of linkage and/or rate of recombination than samples from Duffy-positives (Table 2).  $I_A^S$  values of *P. vivax* from Duffy-negatives ranged from 0.03 (Jimma, Ethiopia) to 0.77 (Khartoum, Sudan), whereas  $I_A^S$  values ranged from 0.04 (Gojeb, Ethiopia) to 0.25 (Khartoum, Sudan) in Duffy-positives.

*P. vivax* from Duffy-negatives and Duffy-positives showed a comparable rate of polyclonal infections (15% and 14%, respectively; Table 2). Among the samples from Duffy-negatives, the highest rate of polyclonal infections was observed in Jimma, Ethiopia (JM:

17.2%), and no polyclonal infections in Khartoum, Sudan (KH) and Gojeb, Ethiopia (GJ), although there were few samples from Duffy-negatives in these locations. Among the samples from Duffy-positives, the highest rate of polyclonal infections was observed in Gojeb, Ethiopia (30.7%), followed by River Nile, Sudan (21%); whereas the lowest was observed in Khartoum (5.8%; Table 2). MOI was also similar between the Duffy-negative (mean = 1.17) and Duffy-positive (mean = 1.16; Table 2) infections, with a maximum of three clones detected within a sample. Because we were unable to confidently differentiate the genotypes of the different clones in samples with more than 1 alleles in two or more loci, 16 of the polyclonal samples were discarded in the genetic analyses.

### 3.2.2 Genetic diversity and population structure

In Ethiopia and Sudan, *P. vivax* in Duffy-positive individuals showed significantly higher genotypic and allelic diversity than in Duffy-negatives ( $p < 0.05$ ; Table 3). Genetic diversity of *P. vivax* in Duffy-positives was similar between Ethiopia and Sudan. However, the diversity of *P. vivax* in Duffy-negatives from Ethiopia was much higher than that from Sudan, likely due to the differences in sample size. Interestingly, genotypic evenness of *P. vivax* was higher in Duffy-negative than Duffy-positive infections in both countries, though it was not significant ( $p = 0.076$ ; Table 3). Given that *P. vivax* in Duffy-negative and Duffy-positive individuals shared a similar set of alleles in each of the studied loci, we found no evidence of population bottleneck in both Duffy groups.

STRUCTURE analyses indicated two most probable genetic clusters among all samples at the site level (purple and yellow clusters; Figure 2). In Ethiopia, most of the samples from Arjo, Gojeb, and Jimma predominately belonged to the purple cluster. No distinguishable differences were detected between samples from Duffy-positive and Duffy-negative infections.

In Sudan, however, a mixed clustering pattern was observed. About 80% of the samples from Duffy-positives in Khartoum belonged to the yellow cluster (Figure 3), whereas those in New Halfa and River Nile had a mixture of yellow and purple clusters. When the samples were analyzed by country and Duffy status rather than by site, three clusters were indicated (purple, blue, and yellow; Figure 4). In Ethiopia, *P. vivax* from Duffy-positive individuals had majority purple cluster and *P. vivax* from Duffy-negatives had both purple and blue clusters. In Sudan, *P. vivax* from Duffy-positive individuals had mostly the yellow cluster and *P. vivax* from Duffy-negatives had mixed yellow, blue, and purple clusters. No marked difference was observed between Duffy-positive and Duffy-negative individuals in respective countries. Similar to STRUCTURE results, DAPC analyses showed that *P. vivax* from individuals in Khartoum, Sudan was distinct from the others (Figure 3). In general, *P. vivax* from Duffy-positive and Duffy-negative individuals in the same site were not clearly distinguishable, except for samples in Jimma and Gojeb. In Jimma, samples from Duffy-negatives were slightly separated from Duffy-positives. In Gojeb, the number of Duffy-negative samples was too small to indicate clear differentiations. Analyses at the population levels also showed no clear distinction among samples by Duffy status or country (Figure 5).

### 3.2.3 Source-sink dynamics and direction of transmission

The transmission networks produced by StrainHub showed that *P. vivax* from Duffy-positive and Duffy-negative individuals in Ethiopia served as the primary source, and *P. vivax* from the Sudanese Duffy-negative individuals was the sink population (Figure 6a). It is noted that the weight of the arrows was not normalized by sample size. Although the Ethiopian Duffy-negative population had a high Source Hub Ratio, the weight of the arrows leading from this

population was not the thickest compared to Duffy-positives indicating that fewer transitions of *P. vivax* were from Duffy-negatives in Ethiopia. Based on IBD analyses, the average relatedness of *P. vivax* between Duffy-negative and Duffy-positive individuals was low but not significantly different to the values with the same Duffy status (Table 4). Despite smaller samples from Duffy-negatives, these results suggested similar levels of transmission and recombination of *P. vivax* in individuals regardless of Duffy status and supported the StrainHub network showing that transition occurred both ways between Duffy-negative and Duffy-positive individuals (Figure 6a). At a site level, *P. vivax* from Arjo (AJ) was a source, and *P. vivax* from infections in New Halfa (HA) was a sink (Figure 6b) for both phenotypes. The weight of the arrows suggest that Arjo had more transitions with the other populations in Ethiopia (GJ and JM) than those in Sudan.

#### 3.2.4 Influence of geographic and landscape factors

The Mantel test indicated a pattern of isolation-by-distance in the population  $F_{ST}$ -values ( $r_M$ -value=0.325;  $p$ -value=0.017). Using a confidence threshold of 0.05, the null hypothesis of no relationship between genetic and geographic distance should be rejected. Based on the AICc score and ranking, the resistance surface based on a single covariate that best fit the  $F_{ST}$ -values was land cover (Figure 7a), while road density and elevation comprised the best-fitting combination surface (Figure 7b). All resistance surfaces were significant ( $p$ -value < 0.05; Table 5), and the analysis showed that geographic distance alone does not explain the genetic distances in our dataset ( $p$ -value>0.025 for a two-tailed test). ResistanceGA weighted elevation as 92% of the combination surface (Figure 7b), constituting most of the variation in resistance. Visual inspection suggests the exception is in the vicinity of Khartoum, where high resistance

values were associated with high road density. On the other hand, land cover had the lowest AICc of any of the individual surfaces and all composite surfaces containing land cover were ranked close behind, with slightly higher AICc scores, suggesting land cover played an important role in explaining genetic distances, despite lower-ranked surface. Of the different land cover classes, grasslands and croplands were associated with low resistance, while savannas and open shrublands were modeled to have higher resistance. Taken together, the Mantel test and ResistanceGA analyses indicated that elevation and land cover were key factors in explaining *P. vivax* gene flow among our study sites in Ethiopia and Sudan, while geographic distance alone is less important.

### 3.3 Discussion

*P. vivax* malaria was previously thought to be rare or absent in African populations who lack the Duffy blood group antigen expression (2). However, recent studies reported several cases of *P. vivax* infection in Duffy-negative people in different parts of Africa (199), including countries where Duffy-negatives are predominant (16). Such a distribution raises important questions of whether *P. vivax* is transmitted among Duffy-negative individuals and between Duffy-negative and Duffy-positive populations, and what landscape factors govern *P. vivax* transmission. This information is crucial to estimating the ability of *P. vivax* malaria to transmit and spread through Duffy-negative populations in Africa. This study provides critical insights into these questions using samples from Duffy-negative and Duffy-positive individuals in Ethiopia and Sudan. These countries were chosen because many *P. vivax* cases were recorded (24, 200) and Duffy-negative and Duffy-positive individuals live together in the same areas (14, 198).

No clear differentiation was detected in *P. vivax* between Duffy-positives and Duffy-negatives for most of the studied sites. The StrainHub network indicated that transmission of *P. vivax* occurred from Duffy-positives to Duffy-negatives and vice versa. This suggests that Duffy-negative hosts are not a dead-end for *P. vivax* that only result in infection and/or clinical symptoms, but that the parasite can also spread from one Duffy-negative host to another. *P. vivax* from Duffy-negative individuals in Sudan was identified as a sink population. While this might imply limited onward transmission, larger samples are needed to confirm this finding. Interestingly, our findings showed that the MOI was similar between the Duffy-negative and Duffy-positive infections. Based on microsatellites, about 9-18% of the samples were polyclonal, consistent to our recent study that showed 18% (8 out of 44) of *P. vivax* in Duffy-positives from Ethiopia were polyclonal by whole genome sequences (24). Such moderate levels of polyclonality could be due to relapse clones (207) or submicroscopic infections, especially in Duffy-negative individuals with low parasitemia where different parasite clones may persist in the host for a long-time without detection and treatment (208). Additionally, transmission intensity, demographic factors, mosquito density, and vectoral capacity may contribute to the differences in MOI among the study populations. Previous studies on *P. falciparum* have shown that areas with a higher abundance of mosquitoes, higher population density, and a younger age group are associated with a higher entomological inoculation rate (209). These factors may apply equally to *P. vivax* in Duffy-negative and Duffy-positive populations, and consequently increase MOI.

The significantly lower genetic diversity observed in Duffy-negative infections compared to Duffy-positive infections suggested a lower transmission frequency and possibly less infectious amongst Duffy-negative Africans. It is noteworthy that the low number of Duffy-

negative infections in Gojeb, Khartoum, and New Halfa might also influence genetic diversity measures. While *P. vivax* from Duffy-negative individuals in Sudan was identified as a sink population and may imply limited onward transmission, further study is needed with larger samples to confirm these findings. To allow transmission in Duffy-negative individuals, *P. vivax* merozoites may have used non-Duffy receptors to invade human erythrocytes. Candidate genes for invasion such as glycosylphosphatidylinositol-anchored micronemal antigen (GAMA) and tryptophan-rich antigens have been shown to be expressed in patients with low parasite density. Also, CD71 (Transferrin Receptor 1, TfR1) has been shown to bind readily with the reticulocyte binding proteins based on *in-vitro* experiments (210). These alternative ligand/receptor proteins may play a key role in erythrocyte invasion (16). Further investigations at the whole-genome level are needed to uncover the Duffy-independent invasion pathway and transmission mechanism in Duffy-negative individuals (211).

Parasite populations from Ethiopia and Sudan showed overlapping clustering patterns, except for Khartoum that was slightly different from the other samples. Low levels of linkage disequilibrium were observed among samples in most of our study sites, except for Khartoum that showed a high  $I_A^S$ -value, likely due to low parasite transmission in the capitol of Sudan, an urban setting with adequate local public health infrastructure (212). While the Mantel test indicated that gene flow is associated with geographical distance, the resistance surface analysis suggested that landscape factors including land cover and elevation play a more important role in determining gene flow. The only exception was in Khartoum, where road density has been fit to a high resistance value, likely to explain the considerable genetic differentiation between Khartoum and the other populations. This could be attributed to road density indicating greater infrastructure, resulting in less transmission. The results suggest that *P. vivax* gene flow

occurred more readily in the rural parts of Ethiopia and Sudan than in the more urban setting of Khartoum, consistent with other studies that showed higher diversity of *P. vivax* in areas close to the country border of Sudan and in agriculture areas outside the capitol (213). These findings show that while sheer geographic distance serves as a barrier to gene flow, the specific features of the rural landscape in East Africa likely do not. Given that the Mantel test provides low analytical power (214) and there were few sample sites in this study, further investigations with additional sites, higher coverage of urban areas, and genome-wide data to investigate *P. vivax* adaptations to Duffy-negative red blood cells are suggested to confirm these findings. Additionally, it might be informative to explore other environmental variables related to human activities and/or mosquito habitats, beyond the landscape data examined here.



## 3.4 Tables

Table 2. Host duffy status, linkage disequilibrium, and complexity of infection among *P. vivax* samples by study site. Asterisk denotes a significant level at  $P < 0.05$ .

Country	Site	Duffy Status	Sample size	$I_A^S$	Number of polyclonal infections (%)	Mean MOI, Median (range)
Ethiopia						
	Arjo (AJ)	Duffy-Positive	56	0.07*	4 (7.14%)	1.08, 1 (1-2)
		Duffy-Negative	15	0.15*	2 (13.33%)	1.13, 1 (1-2)
	Gojeb (GJ)	Duffy-Positive	62	0.04*	19 (30.65%)	1.44, 1 (1-2)
		Duffy-Negative	4	0.26*	0	1, 1 (1)
	Jimma (JM)	Duffy-Positive	32	0.07*	4 (12.5%)	1.18, 1, (1-3)
		Duffy-Negative	64	0.03*	11 (17.19%)	1.21, 1 (1-2)
	<b>Total</b>	<b>Duffy-Positive</b>	<b>150</b>	<b>0.03*</b>	<b>27 (18%)</b>	<b>1.20, 1 (1-3)</b>
		<b>Duffy-Negative</b>	<b>83</b>	<b>0.04*</b>	<b>13 (15.66%)</b>	<b>1.18, 1 (1-2)</b>
Sudan						
	Khartoum (KH)	Duffy-Positive	86	0.25*	5 (5.81%)	1.06, 1 (1-2)
		Duffy-Negative	7	0.77*	0	1, 1 (1)
	New Halfa (HA)	Duffy-Positive	36	0.04*	3 (8.33%)	1.09, 1 (1-2)
		Duffy-Negative	2	N/A	1 (50%)	1.5, 1 (1-2)
	River Nile (RN)	Duffy-Positive	33	0.08*	7 (21.21%)	1.31, 1 (1-3)
		Duffy-Negative	15	0.12*	2 (13.33%)	1.15, 1 (1-2)
	<b>Total</b>	<b>Duffy-Positive</b>	<b>155</b>	<b>0.12*</b>	<b>15 (9.68%)</b>	<b>1.11, 1 (1-3)</b>
		<b>Duffy-Negative</b>	<b>24</b>	<b>0.20*</b>	<b>3 (12.50%)</b>	<b>1.14, 1 (1-2)</b>
	<b>All Sites</b>	<b>Duffy-Positive</b>	<b>305</b>	<b>0.05*</b>	<b>42 (13.77%)</b>	<b>1.16, 1 (1-3)</b>
		<b>Duffy-Negative</b>	<b>107</b>	<b>0.04*</b>	<b>16 (14.95%)</b>	<b>1.17, 1 (1-2)</b>

Table 3. Comparison of genetic diversity based on microsatellite markers in Duffy-negative and Duffy-positive *P. vivax* infections. Statistical tests were performed between Duffy-positive and Duffy-negative individuals of all study sites. Asterisks indicate *p*-values <0.05 that are significant.

Country	Study site	Duffy status	Sample size	Genotypic diversity			Gene diversity	
				<i>G</i>	<i>D</i>	<i>E</i>	<i>N<sub>e</sub></i>	<i>H<sub>e</sub></i>
Ethiopia								
	Arjo	Duffy-positive	56	41	0.94	0.44	8.48	0.87
		Duffy-negative	15	15	0.93	1	5.48	0.85
	Bonga	Duffy-positive	62	35	0.94	0.49	8.07	0.85
		Duffy-negative	4	2	0.38	0.80	1.95	0.65
	Jimma	Duffy-positive	64	40	0.94	0.71	8.47	0.84
		Duffy-negative	32	24	0.91	0.29	7.72	0.88
	Total	Duffy-positive	182	116	0.94	0.55	25	0.85
		Duffy-negative	51	41	0.74	0.70	15	0.79
Sudan								
	Khartoum	Duffy-positive	86	39	0.86	0.27	5.65	0.81
		Duffy-negative	7	3	0.57	1	2.20	0.63
	New Halfa	Duffy-positive	36	22	0.83	0.27	8.00	0.88
		Duffy-negative	2	1	0	1	1.13	0.13
	River Nile	Duffy-positive	33	19	0.88	0.43	7.00	0.86
		Duffy-negative	15	6	0.60	0.42	5.82	0.91
	Total	Duffy-positive	155	80	0.86	0.32	20.65	0.85
		Duffy-negative	24	10	0.39	0.81	9.15	0.56
<i>P</i> -value		--	--	0.025*	0.076	0.009*	0.105	

*G*: Number of multilocus genotypes corrected for sample size

*D*: Simpson's diversity index corrected for sample size

*E*: Genotypic evenness

*N<sub>e</sub>*: Number of effective alleles (Nielsen et al. 2003)

*H<sub>e</sub>*: Expected heterozygosity corrected for sample size (Nei 1978)

Table 4. Average genetic relatedness among individuals by site and host Duffy status using the identical-by-descent (IBD) method described in Taylor *et al.* IBD calculates the probability of alleles sampled from two individuals at any loci being identical due to inheritance from a common ancestor rather than by chance. Thus, the average relatedness between two groups provides a measure of genetic similarity that accounts for recombination.

Pairwise IBD of individuals	Arjo	Gojeb	Jimma	Khartoum	New Halfa	River Nile	<b>Average</b>
Duffy - and Duffy -	0.169	0.448	0.164	0.355	1	0.091	<b>0.371<sup>ns</sup></b>
Duffy + and Duffy -	0.125	0.105	0.092	0.143	0.042	0.087	<b>0.099<sup>ns</sup></b>
Duffy + and Duffy +	0.13	0.121	0.116	0.182	0.119	0.128	<b>0.133<sup>ns</sup></b>

\* Only one comparison was made in New Halfa with two Duffy-negative individuals.

ns: not significant at  $P > 0.05$

Table 5. Fit criteria used to rank the resistance surfaces, and the slope and significance of the relationship between resistance and genetic distance for each surface.

<b>Resistance surface</b>	<b>AIC</b>	<b>AICc</b>	<b>Delta AICc</b>	<b>Slope coefficient</b>	<b>p-value</b>
Road Density and Elevation	-75.834	-125.834	0.000	0.011	0.009
Land Cover	-75.665	-102.331	23.503	0.015	0.010
Road Density and Land Cover	-76.988	-101.988	23.846	0.014	0.005
Road Density, Land Cover, and Elevation	-76.965	-100.965	24.869	0.015	0.005
Land Cover and Elevation	-75.413	-100.413	25.422	0.015	0.011
Null	-71.127	-74.127	51.707	NA	NA
Distance	-73.208	-73.208	52.626	0.006	0.028
Elevation	-75.770	-35.770	90.064	0.011	0.009
Road Density	-73.887	-33.887	91.948	0.007	0.021

## 3.5 Figures

Figure 1. Study sites with *P. vivax* incidence heatmap for reference. Each point corresponds to one of the six sample locations, and the gray lines represent the borders of Ethiopia and Sudan. The incidence layer was modeled by Battle *et al.* and represents the estimated cases per 1000 people in 2017.

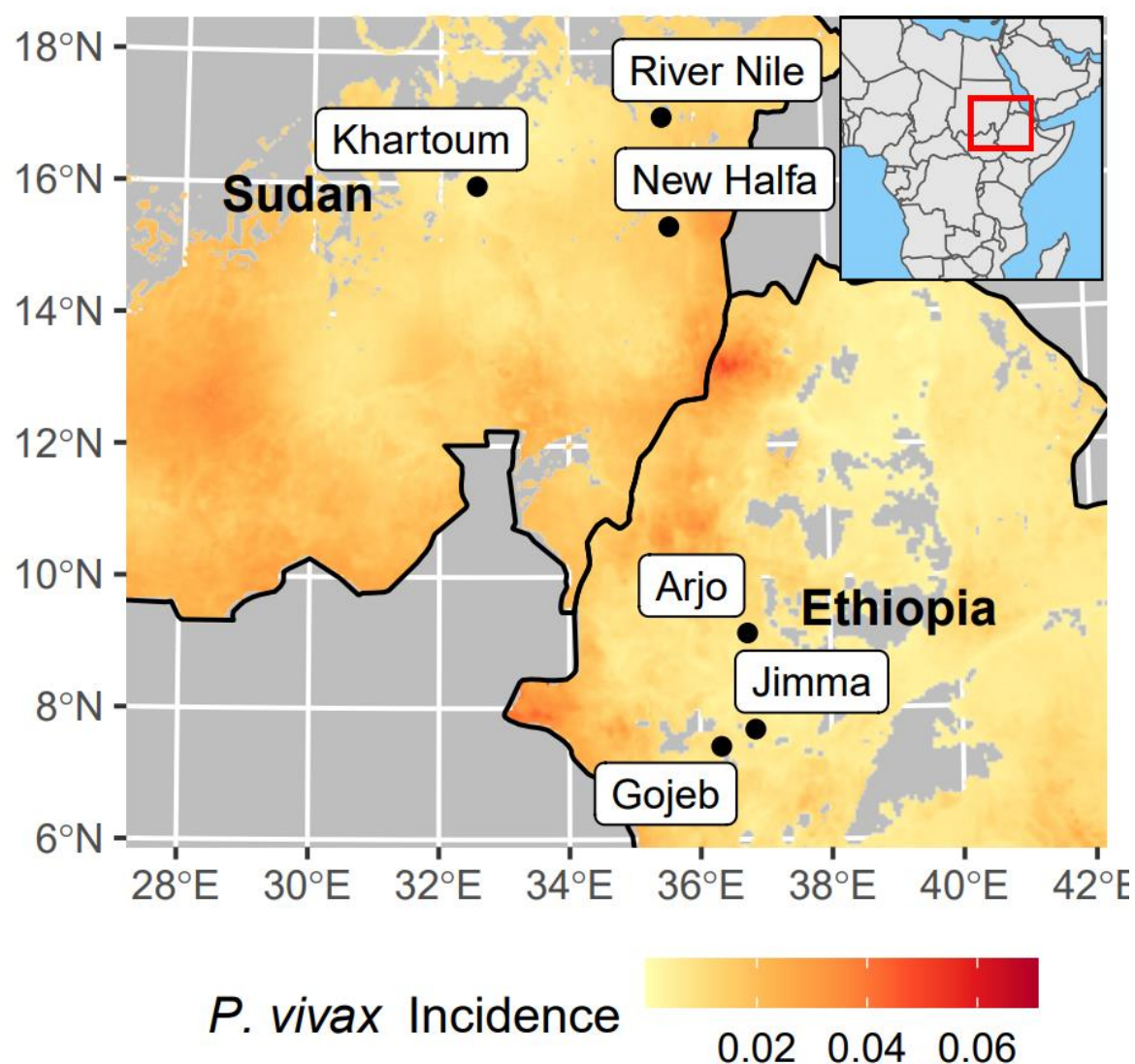


Figure 2. Bayesian inferences of the  $K$  cluster estimated by STRUCTURE for the *P. vivax* samples, according to host Duffy status and location. The most probable clusters are labeled by different colors, and individuals are represented as columns.

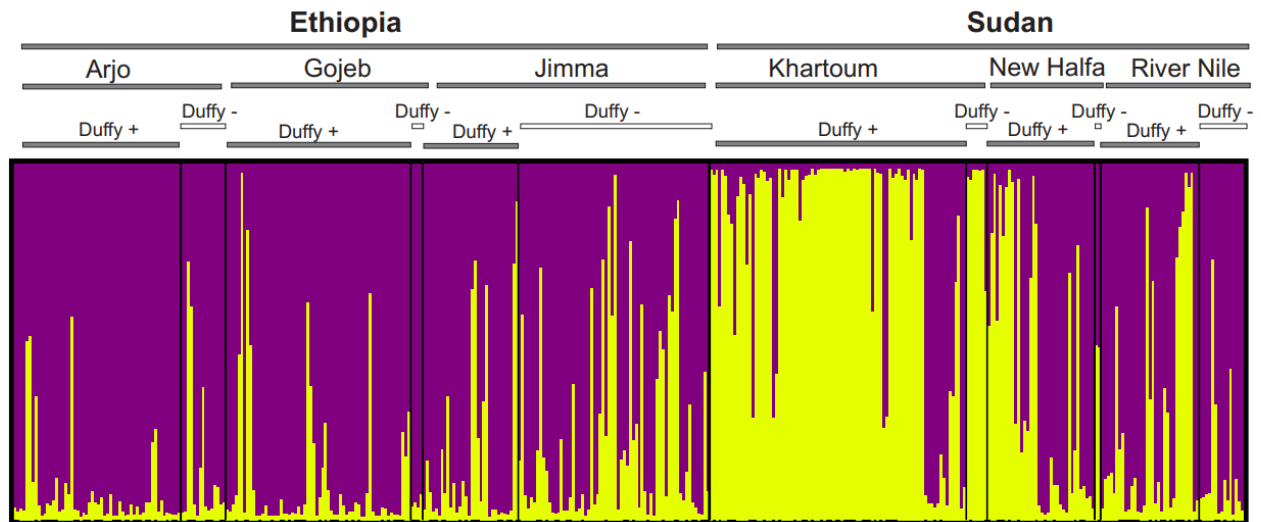


Figure 3. Results of DAPC analyses showing the first two principal components of the data grouped by site and host Duffy status. Dots are individuals, and clusters are identified by symbol color, symbol shape, and inertia ellipses. Eigenvalues are shown in the inset.

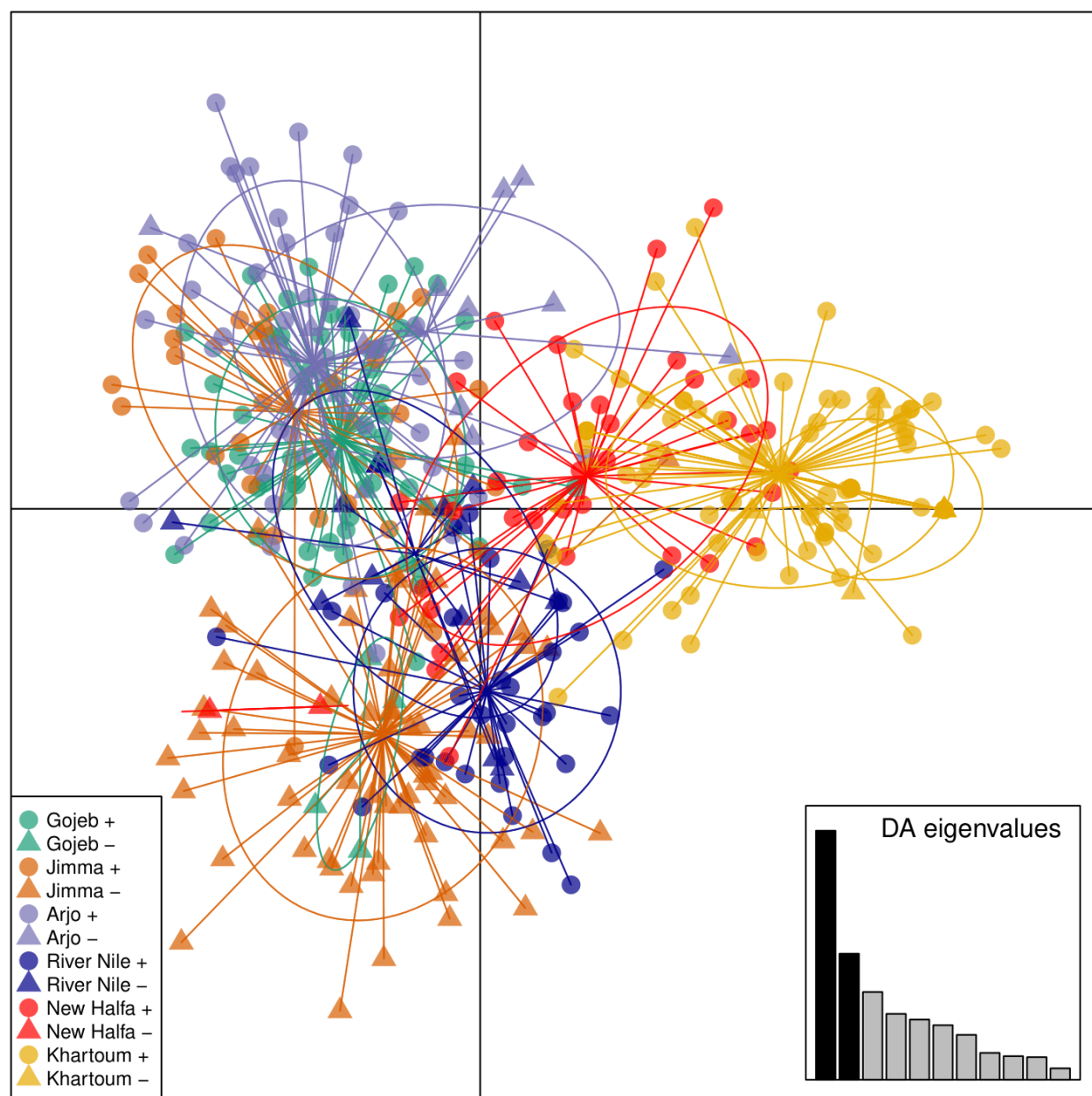


Figure 4. Bayesian inferences of the  $K$  cluster estimated by STRUCTURE for the *P. vivax* samples, according to host Duffy status and country. The three most probable clusters are labeled by different colors and individuals are represented by columns.

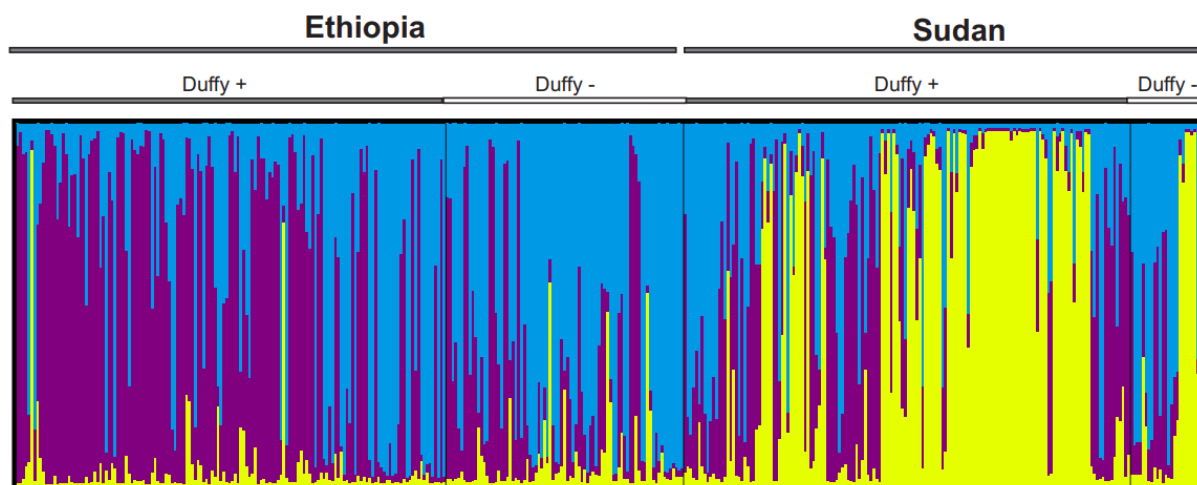




Figure 5. (A) Genetic relatedness among *P. vivax* populations with a large sample size (i.e., *P. vivax* from Duffy-negatives at sites GJ, NH, and KH was excluded) organized by country of origin, shown by color, and host Duffy status, shown by shape. The tree had relatively short internodes with long terminal branches, suggesting the parasite lineages rapidly diverged from one another. (B) Two-dimensional MDS of genetic distance between the same populations (i.e., *P. vivax* from Duffy-negatives at sites GJ, NH, and KH was excluded). Not all Duffy-positive and Duffy-negative infections from the same area were clustered together. No clear distinction was detected among samples from Duffy-positives or Duffy-negatives. (C) Due to the low sample size of Duffy-negative infections in sites GJ, NH, and KH that may skew branch length and the observed clustering pattern, a phylogenetic tree was constructed without these three populations. Similar genetic relationships were observed. (D) The MDS results with reduced Duffy-negative populations mirrored the tree clustering patterns, showing no clear distinction among samples by Duffy status or country.

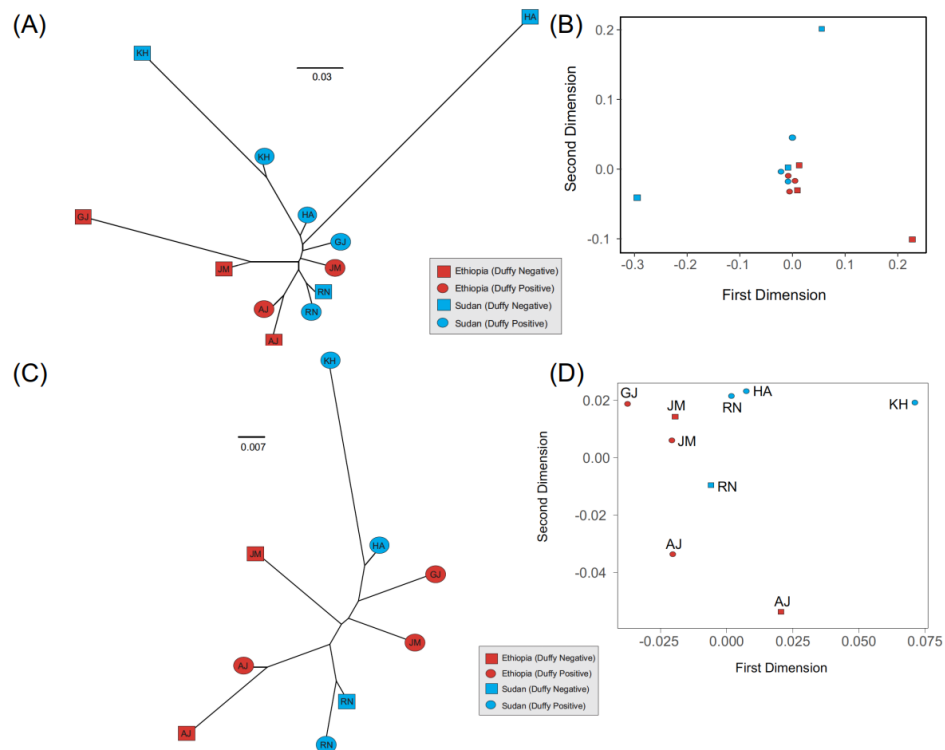


Figure 6. Source Hub Ratio (SHR) networks generated from (A) samples grouped by country and host Duffy status and (B) samples grouped by site. The size of each node is proportional to the node's SHR value. Node colors were randomly assigned to each unique SHR value present in the plot to improve readability. Similarly, arrow colors are paired with the color of the node from which they begin to aid with interpretation. The weight of each arrow is proportional to the number of transitions between those two nodes. The position of nodes is arbitrary and is not equivalent to the position of sample sites in geographic space.

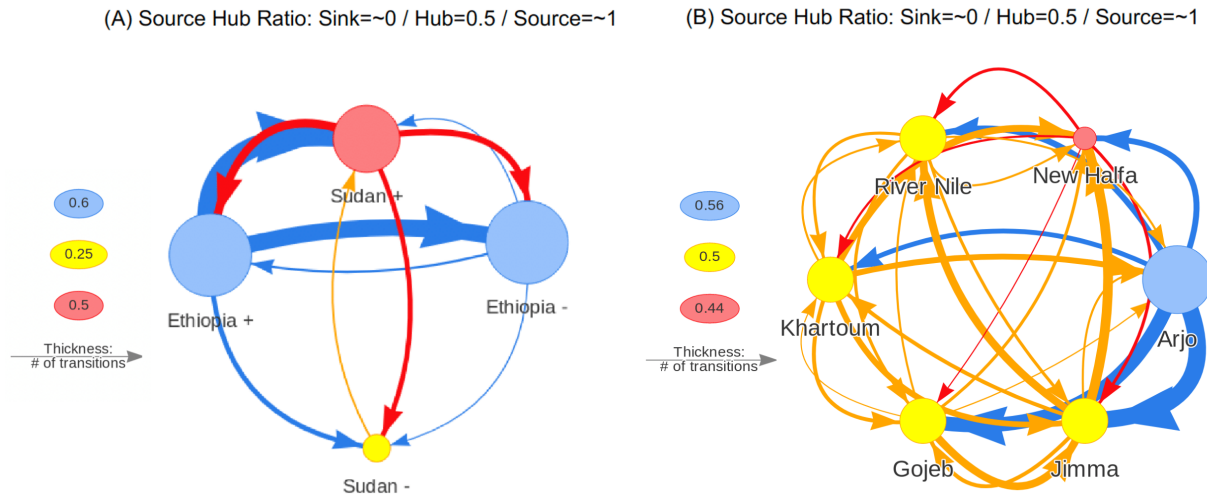
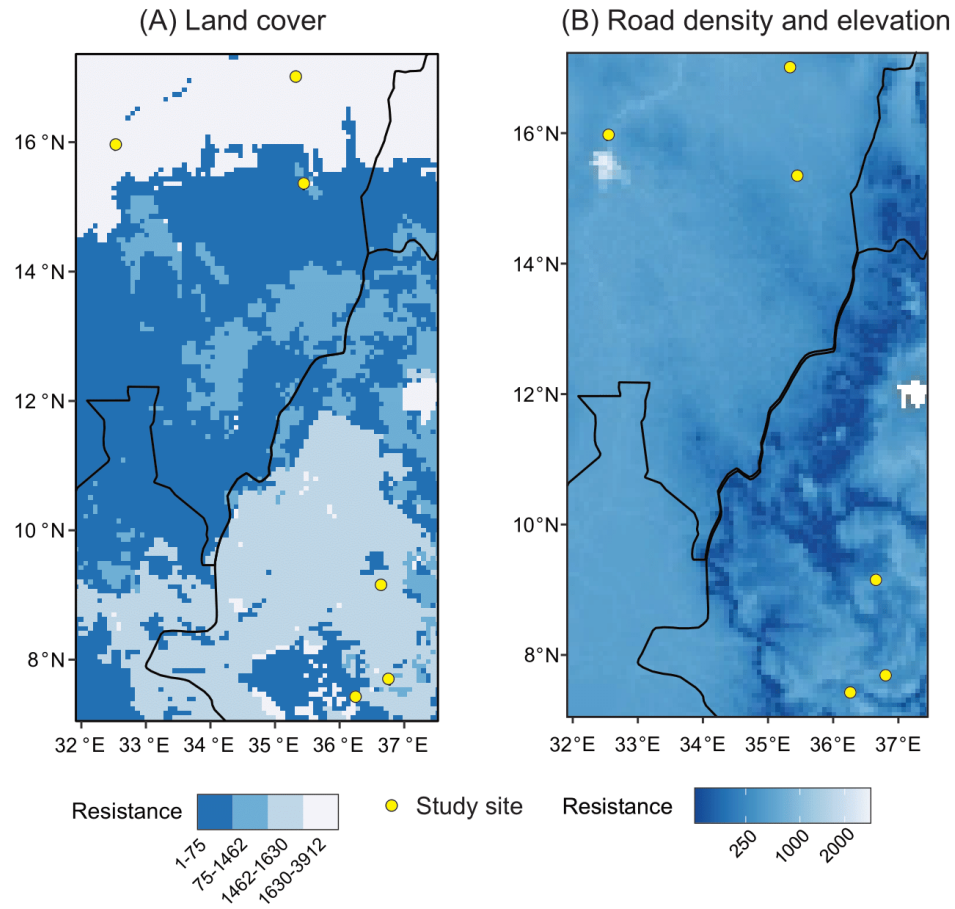


Figure 7. Resistance surfaces fit to genetic distances based on (A) land cover alone and (B) a combination of road density and elevation. Higher values indicate greater obstruction to gene flow. Study sites are denoted by points, and the lines indicate the borders of Ethiopia and Sudan.



## Chapter 4: East African *Plasmodium vivax* transcriptomes reveal differences in gene expression profiles related to erythrocyte invasion and gametocyte detection from other geographical isolates

### 4.1 Rationale

*Plasmodium vivax* is closely related to a large clade of malaria parasites that infect lesser apes and ceropithecoids (old world monkeys) of Southeast Asia (215, 216). The exact origin of human *P. vivax* is still heavily debated, with evidence of *P. vivax* originating in Africa (215) and in Asia (217, 218) both being supported. The first reference genome of *P. vivax* was Salvador I, isolated from *Saimiri boliviensis* monkeys in El Salvador in 2008 (110), followed by the P01 genome isolated from a *P. vivax* patient in Indonesia in 2016 (219). The *P. vivax* nuclear genome is 29 megabases with a 39.8% G-C composition and 6,642 genes distributed amongst 14 chromosomes (219). Several large gene subfamilies have been identified in the P01 genome, including the most abundant *Plasmodium* interspersed repeat (*pir*) genes in the subtelomeric region, followed by unclassified *Plasmodium* exported proteins and tryptophan-rich antigen proteins (219). Remarkably, across the genome, approximately 77% of genes are orthologous between *P. falciparum*, *P. knowlesi*, and *P. yoelii* (110). Genes involved in key metabolic pathways, housekeeping functions, and membrane transporters are highly conserved between *P. vivax* and *P. falciparum* (110). However, *P. vivax* isolates from Africa, Southeast Asia, South America, and Pacific Oceania have significantly higher nucleotide diversity at the genome level compared to *P. falciparum* (20, 24), likely due to variations in transmission intensity, frequency of gene flow via human movement, age of host-pathogen interactions, and host susceptibility (21).

Recent advance in short-term *in vitro* culturing and schizont-enrichment methodologies have enabled transcriptomic sequencing of *P. vivax* enabling a comprehensive review of stage-specific gene expression profile and structure, of which thousands of splices and unannotated untranslated regions were characterized (220). The transcriptomes of Cambodian (52) and Brazilian (194) *P. vivax* field isolates showed high expression levels and large populational variation amongst host-interaction transcripts. For example, the MSP1 gene family was highly upregulated in the Cambodian *P. vivax* compared to the Brazilian ones. Similar trends were also observed in *PvDBP1*, *PvEBP*, *PvMA*, *PvRA*, *PvRBP2a*, *PvMSP5*, and *PvMSP4*, highlighting geographical differences in the gene expression profile. In *P. falciparum*, distinct phenotypic and expression levels of erythrocyte binding antigen (EBA) and reticulocyte binding-like homologue (Rh) gene families were observed among geographical isolates due to varying immunogenic pressures (221). Heterogeneity of gene expression has been documented amongst *P. falciparum*-infected samples, implying that the parasites can modulate the gene transcription process through epigenetic regulation (222). However, the transcriptomic profile of African *P. vivax* remains unexplored, and it is unclear if there is heterogeneity among the continental isolates.

In this study, we aimed to 1) examine the overall gene expression profile of 10 Ethiopian *P. vivax* with respect to different intraerythrocytic lifecycle stages; 2) determine the expression levels of previously characterized erythrocyte binding gene candidates (24); 3) compare gene expression profiles of the Ethiopian *P. vivax* with the Cambodian (52) and Brazilian (194) isolates from *in vitro* especially on the erythrocyte binding. These findings are the first to describe *P. vivax* transcriptomes from East Africa and provide critical insights into parasite ligand proteins that may be involved in a non-Duffy invasion pathway. A systematic

comparison of gene expression profiles among the African, Southeast Asian, and South American isolates will deepen our understanding of *P. vivax* transcriptional machinery and invasion mechanisms.

## 4.2 Results

### 4.2.1 Overview of the Ethiopian *P. vivax* transcriptomes

About 64% (4,404 out of 6,830) genes were detected with transcription in the Ethiopian *P. vivax* genome. Of the 4,404 genes, 69% (2,997) were annotated with known functions and 31% (1,407 genes) remain uncharacterized (Figure 8A). Nearly 52% of the detected genes (2,288 genes) were expressed at a higher threshold of 20 TPM (Figure 8B). We normalized each sample expression profile based on the total number of reads in the sample to TPM to remove technical bias in the sequences and ensure gene expressions were directly comparable within and between samples and isolates. Of the 2,997 genes detected with annotation, 21.7% are responsible for housekeeping, and 14.2% genes responsible for post-translation modifications (PTMs) and regulation. The PIR proteins account for 4.8% (212) of all identified genes processes. About 2.8% of the genes are known to be involved in host-pathogen interaction genes, with genes from the RBP and MSP3 families expressed the highest (Figure 8A). Highly transcribed (TPM>20) transcripts showed similar proportions in gene categories including unknown, PTM/regulatory, DNA regulation, replication/elongation, host interaction, cell signaling, and resistance. Only transcripts involved in transport and housekeeping showed a slight increase of 2.9% and 1.48%, respectively, indicating a higher activity relative to the other categories. By contrast, transcripts involved in RNA regulation, PIR, and ribosomal activity

showed a slight decrease of 2.19%, 1.79%, and 1.71%, indicating an overall lower activity compared to other categories (Figure 8B).

#### 4.2.2 Top 30 transcripts of Ethiopian *P. vivax*

Based on deconvolution, all 10 Ethiopian *P. vivax* samples were majority troph and schizont stage, with nine out of 10 being roughly 50% schizont (Figure 9). Schizont proportions were not statistically different between deconvolution and microscopy (Figure 10). Only less than 1% belong to the ring stage and thus were not included. Overall, four genes including PVP01\_1000200 (PIR protein), PVP01\_0202900 (18s rRNA), PVP01\_0319600 (RNA-binding protein), and PVP01\_0319500 (unknown function) were shown to be most highly expressed among the others (Figure 11). Transcripts involved in housekeeping and PTM regulation each account for 23.3% (7/30) of the top 30 highly expressed genes. Among genes involved in host-interactions, PVP01\_0715400 (merozoite organizing protein), PVP01\_0816800 (protein RIPR), PVP01\_1402400 (reticulocyte binding protein 2a), and PVP01\_1469400 (reticulocyte binding protein 3) are highly expressed. For the 10 Ethiopian *P. vivax* transcriptomes, five gene transcripts including PVP01\_1000200 from the PIR family, PVP01\_0319500 of unknown function, PVP01\_0202900 a 18S rRNA, PVP01\_1329600 a putative glutathione S-transferase, and PVP01\_0418800 a putative pentafunctional AROM polypeptide showed most variable expression, with a standard deviation of 20,000 and higher CPM (Figure 11). Three other genes including PVP01\_0202700 (28S ribosomal RNA), PVP01\_1137600 (basal complex transmembrane protein 1), PVP01\_1243600 (replication factor C subunit 3) showed moderate variation ranging from 1,397 to 1,033 CPM. All other genes such as PVP01\_1206500 (elongation factor Tu) and PVP01\_1011500 (an unclassified protein) showed consistent expression level with variation under 1,000 CPM among samples (Figure 11).

#### 4.2.3 Differentially expressed genes among continental *P. vivax*

The overall gene expression profile was similar between the Ethiopian and Cambodian *P. vivax*, but different from the Brazilian ones (Figure 12A). Several genes involved in DNA regulation, host-interactions, replication, ribosomal, and transportation were upregulated in the Ethiopian and Cambodian isolates but showed considerable downregulation in Brazilian ones. Based on the Kenward-Roger DE analyses, a total of 1,831 differentially expressed genes were detected between the Cambodian and Brazilian isolates (CvB), 1,716 between the Ethiopian and Brazilian (EvB), and 721 between the Ethiopian and Cambodian (EvC) isolates (Figure 12B-D). The EvC analysis showed the lowest differentiation with only 10.6% of the entire transcriptome (Figure 12B), while EvB (Figure 12C) and CvB (Figure 12D) showed a greater differentiation of 25.1% and 26.8%, respectively. For the 721 genes that were differentially expressed between the Cambodian and Ethiopian *P. vivax*, nearly half of them were significantly upregulated in Ethiopia compared to Cambodia (Figure 12B). Four genes including PVP01\_0208700 (V-type proton ATPase subunit C), PVP01\_0102800 (chitinase), PVP01\_0404000 (PIR protein), and PVP01\_0808300 (zinc finger (CCCH type protein) showed significant levels of downregulation ( $\log_{10}P$ -value  $> 50$ ; Figure 12B) compared to other DE genes; two genes including PVP01\_1329600 (glutathione S-transferase) and PVP01\_MIT03400 (cytochrome b) were shown to be overexpressed ( $\log_2$ fold change  $> 10$ ) in comparison. For the 1,716 genes that were differentially expressed between the Ethiopian and Brazilian *P. vivax*, 914 of them were significantly upregulated, slightly higher than those downregulated ones (Figure 12C). Of these, three genes including PVP01\_1412800 (M1-family alanyl aminopeptidase), PVP01\_0723900 (protein phosphatase-beta), and PVP01\_0504500 (28S ribosomal RNA) showed a  $\log_{10}P$ -value greater than 75, indicating substantial expressional differences. For the 1,831 genes that were



differentially expressed between the Cambodian and Brazilian *P. vivax*, 948 of them were significantly upregulated, higher than the downregulated ones (Figure 12D). Four genes including PVP01\_1005900 (ATP-dependent RNA helicase DDX41), PVP01\_0318700 (tRNA<sup>His</sup> guanylyltransferase), PVP01\_1334600 (60S ribosomal protein L10), and PVP01\_1125300 (SURP domain-containing protein) showed substantial expressional differences with  $\log_{10}P$ -value greater than 75. Two genes, PVP01\_0010550 (28S ribosomal RNA) and PVP01\_0422600 (early transcribed membrane protein), were shown to be highly downregulated ( $\log_{10}$ fold change > -12) while one gene PVP01\_0901000 (PIR protein) showed substantial upregulation ( $\log_{10}$ fold change > 12). These comparisons further demonstrated the differences in transcriptional patterns between the Old and New World *P. vivax*.

#### 4.2.4 Expression of genes related to erythrocyte invasion

Of the 43 genes associated with erythrocyte binding function, *PvDBP1* on average showed about 10-fold higher expression than *PvEBP/DBP2* in the Ethiopian *P. vivax*, which failed to be expressed in four samples (Figure 13). *PvRBP2b* showed four-fold higher expression than *PvEBP/DBP2*, but 50% less than *PvDBP1*. *PvRBP2a* showed consistently the highest expression across all samples, with about 6-fold, 67-fold, and 15-fold higher expression than *PvDBP1*, *PvEBP/DBP2*, and *PvRBP2b*, respectively. Other genes including *PvMSP3.8*, *PvTRAg14*, and *PvTRAg22* also showed higher expression than *PvDBP1*. Of the 15 *PvTRAg* genes, only *PvTRAg14* and *PvTRAg22* showed expression higher than *PvDBP1*; *PvTRAg23* and *PvTRAg24* showed the lowest expression. Other putatively functional ligands including *PvRA* and *PvRON4* showed 7-10 times lower expression compared to *PvDBP1*, though *PvGAMA*, *PvRhoph3*, *PvAMA1*, and *PvRON2* were expressed higher than *PvEBP/DBP2*.

We further compared the expressional pattern of these 43 genes in the Ethiopian *P. vivax* with the Cambodian and Brazilian isolates (Figure 14). Members of the *PvDBP* and *PvRBP* gene family showed generally higher expression in the Cambodian *P. vivax* than the other isolates (Figure 14A). For instance, the expression of *PvDBP1*, *PvRBP1a*, and *PvRBP1b* were significantly higher in the Cambodian isolates ( $P<0.01$ ), whereas *PvRBP2a* and *PvRBP2b* in the Ethiopian *P. vivax* showed higher expression than the others. Compared to the *PvDBP1*, *PvEBP*, and *PvRBP* gene family, the expression patterns of the MSP family were different (Figure 13B). Most of the *MSP* gene members including *PvMSP3.5*, *PvMSP3.11*, and *PvMSP4* showed substantially higher expression in the Brazilian *P. vivax* than the other isolates ( $P>0.01$ ). Only *PvMSP3.8* of the 12 *PvMSP* genes was expressed significantly higher in the Ethiopian than the others ( $P>0.01$ ; Figure 14B). Of the 16 *PvTRAg* genes, *PvTRAg14* and *PvTRAg22* showed significantly higher expression in the Ethiopian isolates compared to the others ( $P>0.05$ ; Figure 14C). Eight other members including *PvTRAg2b*, *PvTRAg7*, *PvTRAg19*, *PvTRAg20*, *PvTRAg21*, *PvTRAg23*, *PvTRAg24*, and *PvTRAg38* showed significantly higher expression in the Brazilian isolates than the others ( $P<0.05$ ; Figure 14C). The remaining nine putatively functional ligands showed relatively similar expression levels, except *PvMA*, *PvRhopH3*, and *PvTrx-mero* that were highly expressed in the Brazilian isolates ( $P<0.05$ ; Figure 14D).

### 4.3 Discussion

Approximately 32% of all detected transcripts are of unknown function, of which some of these such as PVP01\_0319500, PVP01\_1011500, and PVP01\_1228800 were among the highest expressed. It is not surprising to see 23% of the highly expressed transcripts belong to housekeeping function, such as several zinc fingers and ATP-synthase proteins. However, there is also a large number of highly expressed protein regulators and PTMs that have not been thoroughly examined. For example, PVP01\_1444000, a ubiquitin-activating enzyme, was among the highest expressed transcripts but with no recorded function. Several other protein kinases, lysophospholipases, and chaperones were highly expressed but their role in intercellular signaling pathways is unclear. It is worth noting that a greater proportion of transcripts responsible for ribosomal protein production were upregulated (TPM > 20) than other gene categories, likely from increased production due to merozoite development in the schizont cultures.

Four genes involved in host interactions, two of which belong to the RBP family *PvRBP2a* and *PvRBP3*, were among the top 30 highly expressed gene transcripts. In addition, *PvRBP1a*, *PvRBP2e*, *PvRBP2a* and *PvRBP2b* were also found to be consistently highly expressed (TPM > 40) across the Ethiopian and Cambodian but not the Brazilian isolates, indicative of potential functional differences in erythrocyte invasion. Recent studies showed that the binding regions of *PvRBP1a* and *PvRBP1b* are homologous to that of *PfRh4*, and the amino acids at site ~339-599 were confirmed to interact with human reticulocytes (113). Though the host receptors of both *PvRBP1a* and *PvRBP1b* proteins are unclear, their receptors have been shown to be neuraminidase resistant (82). Recently, transferrin receptor 1 (TfR1) has been identified as the receptor for *PvRBP2b* and the *PvRBP2b-TfR1* interaction plays a critical role in

reticulocyte invasion in Duffy-positive infections (116). *PvRBP2d*, *PvRBP2e*, and *PvRBP3* are pseudogenes that share homology with other *PvRBPs* but encode for nonfunctional proteins (117). The extent to which of these *PvRBP* genes involve, if any, in erythrocyte invasion remains unclear and requires further functional assays with a larger sample size. The expressional differences in *PvRBP* genes in Ethiopia could be due to a greater proportion of individuals having low levels of Duffy expression (i.e., Duffy-negatives) (14), where *P. vivax* can infect and adapt to both Duffy-positive and Duffy-negative populations (223); whereas in Cambodia and the inland regions of Brazil populations are predominantly Duffy-positive (14). Given that *P. falciparum* can modulate gene expression in response to their hosts through epigenetic regulation (52, 222), higher *PvRBP* expression in the Ethiopian *P. vivax* could be a response to the host Duffy phenotype, though this has not been studied in *P. vivax*. Further investigation on the expression and binding affinity of these *PvRBP* genes with varying expression levels of Duffy is needed for validation.

Another invasion protein, RPR, was also among the highly expressed transcripts. RPR is currently known as a vaccine target in *P. falciparum* (224), where RPR (PfRH5) binds to the erythrocyte receptor basigin (85, 86). The PfRh5 complex is composed of PfRh5, Rpr, CyRPA, and Pf113, which collectively promote successful merozoite invasion of erythrocytes by binding to basigin (BSG, CD147) (84, 85). A BSG variant on erythrocytes, known as Ok<sup>a</sup>, has been shown to reduce merozoite binding affinities and invasion efficiencies (86), though this has only been reported in individuals of Japanese ancestry (87). Despite the clear role of RPR in *P. falciparum*, *P. vivax* RPR does not seem to bind to BSG (225) and the exact role of RPR and its binding target(s) remains unclear in *P. vivax*.

The KR-DE analysis showed 10-26% variation among the transcriptomes of the three countries, with the Ethiopian and Cambodian *P. vivax* being most similar whereas the Cambodian and Brazilian *P. vivax* most different. Genes that showed the highest levels of variation among all countries were those involved in housekeeping, PIR, or ribosomal functions. The exact reason for such differences amongst the continental *P. vivax* remains unclear, though prior studies in *P. falciparum* have shown host nutrition can significantly alter gene expression related to housekeeping, metabolism, replication, and invasion/transmission (226). In addition, malnourishment was shown protective to *P. vivax* subsequent infections in the Western Brazilian Amazon (227). Furthermore, in zebra fish, sex determination can cause significant expressional differences in the housekeeping genes (228), suggesting that sexual development factors may also alter expression profiles.

*P. vivax* PIR genes support a wide range of functions, including antigenic variation, immune evasion, sequestration, and adhesion (229, 230). Gene expression studies suggested their prominent role in virulence and chronic infections. In *P. berghei*, the *pir* transcriptional repertoire is diverse with different members or subfamilies expressed at different time throughout the parasite developmental cycle (231). PIR proteins have been shown to be targeted by antibodies (232). The high expression observed for some PIR proteins, such as PVP01\_1000200, in the Cambodian and Ethiopian *P. vivax* may indicate epigenetic regulation associated with host exposure and immune responses (52, 222). Varying expression of ribosomal proteins, such as PVP01\_0827400 (60S ribosomal protein L26) and PVP01\_1013900 (40S ribosomal protein S9, putative) may be attributed to host nutrition, which is directly proportional to the speed of replication in *P. berghei* (226). Future studies should examine factors associated with the expression of these genes in *P. vivax*.

The deconvolution of stage-specific transcripts from the RNA-seq data was based on the *P. berghei* orthologues due to a lack of single-cell RNA-seq data ring-staged *P. vivax*. To date, *P. berghei* remains the most comprehensively characterized single-cell data for both sexual and asexual blood stages of *Plasmodium* (233, 234). *P. berghei* orthologues have been previously shown to be reliable for determination of stage-specific transcripts (235). In primates, *P. vivax* has been shown to transcribe most genes during a short period in the intraerythrocytic cycle (236) with a high proportion of late-schizont transcripts shown to be expressed as early as the trophozoite stage. In *P. berghei*, the process of gametocyte development and genes involved in sequestration are transcribed much earlier during the trophozoite-schizont transition stage. Furthermore, male gametocyte development precursors are expressed in the asexual stages despite gametocyte development not taking place (237, 238). These factors hinder deconvolution efforts and make it challenging to classify which genes are transcribed in each stage computationally, while the speed of gametocyte development in trophozoites can lead to false negatives when using microscopy (239). Future studies should seek both combinations to eliminate false positives and negatives from stage determination until a reliable species-specific single cell model is available.

## 4.4 Figures

Figure 8. Categorization of (A) all detectable transcripts and (B) upregulated (TPM > 20) transcripts for the Ethiopian *P. vivax* by gene function. The numbers shown represent the number of transcripts along with the overall percentage compared to all detected transcripts. Transcripts that were not detected were removed from the analysis. Only transcripts involved in transport and housekeeping showed a slight increase of 2.9% and 1.48%, respectively in the number of upregulated transcripts, indicating a higher activity relative to the other categories.

By contrast, transcripts involved in RNA regulation, PIR, and ribosomal activity showed a slight decrease of 2.19%, 1.79%, and 1.71%, indicating an overall lower activity compared to other categories.

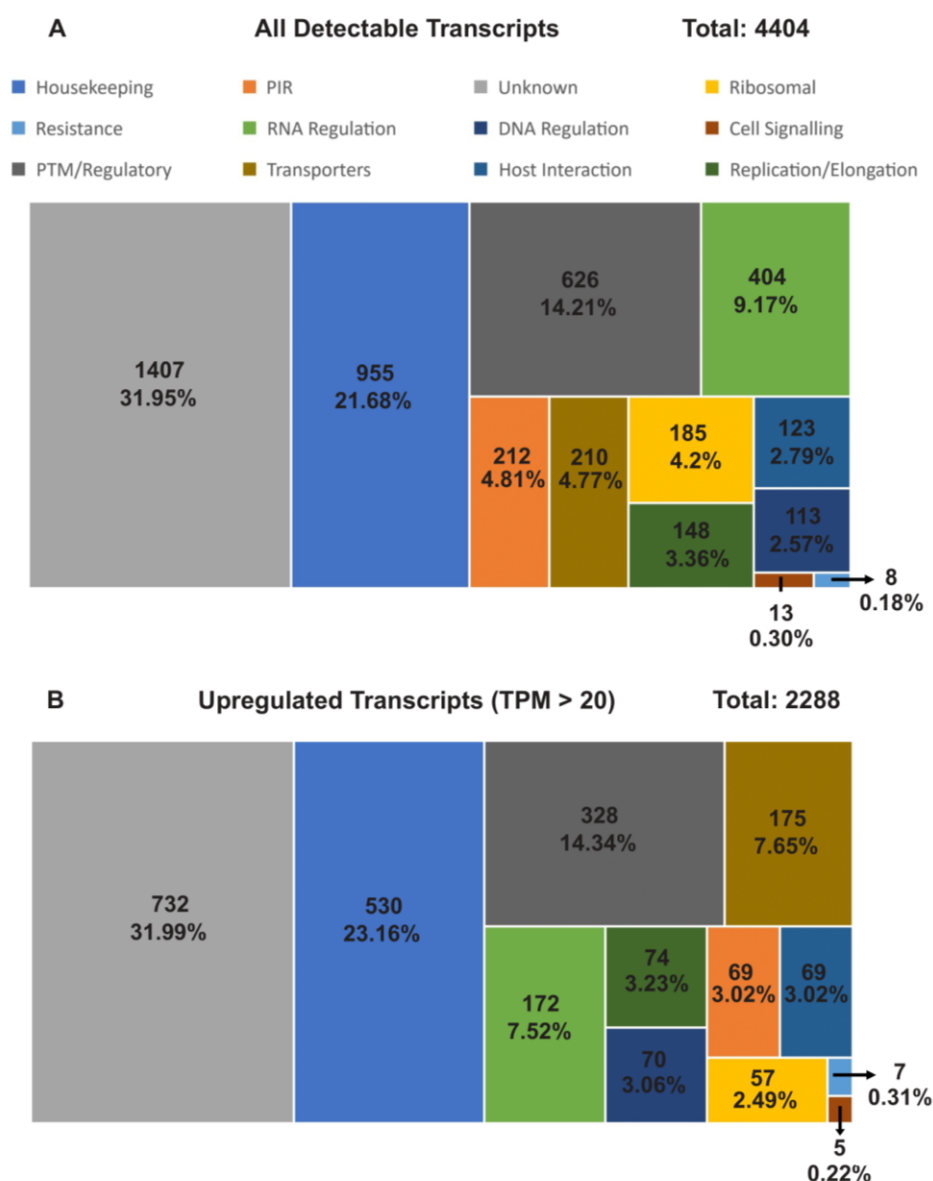


Figure 9. CIBERSORTx deconvolution of the 10 Ethiopian *P. vivax* transcriptomes, the four Cambodian *P. vivax* transcriptomes, and the two Brazilian transcriptomes using a *P. berghei* homologue matrix. No significant difference was observed between the amount of trophozoites or schizonts amongst the isolates ( $P>0.05$ ).

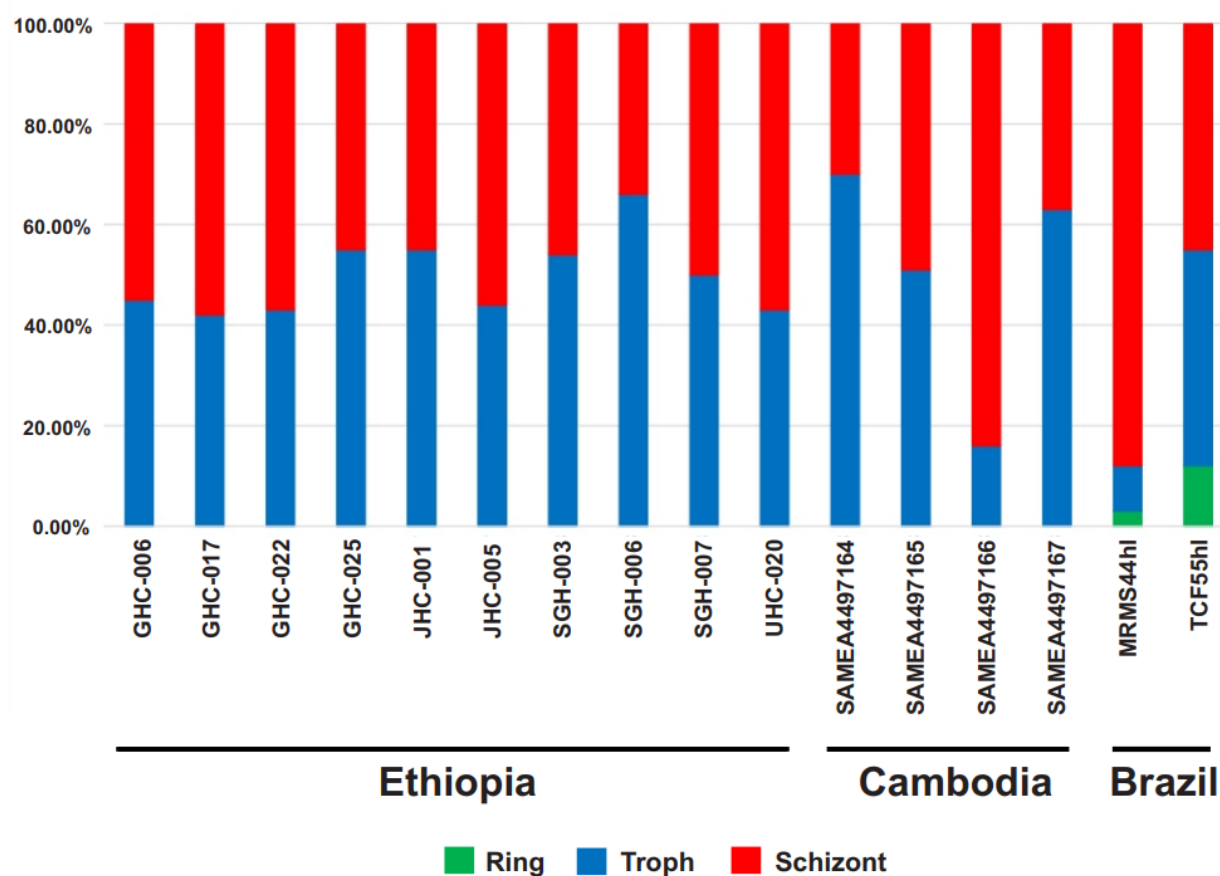




Figure 10. Microscopy analysis of five Ethiopian *P. vivax* samples. No significant difference was observed between microscopy and computational deconvolution ( $P>0.05$ ).

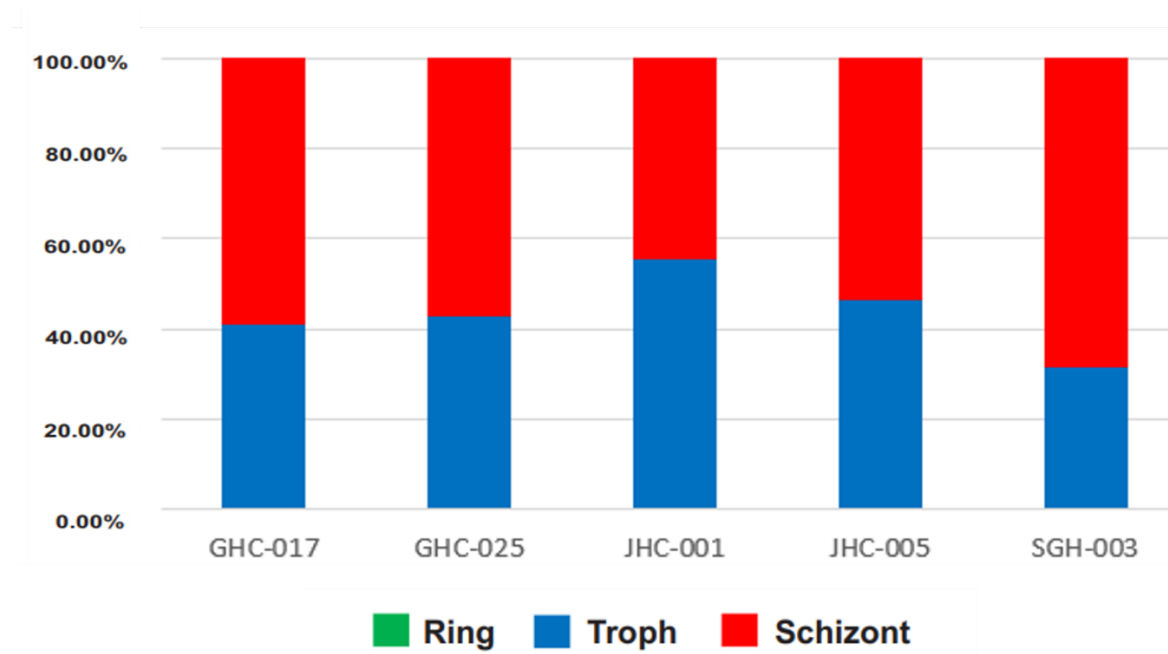


Figure 11. Heat map showing the top 30 highly transcribed genes based on  $\log_2(\text{CPM}+1)$ . Genes are arranged by different functions as indicated on the y-axis. Overall, four genes including PVP01\_1000200 (PIR protein), PVP01\_0202900 (18s rRNA), PVP01\_0319600 (RNA-binding protein), and PVP01\_0319500 (unknown function) from four different functional groups were shown to be most highly expressed among the others. Of interest, PVP01\_0715400 (merozoite organizing protein), PVP01\_0816800 (protein RIPR), PVP01\_1402400 (reticulocyte binding protein 2a), and PVP01\_1469400 (reticulocyte binding protein 3) were among the top 30 highly expressed genes involved in host interactions.

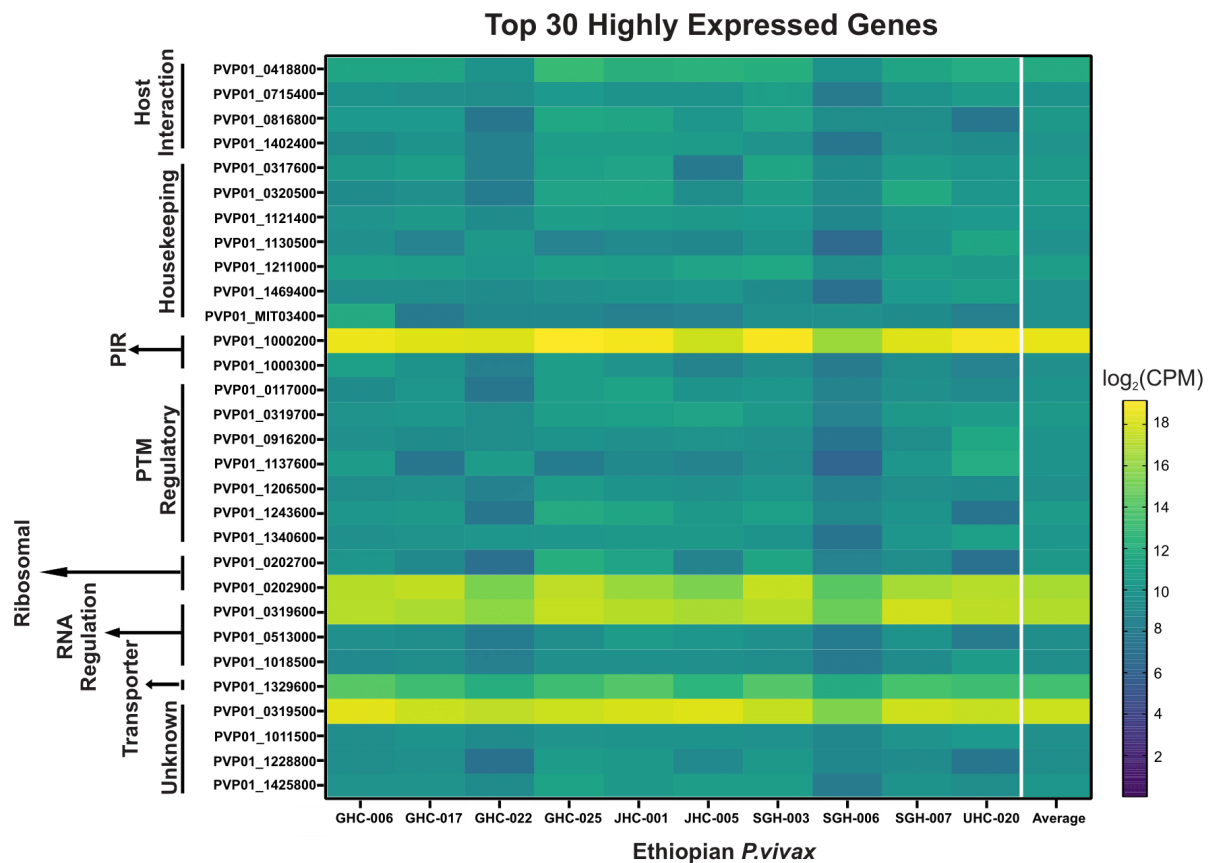
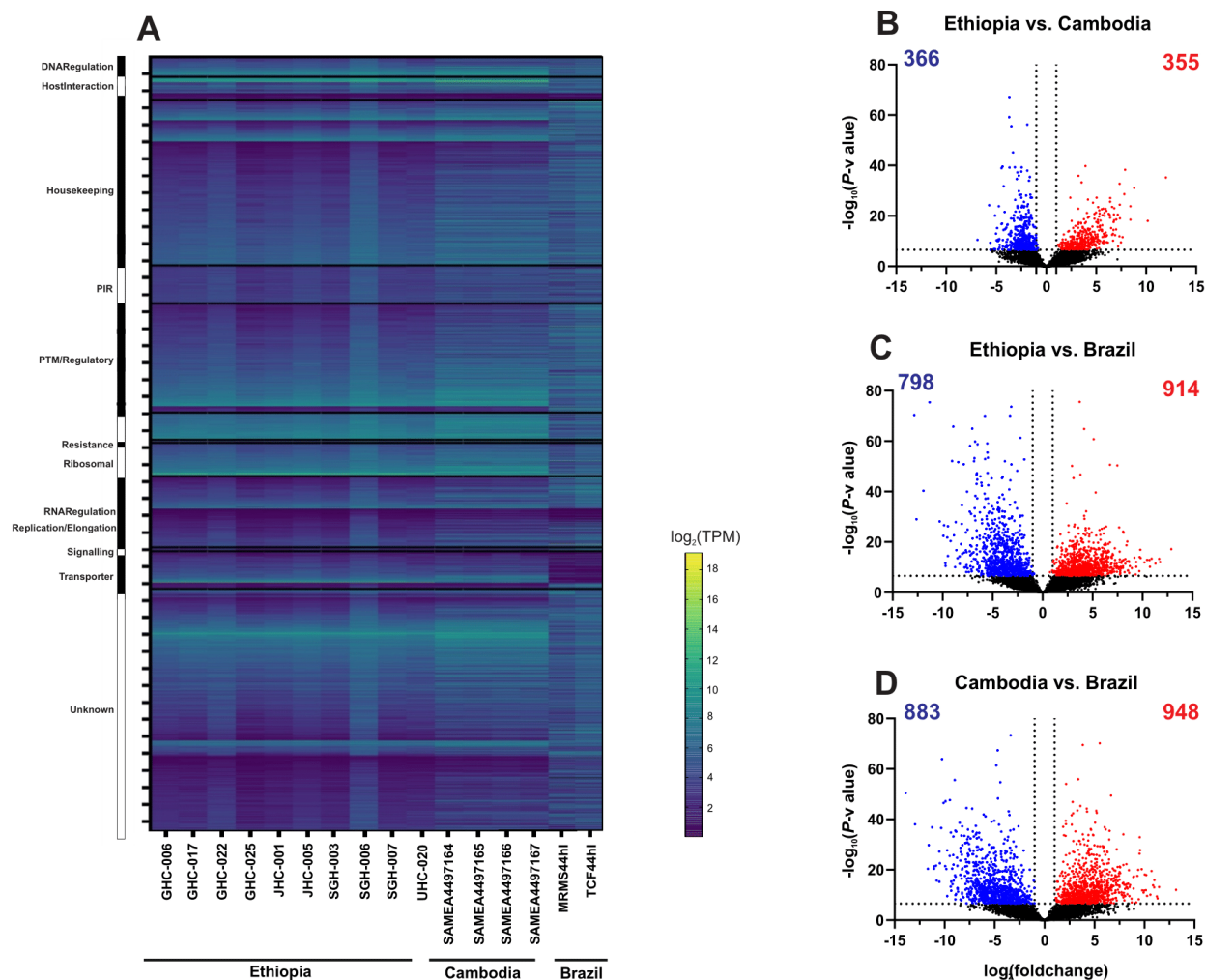


Figure 12. (A) Comparisons of the entire transcriptomes with genes sorted by functionality among the Ethiopian, Cambodian, and Brazilian *P. vivax*. The overall gene expression profile was nearly identical between the Ethiopian and Cambodian *P. vivax*, but different from the Brazilian isolates. Several genes involved in DNA regulation, host-interactions, replication, ribosomal, and transportation were upregulated in the Ethiopian and Cambodian isolates but showed considerable downregulation in Brazilian ones. (B-D) Volcano plots based on the Kenward-Roger DE analyses comparing differentially expressed genes between the (B) Ethiopian and Cambodian; (C) Ethiopian and Brazilian; (D) Cambodian and Brazilian isolates. Blue dots represent single genes that are downregulated in the comparison while red dots represent upregulated genes by comparison. About 10% of the detectable transcripts were differentially expressed between the Ethiopian and Cambodian *P. vivax*, but about 25% and 27% variations were detected between the Ethiopian and Brazilian as well as the Cambodian and Brazilian *P. vivax*, respectively. Overall, the Brazilian isolates had more genes that were upregulated compared to the Ethiopian and Cambodian ones.



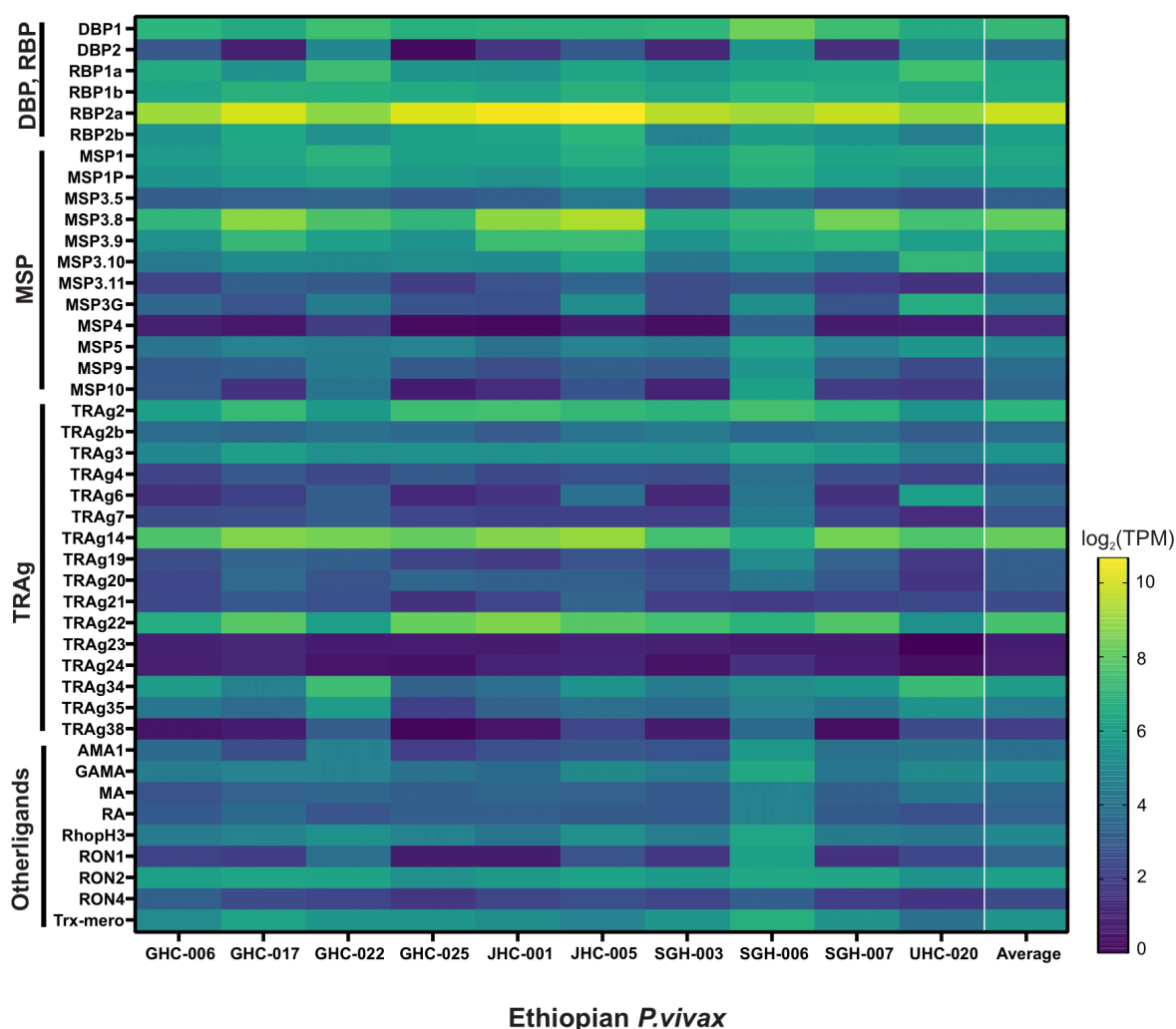
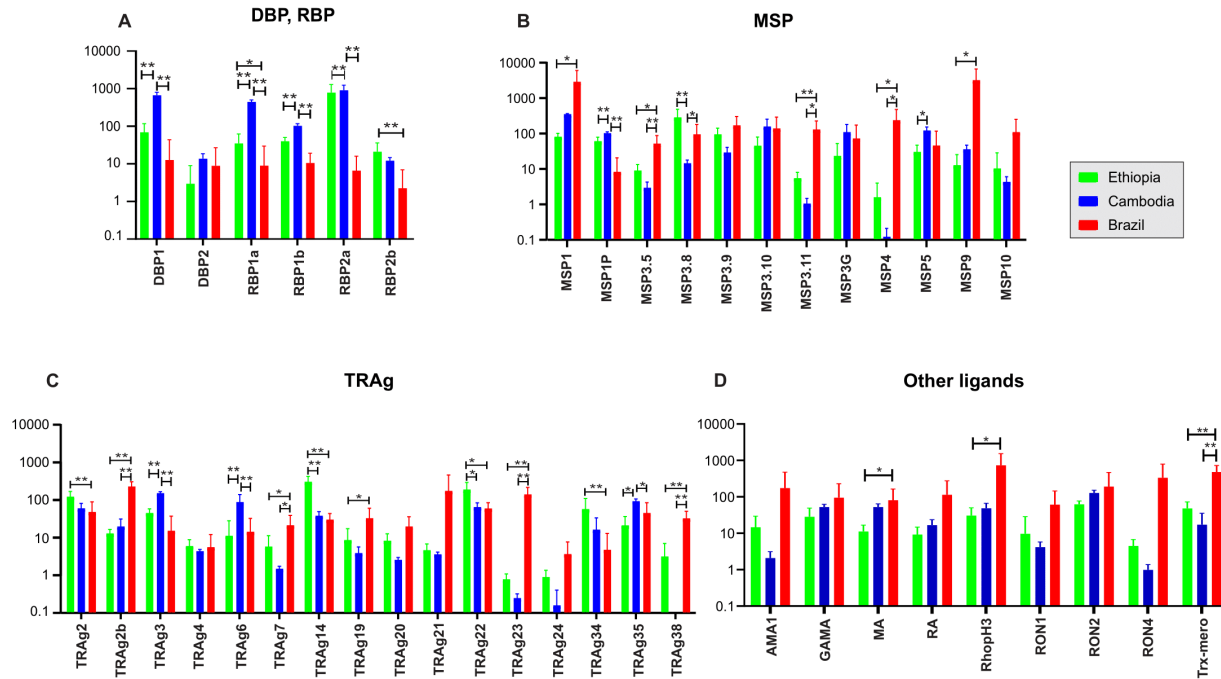


Figure 14. Comparisons of 43 genes associated with erythrocyte binding function based on  $\log(2)\text{TPM}+1$  values across the Ethiopian, Cambodian, and Brazilian *P. vivax* for (A) *PvDBP1*, *PvEBP*, and *PvRBP* genes; (B) *PvMSP* genes; (C) *PvTRAg* genes; (D) other putatively functional ligands. \* denotes  $P$ -value  $> 0.05$ ; \*\* denote  $P$ -value  $> 0.01$ .



## Chapter 5: From Genes to Biomarkers: Understanding The Biology of Malaria Gametocytes and their Detection

### 5.1 Rationale

The lifecycle of *Plasmodium* is divided into two stages: the human asexual reproduction stage (also known as the erythrocytic stage) and the mosquito sexual reproduction stage (known as the sporogonic cycle) (240), both of which are necessary for population growth and genetic diversification (241). The parasite first enters the human body in the form of sporozoites through the infected salivary gland of an *Anopheles* mosquito during a blood meal. Within minutes, sporozoites infect the liver and begin asexual replication to form schizonts (a process called exoerythrocytic schizogony) within a few days to a few weeks (240). Once matured, schizonts burst to release hundreds of merozoites into the blood stream (240). *P. falciparum*, *P. ovale*, *P. malariae*, and *P. simium* infect mature erythrocytes (241-243) while *P. vivax* and *P. knowlesi* infect younger reticulocytes (241, 242, 244-246) to feast on hemoglobin and further reproduce asexually (241, 242). At this stage, the intracellular *Plasmodium* is considered as a ring stage parasite because the young parasite takes up hemoglobin in a single, large vacuole that looks like a ring. Once the hemoglobin is engulfed, the parasite then begins feeding and hemoglobin is acquired by endocytosis of erythrocyte cytoplasm within cytostomes, known as the trophozoite stage. After the hemoglobin is consumed, the trophozoite may either undergo schizogony to asexually reproduce and start the erythrocytic cycle with new merozoites or mature into a macrogametocyte (egg) or microgametocyte (sperm). Because human body temperature is considerably warm for *Plasmodium* sexual reproduction (247), both forms of gametocytes are taken up by an *Anopheles* mosquito where sexual reproduction occurs within the gut of the mosquito producing zygotes. Once matured, the zygote will become mobile and elongated,

developing into ookinete to infect the midgut wall of the mosquito (248) and develop further into oocyst. Oocysts asexually divide and eventually rupture into sporozoites that travel to the salivary gland of the mosquito to infect a new human host (241, 242).

All six human malaria parasites require gametocytes to infect female *Anopheles* mosquito to reproduce sexually and continue development into sporozoites before infecting a new human host (249). This has led to complications in the control of malaria transmission and gametocyte detection (250). Furthermore, *P. vivax* and *P. ovale*'s unique ability to form dormant stage hypnozoites complicates parasite clearance and can reintroduce old parasite strains into transmission reservoirs (241, 242) Gametocytes are critical for malaria transmission and possible immune evasion in both the human and mosquito hosts (192, 251), emphasizing the importance of accurate detection. The current standard for *P. vivax* gametocyte detection involves PCR screening for *Pvs25* and *Pvs16*, which only accounts for female gametocytes; may grossly underestimate true gametocyte load and transmission potential. This research aims to examine the transcriptional activity of 25 previously published *P. vivax* gametocyte genes across three continental isolates. While these genes have a potential to be used for gametocyte detection, it remains unclear if such expressional patterns are similar in other geographical isolates.

## 5.2 Results

### 5.2.1 Sub-microscopic gametocyte densities

Previous study has indicated that approximately 60% of *P. vivax* infections had concurrent detectable low-density gametocytemia (252). Gametocyte densities are directly associated with total asexual parasite densities (Figure 15A) and typically lower than asexual parasite densities (Figure. 15B). Given the relatively low gametocyte densities, it is conceivable



that many of these infections are submicroscopic and remain undetected in communities where malaria occurs, contributing to continuous transmission.

### 5.2.2 Expression of female and male *P. vivax* gametocyte genes

Based on the expression level of AP2-G and *Pvs25* (PvP01\_0616100), all 10 *in vitro* *P. vivax* samples from Ethiopia contained submicroscopic gametocytes, in addition to the four schizont samples from Cambodia and two samples from Brazil (Figure 16). Amongst the gametocyte-positive samples, PVP01\_1403000 (gametocyte associated protein, GAP) and PVP01\_1208000 (*Pvs47*) from female and male gametocytes, respectively, showed the highest expression across Ethiopian, Cambodian, and Brazilian isolates, and were consistently higher than *Pvs25*. This expression pattern suggests the potential utility of these two genes as female and male gametocyte detection biomarkers. The female gametocyte gene PVP01\_0904300 (CPW-WPC family protein) showed consistently high levels of expression in both the Ethiopian and Cambodian isolates, though much lower in the Brazilian ones. This gene was also found to be highly expressed (TPM>100) in both the trophozoite and schizont stages of the Ethiopian isolates (Figure 16). On the other hand, PVP01\_1302200 (high mobility group protein B1) and PVP01\_1262200 (fructose 1,6-bisphosphate aldolase) from the female and male gametocytes showed the highest expression levels in Brazilian *P. vivax* but not the Ethiopian and Cambodian ones, highlighting differential expression patterns between continents.

### 5.3 Discussion

For *P. vivax*, Pvs 25 and Pvs16 that are specific to female gametocytes are two conventional gene markers for gametocyte detection (253). One gametocyte roughly corresponds to 4 Pvs25 transcripts per cell (254), and Pvs25 can detect from a mean of 0.34 gametocytes per  $\mu\text{L}$  blood from *P. vivax* patients in Papua New Guinea (253) to a mean of 2 gametocytes per  $\mu\text{L}$  blood in patients from Ethiopia (252). Such low gametocyte densities make them extremely difficult to be detected by microscopy. The number of Pvs25 gene transcript copies detected by qRT-PCR directly correlates with the number of mature gametocytes as well as the overall parasite densities (255, 256) and was shown a nearly normal distribution with a mean of  $1.2 \times 10^7$  copies/ $\mu\text{L}$  (ranging from  $1.1$  to  $4.8 \times 10^8$  copies/ $\mu\text{L}$ ) blood among 42 symptomatic *P. vivax* patients from northwestern Brazil (257). Prior studies showed that age is tightly associated with gametocytemia. A lower proportion of infections with gametocytes was found with increasing age (254, 258). Gametocytes are generally detected in ~20% of the infections among adults (256), but at much higher proportions in children under the age of 12 (258, 259). Yet, gametocytemia in adults is up to 20-fold higher than in children (260, 261). In areas with low levels of transmission, a large proportion of infections that are undetected by microscopy could be reservoir for parasites with high infectious gametocytes (262). In Ethiopia, symptomatic *P. vivax* infections are nearly four times more infectious than asymptomatic ones (263). Other factors such as host immune response, parasite strains, red blood cell density, antimalarial drug use, and relapse can also affect gametocyte production (254, 264, 265).

Prior studies have demonstrated that low density *P. vivax* gametocytes in asymptomatic carriers significantly contribute to transmission and genetic diversity (266, 267). In areas with low levels of transmission, submicroscopic infections could be hidden reservoirs for parasites

with high proportions of infectious gametocytes (262). *Pvs25* and *Pvs16* only account for female gametocytes, grossly underestimating the total gametocyte densities that include male gametocytes. We previously described two alternative female (PVP01\_0415800 and PVP01\_0904300) and one male (PVP01\_1119500) gametocyte genes that show higher expression than *Pvs25* in the Ethiopian isolates (268). The two female gametocytes genes were moderately expressed (TPM > 10) in the Cambodian and Brazilian isolates, but the male gametocytes gene showed low expression (TPM > 3). In comparison, PVP01\_1403000 of the female gametocytes and PVP01\_1208000 of the male gametocytes were moderately expressed (TPM > 15) across all continental isolates. Further investigations on the polymorphic nature and the utility of these genes as gametocyte biomarkers, as well as their exact role in gametocyte development are needed.

## 5.4 Figures

Figure 15. (A) Comparison of infected red blood cells and gametocytemia among *P. vivax* infections from Ethiopia. (B) Significant correlation was observed between asexual parasitemia and gametocytemia.

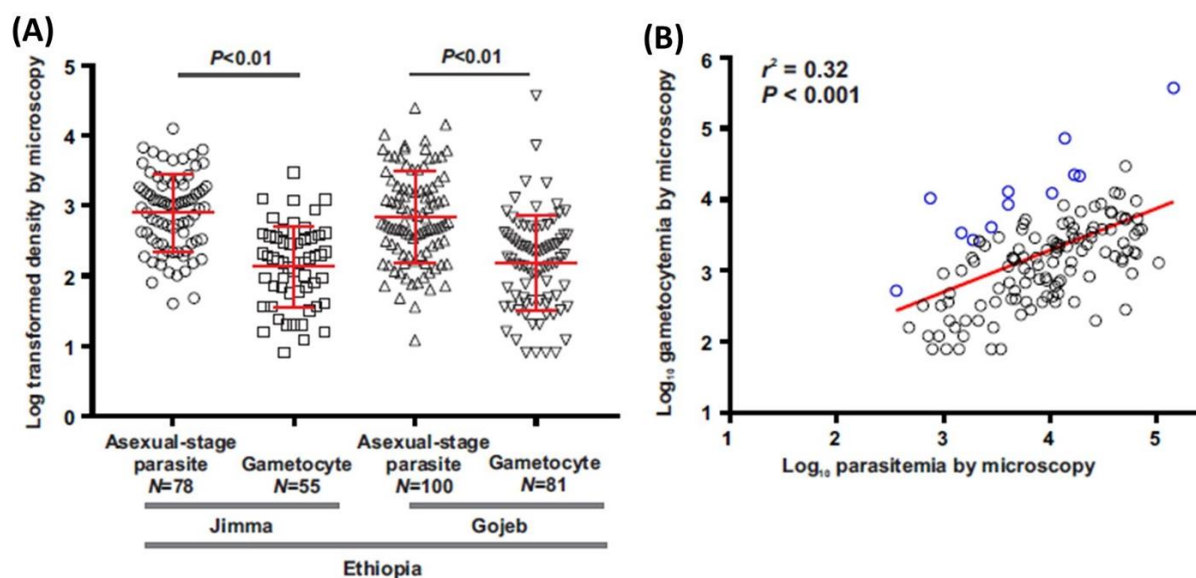
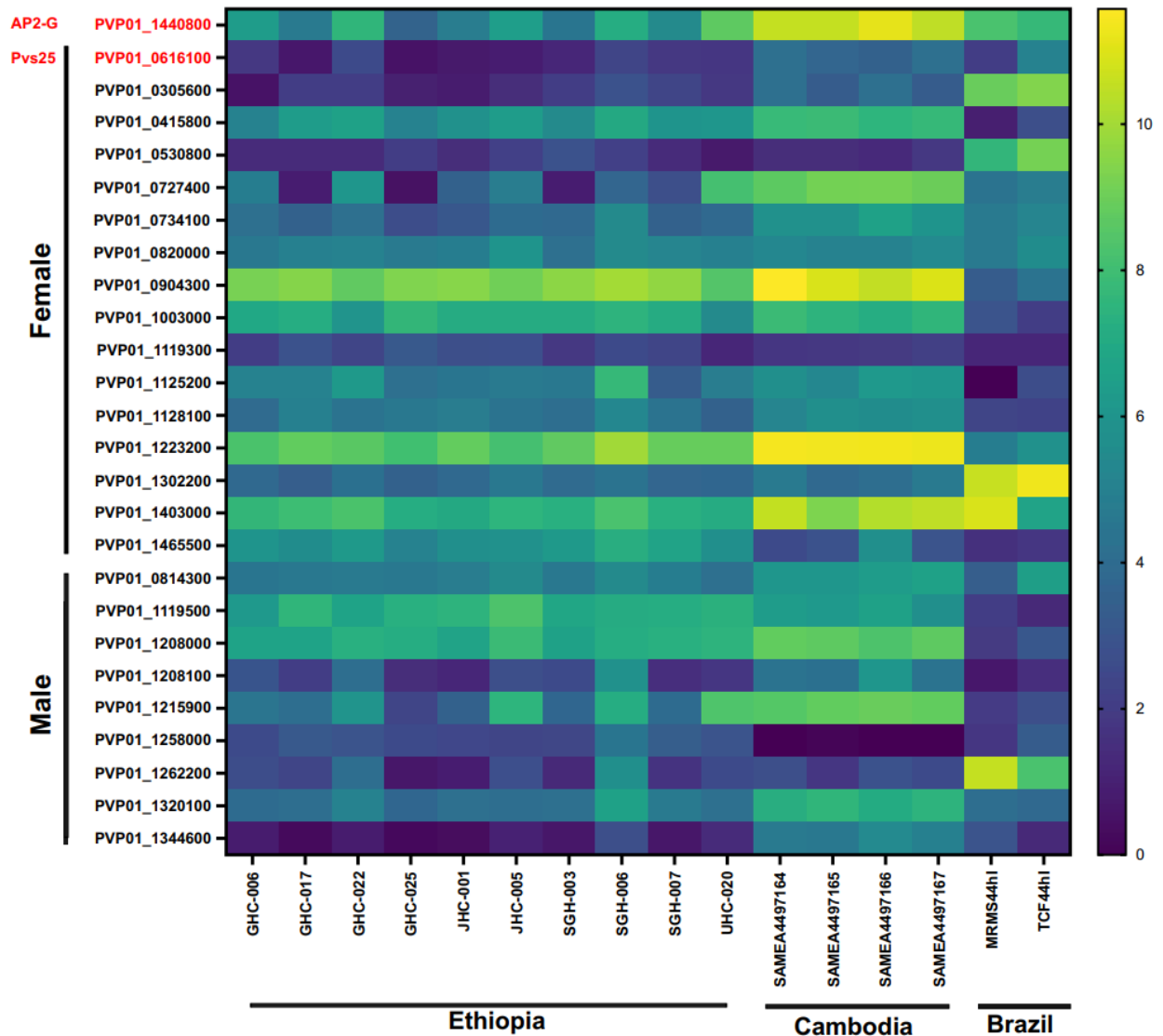


Figure 16. Heatmap comparing 26 *P. vivax* gametocyte biomarker candidates across the Ethiopian, Cambodian, and Brazilian *P. vivax*. Based on the expression level of AP2-G and *Pvs25*, all 10 *in vitro* *P. vivax* samples from Ethiopia contained gametocytes, in addition to all four samples from Cambodia and four samples from Brazil. Two genes, PVP01\_1403000 (gametocyte associated protein, GAP) and PVP01\_1208000 (*Pvs47*) from female and male gametocytes, respectively, showed the highest expression across all continental isolates, and were consistently higher than *Pvs25*.



## Chapter 6: Summary Conclusions

### 6.1 *Plasmodium vivax* from Duffy-Negative and Duffy-Positive Individuals Shares Similar Gene Pool Indicative of Between-Host Transmission

Our study is the first to show that *P. vivax* can transmit to and from Duffy-negative individuals and shed light on the transmission pathways of Duffy-negative *P. vivax* in endemic-regions of East Africa. Apart from the spread of *P. vivax* between Duffy-positive and Duffy-negative hosts, this study also reveals the potential of *P. vivax* to spread through the physical environments in East Africa. This was performed through integrating genetic with landscape data and found that urban environments pose a greater hindrance to the transmission of *P. vivax* than rural and less-developed areas. The generally high genetic diversity of *P. vivax* in most study sites could be related to high transmission and frequent gene flow between Duffy-negative and Duffy-positive individuals as well as across country-border. Future investigations using whole genome sequence data with expanded *P. vivax* samples in East Africa are imperative to confirm these findings. Knowledge of *P. vivax* transmission mechanisms involving gametocyte infectivity experiments and *in vitro* invasion assays in Duffy-negative individuals would bring attention to the need for diagnosing and controlling *P. vivax* in Africa.

## 6.2 East African *Plasmodium vivax* transcriptomes are different in gene expression profiles related to erythrocyte invasion

This study characterized the first *P. vivax* transcriptome from the African field isolates and identified several host-interaction gene transcripts, including *PvRBP2a*, *PvMSP3.8*, *PvTRAg14*, and *PvTRAg22* that were highly expressed compared to *PvDBP1* in Duffy-positive individuals. We further demonstrated 10% to 26% differences in the gene expression profile amongst the continental isolates, with the Ethiopian and Cambodian *P. vivax* being most similar. Furthermore, we compared the expressional pattern of 43 erythrocyte invasion gene candidates and found differential expression amongst the three isolates. Specifically, *PvRBP1a*, *PvRBP2a*, and *PvRBP2b* showed high expression in the Ethiopian *P. vivax*, while *PvTRAg3*, *PvTRAg14*, *PvTRAg22*, and *PvTRAg35* showed high expression in both the Ethiopian and Cambodian isolates. These findings provide an important baseline for future comparisons of *P. vivax* transcriptomes with Duffy-negative infections. Further investigations examining binding affinity and functionality of *P. vivax* ligands, especially *PvRBP2a*, *PvMSP3.8*, *PvTRAg14*, and *PvTRAg22* are imperative to identify Duffy-independent invasion pathways.

### 6.3 Alternative biomarkers for male and female *P. vivax* detection show higher expression compared to *Pvs25* and *Pvs16*

Gametocytogenesis and gametocyte transmission tracking remained largely uncharacterized due to low prevalence and technological hurdles. As several countries approach the elimination phase for malaria, the need for sensitive and reliable biomarkers for gametocyte detection is more urgent than ever. Microscopy has low detection limit to overcome low parasitemia loads and existing qPCR biomarkers fail to accurately detect both sexes of the parasites. Knowledge of gametocyte reservoirs and their interactions with host immune system will help develop effective treatment and preventive strategies to minimize the risk of malaria transmission. we successfully identified one female (PVP01\_1403000) and one male (PVP01\_1208000) gametocyte gene markers showed higher expression than the standard *Pvs25* consistently in all three continental *P. vivax* isolates. These gene markers may provide alternative biomarkers for field *P. vivax* gametocyte detection. Future studies should evaluate the sensitivity and specificity of these biomarkers for female and male gametocyte detection, especially in low parasitemia infections. We also recommend studies focus on gene interactions and protein functions involved in gametocyte development, as well as polymorphisms in novel gametocyte genes that could be targets for developing better diagnostics or transmission blocking vaccines.



## References

1. Organization WH. World Malaria Report. 2018.
2. Price RN, Tjitra E, Guerra CA, Yeung S, White NJ, Anstey NM. Vivax malaria: neglected and not benign. *Am J Trop Med Hyg.* 2007;77(6 Suppl):79-87.
3. Elgoraish AG, Elzaki SEG, Ahmed RT, Ahmed AI, Fadlalmula HA, Abdalgader Mohamed S, et al. Epidemiology and distribution of Plasmodium vivax malaria in Sudan. *Trans R Soc Trop Med Hyg.* 2019.
4. Lo E, Hemming-Schroeder E, Yewhalaw D, Nguyen J, Kebede E, Zemene E, et al. Transmission dynamics of co-endemic Plasmodium vivax and P. falciparum in Ethiopia and prevalence of antimalarial resistant genotypes. *PLoS Negl Trop Dis.* 2017;11(7):e0005806.
5. Herrera S, Corradin G, Arevalo-Herrera M. An update on the search for a Plasmodium vivax vaccine. *Trends Parasitol.* 2007;23(3):122-8.
6. White NJ. The role of anti-malarial drugs in eliminating malaria. *Malar J.* 2008;7 Suppl 1:S8.
7. Chu CS, White NJ. Management of relapsing Plasmodium vivax malaria. *Expert Rev Anti Infect Ther.* 2016;14(10):885-900.
8. White NJ. Determinants of relapse periodicity in Plasmodium vivax malaria. *Malar J.* 2011;10:297.
9. Lawpoolsri S, Sattabongkot J, Sirichaisinthop J, Cui L, Kiattibutr K, Rachaphaew N, et al. Epidemiological profiles of recurrent malaria episodes in an endemic area along the Thailand-Myanmar border: a prospective cohort study. *Malar J.* 2019;18(1):124.
10. Robinson LJ, Wampfler R, Betuela I, Karl S, White MT, Li Wai Suen CS, et al. Strategies for understanding and reducing the Plasmodium vivax and Plasmodium ovale hypnozoite reservoir in Papua New Guinean children: a randomised placebo-controlled trial and mathematical model. *PLoS Med.* 2015;12(10):e1001891.
11. Taylor AR, Watson JA, Chu CS, Puaprasert K, Duanguppama J, Day NPJ, et al. Resolving the cause of recurrent Plasmodium vivax malaria probabilistically. *Nat Commun.* 2019;10(1):5595.
12. Chitnis CE, Miller LH. Identification of the erythrocyte binding domains of Plasmodium vivax and Plasmodium knowlesi proteins involved in erythrocyte invasion. *J Exp Med.* 1994;180(2):497-506.
13. Fang XD, Kaslow DC, Adams JH, Miller LH. Cloning of the Plasmodium vivax Duffy receptor. *Mol Biochem Parasitol.* 1991;44(1):125-32.
14. Howes RE, Patil AP, Piel FB, Nyangiri OA, Kabaria CW, Gething PW, et al. The global distribution of the Duffy blood group. *Nat Commun.* 2011;2:266.
15. Gunalan K, Lo E, Hostetler JB, Yewhalaw D, Mu J, Neafsey DE, et al. Role of Plasmodium vivax Duffy-binding protein 1 in invasion of Duffy-null Africans. *Proc Natl Acad Sci U S A.* 2016;113(22):6271-6.
16. Gunalan K, Niangaly A, Thera MA, Doumbo OK, Miller LH. Plasmodium vivax Infections of Duffy-Negative Erythrocytes: Historically Undetected or a Recent Adaptation? *Trends Parasitol.* 2018;34(5):420-9.
17. Howes RE, Reiner RC, Jr., Battle KE, Longbottom J, Mappin B, Ordanovich D, et al. Plasmodium vivax Transmission in Africa. *PLoS Negl Trop Dis.* 2015;9(11):e0004222.

18. Menard D, Barnadas C, Bouchier C, Henry-Halldin C, Gray LR, Ratsimbaoa A, et al. Plasmodium vivax clinical malaria is commonly observed in Duffy-negative Malagasy people. *Proc Natl Acad Sci U S A*. 2010;107(13):5967-71.
19. Menard D, Chan ER, Benedet C, Ratsimbaoa A, Kim S, Chim P, et al. Whole genome sequencing of field isolates reveals a common duplication of the Duffy binding protein gene in Malagasy Plasmodium vivax strains. *PLoS Negl Trop Dis*. 2013;7(11):e2489.
20. White MT, Shirreff G, Karl S, Ghani AC, Mueller I. Variation in relapse frequency and the transmission potential of Plasmodium vivax malaria. *Proc Biol Sci*. 2016;283(1827):20160048.
21. Auburn S, Benavente ED, Miotto O, Pearson RD, Amato R, Grigg MJ, et al. Genomic analysis of a pre-elimination Malaysian Plasmodium vivax population reveals selective pressures and changing transmission dynamics. *Nat Commun*. 2018;9(1):2585.
22. Diez Benavente E, Ward Z, Chan W, Mohareb FR, Sutherland CJ, Roper C, et al. Genomic variation in Plasmodium vivax malaria reveals regions under selective pressure. *PLoS One*. 2017;12(5):e0177134.
23. Parobek CM, Lin JT, Saunders DL, Barnett EJ, Lon C, Lanteri CA, et al. Selective sweep suggests transcriptional regulation may underlie Plasmodium vivax resilience to malaria control measures in Cambodia. *Proc Natl Acad Sci U S A*. 2016;113(50):E8096-E105.
24. Ford A, Kepple D, Abagero BR, Connors J, Pearson R, Auburn S, et al. Whole genome sequencing of Plasmodium vivax isolates reveals frequent sequence and structural polymorphisms in erythrocyte binding genes. *PLoS Negl Trop Dis*. 2020;14(10):e0008234.
25. Guy AJ, Irani V, Richards JS, Ramsland PA. Structural patterns of selection and diversity for Plasmodium vivax antigens DBP and AMA1. *Malar J*. 2018;17(1):183.
26. Jang JW, Yun SG, Woo MK, Han ET, Lu F, Gao Q, et al. Sequence polymorphisms of Plasmodium vivax tryptophan and alanine rich antigen (PvTARAg55). *Acta Trop*. 2015;142:122-6.
27. Lo E, Hostetler JB, Yewhalaw D, Pearson RD, Hamid MMA, Gunalan K, et al. Frequent expansion of Plasmodium vivax Duffy Binding Protein in Ethiopia and its epidemiological significance. *PLoS Negl Trop Dis*. 2019;13(9):e0007222.
28. Roesch C, Popovici J, Bin S, Run V, Kim S, Ramboarina S, et al. Genetic diversity in two Plasmodium vivax protein ligands for reticulocyte invasion. *PLoS Negl Trop Dis*. 2018;12(10):e0006555.
29. Han JH, Cho JS, Ong JJY, Park JH, Nyunt MH, Sutanto E, et al. Genetic diversity and neutral selection in Plasmodium vivax erythrocyte binding protein correlates with patient antigenicity. *PLoS Negl Trop Dis*. 2020;14(7):e0008202.
30. Zeeshan M, Bora H, Sharma YD. Presence of memory T cells and naturally acquired antibodies in Plasmodium vivax malaria-exposed individuals against a group of tryptophan-rich antigens with conserved sequences. *J Infect Dis*. 2013;207(1):175-85.
31. Hwang SY, Kim SH, Kho WG. Genetic characteristics of polymorphic antigenic markers among Korean isolates of Plasmodium vivax. *Korean J Parasitol*. 2009;47 Suppl:S51-8.
32. Goryacheva, II, Baranova AM, Lukashev AN, Gordeev MI, Usenbaev NT, Shaikevich EV. Genetic characterization of Plasmodium vivax in the Kyrgyz Republic. *Infect Genet Evol*. 2018;66:262-8.
33. Xainli J, Adams JH, King CL. The erythrocyte binding motif of plasmodium vivax duffy binding protein is highly polymorphic and functionally conserved in isolates from Papua New Guinea. *Mol Biochem Parasitol*. 2000;111(2):253-60.

34. Cheng CW, Putaporntip C, Jongwutiwes S. Polymorphism in merozoite surface protein-7E of *Plasmodium vivax* in Thailand: Natural selection related to protein secondary structure. *PLoS One*. 2018;13(5):e0196765.
35. Arevalo-Pinzon G, Bermudez M, Curtidor H, Patarroyo MA. The *Plasmodium vivax* rhoptry neck protein 5 is expressed in the apical pole of *Plasmodium vivax* VCG-1 strain schizonts and binds to human reticulocytes. *Malar J*. 2015;14:106.
36. Baquero LA, Moreno-Perez DA, Garzon-Ospina D, Forero-Rodriguez J, Ortiz-Suarez HD, Patarroyo MA. PvGAMA reticulocyte binding activity: predicting conserved functional regions by natural selection analysis. *Parasit Vectors*. 2017;10(1):251.
37. Gunalan K, Sa JM, Moraes Barros RR, Anzick SL, Caeon RL, Mershon JP, et al. Transcriptome profiling of *Plasmodium vivax* in Saimiri monkeys identifies potential ligands for invasion. *Proc Natl Acad Sci U S A*. 2019;116(14):7053-61.
38. Tyagi K, Hossain ME, Thakur V, Aggarwal P, Malhotra P, Mohammed A, et al. *Plasmodium vivax* Tryptophan Rich Antigen PvTRAg36.6 Interacts with PvETRAMP and PvTRAg56.6 Interacts with PvMSP7 during Erythrocytic Stages of the Parasite. *PLoS One*. 2016;11(3):e0151065.
39. Wang B, Lu F, Cheng Y, Chen JH, Jeon HY, Ha KS, et al. Correction for Wang et al., "Immunoprofiling of the Tryptophan-Rich Antigen Family in *Plasmodium vivax*". *Infect Immun*. 2018;86(4).
40. Udomsangpetch R, Somsri S, Panichakul T, Chotivanich K, Sirichaisinthop J, Yang Z, et al. Short-term in vitro culture of field isolates of *Plasmodium vivax* using umbilical cord blood. *Parasitol Int*. 2007;56(1):65-9.
41. Golenda CF, Li J, Rosenberg R. Continuous in vitro propagation of the malaria parasite *Plasmodium vivax*. *Proc Natl Acad Sci U S A*. 1997;94(13):6786-91.
42. Borlon C, Russell B, Sriprawat K, Suwanarusk R, Erhart A, Renia L, et al. Cryopreserved *Plasmodium vivax* and cord blood reticulocytes can be used for invasion and short term culture. *Int J Parasitol*. 2012;42(2):155-60.
43. Anderson DC, Lapp SA, Barnwell JW, Galinski MR. A large scale *Plasmodium vivax*-Saimiri boliviensis trophozoite-schizont transition proteome. *PLoS One*. 2017;12(8):e0182561.
44. Peterson MS, Joyner CJ, Cordy RJ, Salinas JL, Machiah D, Lapp SA, et al. *Plasmodium vivax* Parasite Load Is Associated With Histopathology in Saimiri boliviensis With Findings Comparable to *P. vivax* Pathogenesis in Humans. *Open Forum Infect Dis*. 2019;6(3):ofz021.
45. Obaldia N, 3rd, Meibalan E, Sa JM, Ma S, Clark MA, Mejia P, et al. Bone Marrow Is a Major Parasite Reservoir in *Plasmodium vivax* Infection. *mBio*. 2018;9(3).
46. Galinski MR, Medina CC, Ingravallo P, Barnwell JW. A reticulocyte-binding protein complex of *Plasmodium vivax* merozoites. *Cell*. 1992;69(7):1213-26.
47. Hadley TJ. Invasion of erythrocytes by malaria parasites: a cellular and molecular overview. *Annu Rev Microbiol*. 1986;40:451-77.
48. Kanjee U, Rangel GW, Clark MA, Duraisingh MT. Molecular and cellular interactions defining the tropism of *Plasmodium vivax* for reticulocytes. *Curr Opin Microbiol*. 2018;46:109-15.
49. Malleret B, Renia L, Russell B. The unhealthy attraction of *Plasmodium vivax* to reticulocytes expressing transferrin receptor 1 (CD71). *Int J Parasitol*. 2017;47(7):379-83.
50. Almeida ACG, Kuehn A, Castro AJM, Vitor-Silva S, Figueiredo EFG, Brasil LW, et al. High proportions of asymptomatic and submicroscopic *Plasmodium vivax* infections in a peri-urban area of low transmission in the Brazilian Amazon. *Parasit Vectors*. 2018;11(1):194.

51. Huh AJ, Kwak YG, Kim ES, Lee KS, Yeom JS, Cho YK, et al. Parasitemia characteristics of *Plasmodium vivax* malaria patients in the Republic of Korea. *J Korean Med Sci.* 2011;26(1):42-6.
52. Siegel SV, Chappell L, Hostetler JB, Amaratunga C, Suon S, Bohme U, et al. Analysis of *Plasmodium vivax* schizont transcriptomes from field isolates reveals heterogeneity of expression of genes involved in host-parasite interactions. *Sci Rep.* 2020;10(1):16667.
53. Adams JH, Mueller I. The Biology of *Plasmodium vivax*. *Cold Spring Harb Perspect Med.* 2017;7(9).
54. Battle KE, Karhunen MS, Bhatt S, Gething PW, Howes RE, Golding N, et al. Geographical variation in *Plasmodium vivax* relapse. *Malar J.* 2014;13:144.
55. Mikolajczak SA, Vaughan AM, Kangwanransan N, Roobsoong W, Fishbaugher M, Yimamnuaychok N, et al. *Plasmodium vivax* liver stage development and hypnozoite persistence in human liver-chimeric mice. *Cell Host Microbe.* 2015;17(4):526-35.
56. Craig MH, Snow RW, le Sueur D. A climate-based distribution model of malaria transmission in sub-Saharan Africa. *Parasitol Today.* 1999;15(3):105-11.
57. Ikeda T, Behera SK, Morioka Y, Minakawa N, Hashizume M, Tsuzuki A, et al. Seasonally lagged effects of climatic factors on malaria incidence in South Africa. *Sci Rep.* 2017;7(1):2458.
58. Midekisa A, Beyene B, Mihretie A, Bayabil E, Wimberly MC. Seasonal associations of climatic drivers and malaria in the highlands of Ethiopia. *Parasit Vectors.* 2015;8:339.
59. Rodriguez LE, Urquiza M, Ocampo M, Curtidor H, Suarez J, Garcia J, et al. *Plasmodium vivax* MSP-1 peptides have high specific binding activity to human reticulocytes. *Vaccine.* 2002;20(9-10):1331-9.
60. O'Donnell RA, Hackett F, Howell SA, Treeck M, Struck N, Krnajski Z, et al. Intramembrane proteolysis mediates shedding of a key adhesin during erythrocyte invasion by the malaria parasite. *J Cell Biol.* 2006;174(7):1023-33.
61. Sim BK, Narum DL, Liang H, Fuhrmann SR, Obaldia N, 3rd, Gramzinski R, et al. Induction of biologically active antibodies in mice, rabbits, and monkeys by *Plasmodium falciparum* EBA-175 region II DNA vaccine. *Mol Med.* 2001;7(4):247-54.
62. Koch M, Wright KE, Otto O, Herbig M, Salinas ND, Tolia NH, et al. *Plasmodium falciparum* erythrocyte-binding antigen 175 triggers a biophysical change in the red blood cell that facilitates invasion. *Proc Natl Acad Sci U S A.* 2017;114(16):4225-30.
63. Sisqueira X, Nebl T, Thompson JK, Whitehead L, Malpede BM, Salinas ND, et al. *Plasmodium falciparum* ligand binding to erythrocytes induce alterations in deformability essential for invasion. *Elife.* 2017;6.
64. Paing MM, Salinas ND, Adams Y, Oksman A, Jensen AT, Goldberg DE, et al. Shed EBA-175 mediates red blood cell clustering that enhances malaria parasite growth and enables immune evasion. *Elife.* 2018;7.
65. Maier AG, Baum J, Smith B, Conway DJ, Cowman AF. Polymorphisms in erythrocyte binding antigens 140 and 181 affect function and binding but not receptor specificity in *Plasmodium falciparum*. *Infect Immun.* 2009;77(4):1689-99.
66. Mayer DC, Jiang L, Achur RN, Kakizaki I, Gowda DC, Miller LH. The glycoporphin C N-linked glycan is a critical component of the ligand for the *Plasmodium falciparum* erythrocyte receptor BAEBL. *Proc Natl Acad Sci U S A.* 2006;103(7):2358-62.

67. Gaur D, Storry JR, Reid ME, Barnwell JW, Miller LH. *Plasmodium falciparum* is able to invade erythrocytes through a trypsin-resistant pathway independent of glycophorin B. *Infect Immun*. 2003;71(12):6742-6.
68. Facer CA. Erythrocyte sialoglycoproteins and *Plasmodium falciparum* invasion. *Trans R Soc Trop Med Hyg*. 1983;77(4):524-30.
69. Field SP, Hempelmann E, Mendelow BV, Fleming AF. Glycophorin variants and *Plasmodium falciparum*: protective effect of the Dantu phenotype in vitro. *Hum Genet*. 1994;93(2):148-50.
70. Kariuki SN, Marin-Menendez A, Introini V, Ravenhill BJ, Lin YC, Macharia A, et al. Red blood cell tension protects against severe malaria in the Dantu blood group. *Nature*. 2020;585(7826):579-83.
71. Reyes C, Molina-Franky J, Aza-Conde J, Suarez CF, Pabon L, Moreno-Vranich A, et al. Malaria: Paving the way to developing peptide-based vaccines against invasion in infectious diseases. *Biochem Biophys Res Commun*. 2020;527(4):1021-6.
72. Vera-Bravo R, Valbuena JJ, Ocampo M, Garcia JE, Rodriguez LE, Puentes A, et al. Amino terminal peptides from the *Plasmodium falciparum* EBA-181/JESEBL protein bind specifically to erythrocytes and inhibit in vitro merozoite invasion. *Biochimie*. 2005;87(5):425-36.
73. Rayner JC, Vargas-Serrato E, Huber CS, Galinski MR, Barnwell JW. A *Plasmodium falciparum* homologue of *Plasmodium vivax* reticulocyte binding protein (PvRBP1) defines a trypsin-resistant erythrocyte invasion pathway. *J Exp Med*. 2001;194(11):1571-81.
74. Triglia T, Duraisingh MT, Good RT, Cowman AF. Reticulocyte-binding protein homologue 1 is required for sialic acid-dependent invasion into human erythrocytes by *Plasmodium falciparum*. *Mol Microbiol*. 2005;55(1):162-74.
75. Gao X, Gunalan K, Yap SS, Preiser PR. Triggers of key calcium signals during erythrocyte invasion by *Plasmodium falciparum*. *Nat Commun*. 2013;4:2862.
76. Dvorin JD, Bei AK, Coleman BI, Duraisingh MT. Functional diversification between two related *Plasmodium falciparum* merozoite invasion ligands is determined by changes in the cytoplasmic domain. *Mol Microbiol*. 2010;75(4):990-1006.
77. Duraisingh MT, Triglia T, Ralph SA, Rayner JC, Barnwell JW, McFadden GI, et al. Phenotypic variation of *Plasmodium falciparum* merozoite proteins directs receptor targeting for invasion of human erythrocytes. *EMBO J*. 2003;22(5):1047-57.
78. Espinosa AM, Sierra AY, Barrero CA, Cepeda LA, Cantor EM, Lombo TB, et al. Expression, polymorphism analysis, reticulocyte binding and serological reactivity of two *Plasmodium vivax* MSP-1 protein recombinant fragments. *Vaccine*. 2003;21(11-12):1033-43.
79. Aniwah Y, Gao X, Gunalan K, Preiser PR. PfrH2b specific monoclonal antibodies inhibit merozoite invasion. *Mol Microbiol*. 2016;102(3):386-404.
80. Gunalan K, Gao X, Liew KJ, Preiser PR. Differences in erythrocyte receptor specificity of different parts of the *Plasmodium falciparum* reticulocyte binding protein homologue 2a. *Infect Immun*. 2011;79(8):3421-30.
81. Triglia T, Chen L, Lopaticki S, Dekiwadia C, Riglar DT, Hodder AN, et al. *Plasmodium falciparum* merozoite invasion is inhibited by antibodies that target the PfrH2a and b binding domains. *PLoS Pathog*. 2011;7(6):e1002075.
82. Han JH, Lee SK, Wang B, Muh F, Nyunt MH, Na S, et al. Identification of a reticulocyte-specific binding domain of *Plasmodium vivax* reticulocyte-binding protein 1 that is homologous to the PfrH4 erythrocyte-binding domain. *Sci Rep*. 2016;6:26993.

83. Tham WH, Wilson DW, Lopaticki S, Schmidt CQ, Tetteh-Quarcoo PB, Barlow PN, et al. Complement receptor 1 is the host erythrocyte receptor for *Plasmodium falciparum* PfRh4 invasion ligand. *Proc Natl Acad Sci U S A*. 2010;107(40):17327-32.
84. Partey FD, Castberg FC, Sarbah EW, Silk SE, Awandare GA, Draper SJ, et al. Correction: Kinetics of antibody responses to PfRH5-complex antigens in Ghanaian children with *Plasmodium falciparum* malaria. *PLoS One*. 2018;13(9):e0204452.
85. Volz JC, Yap A, Sisquella X, Thompson JK, Lim NT, Whitehead LW, et al. Essential Role of the PfRh5/PfRipr/CyRPA Complex during *Plasmodium falciparum* Invasion of Erythrocytes. *Cell Host Microbe*. 2016;20(1):60-71.
86. Crosnier C, Bustamante LY, Bartholdson SJ, Bei AK, Theron M, Uchikawa M, et al. Basigin is a receptor essential for erythrocyte invasion by *Plasmodium falciparum*. *Nature*. 2011;480(7378):534-7.
87. Sierra AY, Barrero CA, Rodriguez R, Silva Y, Moncada C, Vanegas M, et al. Splenectomised and spleen intact Aotus monkeys' immune response to *Plasmodium vivax* MSP-1 protein fragments and their high activity binding peptides. *Vaccine*. 2003;21(27-30):4133-44.
88. Lopaticki S, Maier AG, Thompson J, Wilson DW, Tham WH, Triglia T, et al. Reticulocyte and erythrocyte binding-like proteins function cooperatively in invasion of human erythrocytes by malaria parasites. *Infect Immun*. 2011;79(3):1107-17.
89. Stubbs J, Simpson KM, Triglia T, Plouffe D, Tonkin CJ, Duraisingh MT, et al. Molecular mechanism for switching of *P. falciparum* invasion pathways into human erythrocytes. *Science*. 2005;309(5739):1384-7.
90. Amir A, Cheong FW, de Silva JR, Liew JWK, Lau YL. *Plasmodium knowlesi* malaria: current research perspectives. *Infect Drug Resist*. 2018;11:1145-55.
91. Cox-Singh J, Davis TM, Lee KS, Shamsul SS, Matusop A, Ratnam S, et al. *Plasmodium knowlesi* malaria in humans is widely distributed and potentially life threatening. *Clin Infect Dis*. 2008;46(2):165-71.
92. Moon RW, Sharaf H, Hastings CH, Ho YS, Nair MB, Rchiad Z, et al. Normocyte-binding protein required for human erythrocyte invasion by the zoonotic malaria parasite *Plasmodium knowlesi*. *Proc Natl Acad Sci U S A*. 2016;113(26):7231-6.
93. Ahmed AM, Pinheiro MM, Divis PC, Siner A, Zainudin R, Wong IT, et al. Disease progression in *Plasmodium knowlesi* malaria is linked to variation in invasion gene family members. *PLoS Negl Trop Dis*. 2014;8(8):e3086.
94. Bermudez M, Moreno-Perez DA, Arevalo-Pinzon G, Curtidor H, Patarroyo MA. *Plasmodium vivax* in vitro continuous culture: the spoke in the wheel. *Malar J*. 2018;17(1):301.
95. Pasini EM, Zeeman AM, Voorberg VANDERWA, Kocken CHM. *Plasmodium knowlesi*: a relevant, versatile experimental malaria model. *Parasitology*. 2018;145(1):56-70.
96. Tachibana S, Sullivan SA, Kawai S, Nakamura S, Kim HR, Goto N, et al. *Plasmodium cynomolgi* genome sequences provide insight into *Plasmodium vivax* and the monkey malaria clade. *Nat Genet*. 2012;44(9):1051-5.
97. Coatney GR, Elder HA, Contacos PG, Getz ME, Greenland R, Rossan RN, et al. Transmission of the M strain of *Plasmodium cynomolgi* to man. *Am J Trop Med Hyg*. 1961;10:673-8.
98. Eyles DE, Coatney GR, Getz ME. Vivax-type malaria parasite of macaques transmissible to man. *Science*. 1960;131(3416):1812-3.
99. Ta TH, Hisam S, Lanza M, Jiram AI, Ismail N, Rubio JM. First case of a naturally acquired human infection with *Plasmodium cynomolgi*. *Malar J*. 2014;13:68.

100. Tachibana S, Kawai S, Katakai Y, Takahashi H, Nakade T, Yasutomi Y, et al. Contrasting infection susceptibility of the Japanese macaques and cynomolgus macaques to closely related malaria parasites, *Plasmodium vivax* and *Plasmodium cynomolgi*. *Parasitol Int*. 2015;64(3):274-81.
101. Sutton PL, Luo Z, Divis PCS, Friedrich VK, Conway DJ, Singh B, et al. Characterizing the genetic diversity of the monkey malaria parasite *Plasmodium cynomolgi*. *Infect Genet Evol*. 2016;40:243-52.
102. Putaporntip C, Kuamsab N, Jongwutiwes S. Sequence diversity and positive selection at the Duffy-binding protein genes of *Plasmodium knowlesi* and *P. cynomolgi*: Analysis of the complete coding sequences of Thai isolates. *Infect Genet Evol*. 2016;44:367-75.
103. Chua ACY, Ong JJY, Malleret B, Suwanarusk R, Kosaisavee V, Zeeman AM, et al. Robust continuous in vitro culture of the *Plasmodium cynomolgi* erythrocytic stages. *Nat Commun*. 2019;10(1):3635.
104. Singh AP, Ozwara H, Kocken CH, Puri SK, Thomas AW, Chitnis CE. Targeted deletion of *Plasmodium knowlesi* Duffy binding protein confirms its role in junction formation during invasion. *Mol Microbiol*. 2005;55(6):1925-34.
105. Kano FS, de Souza AM, de Menezes Torres L, Costa MA, Souza-Silva FA, Sanchez BAM, et al. Susceptibility to *Plasmodium vivax* malaria associated with DARC (Duffy antigen) polymorphisms is influenced by the time of exposure to malaria. *Sci Rep*. 2018;8(1):13851.
106. King CL, Adams JH, Xianli J, Grimberg BT, McHenry AM, Greenberg LJ, et al. Fy(a)/Fy(b) antigen polymorphism in human erythrocyte Duffy antigen affects susceptibility to *Plasmodium vivax* malaria. *Proc Natl Acad Sci U S A*. 2011;108(50):20113-8.
107. Miller LH, Mason SJ, Clyde DF, McGinniss MH. The resistance factor to *Plasmodium vivax* in blacks. The Duffy-blood-group genotype, FyFy. *N Engl J Med*. 1976;295(6):302-4.
108. Twohig KA, Pfeffer DA, Baird JK, Price RN, Zimmerman PA, Hay SI, et al. Growing evidence of *Plasmodium vivax* across malaria-endemic Africa. *PLoS Negl Trop Dis*. 2019;13(1):e0007140.
109. Hester J, Chan ER, Menard D, Mercereau-Puijalon O, Barnwell J, Zimmerman PA, et al. De novo assembly of a field isolate genome reveals novel *Plasmodium vivax* erythrocyte invasion genes. *PLoS Negl Trop Dis*. 2013;7(12):e2569.
110. Carlton JM, Adams JH, Silva JC, Bidwell SL, Lorenzi H, Caler E, et al. Comparative genomics of the neglected human malaria parasite *Plasmodium vivax*. *Nature*. 2008;455(7214):757-63.
111. Rayner JC, Galinski MR, Ingravallo P, Barnwell JW. Two *Plasmodium falciparum* genes express merozoite proteins that are related to *Plasmodium vivax* and *Plasmodium yoelii* adhesive proteins involved in host cell selection and invasion. *Proc Natl Acad Sci U S A*. 2000;97(17):9648-53.
112. Gaur D, Singh S, Singh S, Jiang L, Diouf A, Miller LH. Recombinant *Plasmodium falciparum* reticulocyte homology protein 4 binds to erythrocytes and blocks invasion. *Proc Natl Acad Sci U S A*. 2007;104(45):17789-94.
113. Gupta S, Singh S, Popovici J, Roesch C, Shakri AR, Guillotte-Blisnick M, et al. Targeting a Reticulocyte Binding Protein and Duffy Binding Protein to Inhibit Reticulocyte Invasion by *Plasmodium vivax*. *Sci Rep*. 2018;8(1):10511.
114. Han JH, Li J, Wang B, Lee SK, Nyunt MH, Na S, et al. Identification of Immunodominant B-cell Epitope Regions of Reticulocyte Binding Proteins in *Plasmodium vivax* by Protein Microarray Based Immunoscreening. *Korean J Parasitol*. 2015;53(4):403-11.

115. Gruszczyk J, Lim NT, Arnott A, He WQ, Nguitragool W, Roobsoong W, et al. Structurally conserved erythrocyte-binding domain in *Plasmodium* provides a versatile scaffold for alternate receptor engagement. *Proc Natl Acad Sci U S A*. 2016;113(2):E191-200.
116. Gruszczyk J, Kanjee U, Chan LJ, Menant S, Malleret B, Lim NTY, et al. Transferrin receptor 1 is a reticulocyte-specific receptor for *Plasmodium vivax*. *Science*. 2018;359(6371):48-55.
117. Hietanen J, Chim-Ong A, Chiramanewong T, Gruszczyk J, Roobsoong W, Tham WH, et al. Gene Models, Expression Repertoire, and Immune Response of *Plasmodium vivax* Reticulocyte Binding Proteins. *Infect Immun*. 2015;84(3):677-85.
118. Bozdech Z, Mok S, Hu G, Imwong M, Jaidee A, Russell B, et al. The transcriptome of *Plasmodium vivax* reveals divergence and diversity of transcriptional regulation in malaria parasites. *Proc Natl Acad Sci U S A*. 2008;105(42):16290-5.
119. Burns JM, Adeeku EK, Belk CC, Dunn PD. An unusual tryptophan-rich domain characterizes two secreted antigens of *Plasmodium yoelii*-infected erythrocytes. *Mol Biochem Parasitol*. 2000;110(1):11-21.
120. Salzwedel K, West JT, Hunter E. A conserved tryptophan-rich motif in the membrane-proximal region of the human immunodeficiency virus type 1 gp41 ectodomain is important for Env-mediated fusion and virus infectivity. *J Virol*. 1999;73(3):2469-80.
121. Bourgard C, Albrecht L, Kayano A, Sunnerhagen P, Costa FTM. *Plasmodium vivax* Biology: Insights Provided by Genomics, Transcriptomics and Proteomics. *Front Cell Infect Microbiol*. 2018;8:34.
122. Mourier T, de Alvarenga DAM, Kaushik A, de Pina-Costa A, Douvropoulou O, Guan Q, et al. The genome of the zoonotic malaria parasite *Plasmodium simium* reveals adaptations to host switching. *BMC Biol*. 2021;19(1):219.
123. Tyagi RK, Sharma YD. Erythrocyte Binding Activity Displayed by a Selective Group of *Plasmodium vivax* Tryptophan Rich Antigens Is Inhibited by Patients' Antibodies. *PLoS One*. 2012;7(12):e50754.
124. Zeeshan M, Tyagi RK, Tyagi K, Alam MS, Sharma YD. Host-parasite interaction: selective Pv-fam-a family proteins of *Plasmodium vivax* bind to a restricted number of human erythrocyte receptors. *J Infect Dis*. 2015;211(7):1111-20.
125. Alam MS, Choudhary V, Zeeshan M, Tyagi RK, Rathore S, Sharma YD. Interaction of *Plasmodium vivax* Tryptophan-rich Antigen PvTRAg38 with Band 3 on Human Erythrocyte Surface Facilitates Parasite Growth. *J Biol Chem*. 2015;290(33):20257-72.
126. Alam MS, Zeeshan M, Mittra P, Choudhary V, Sharma YD. Receptor specific binding regions of *Plasmodium vivax* tryptophan rich antigens and parasite growth inhibition activity of PvTRAg35.2. *Microbes Infect*. 2016;18(9):550-8.
127. Versiani FG, Almeida ME, Mariuba LA, Orlandi PP, Nogueira PA. N-terminal *Plasmodium vivax* merozoite surface protein-1, a potential subunit for malaria vivax vaccine. *Clin Dev Immunol*. 2013;2013:965841.
128. McCaffery JN, Fonseca JA, Singh B, Cabrera-Mora M, Bohannon C, Jacob J, et al. A Multi-Stage *Plasmodium vivax* Malaria Vaccine Candidate Able to Induce Long-Lived Antibody Responses Against Blood Stage Parasites and Robust Transmission-Blocking Activity. *Front Cell Infect Microbiol*. 2019;9:135.
129. Murhandarwati EEH, Herningtyas EH, Puspawati P, Mau F, Chen SB, Shen HM, et al. Genetic diversity of Merozoite surface protein 1-42 (MSP1-42) fragment of *Plasmodium vivax*



from Indonesian isolates: Rationale implementation of candidate MSP1 vaccine. *Infect Genet Evol.* 2020;85:104573.

130. Jiang J, Barnwell JW, Meyer EV, Galinski MR. Plasmodium vivax merozoite surface protein-3 (PvMSP3): expression of an 11 member multigene family in blood-stage parasites. *PLoS One.* 2013;8(5):e63888.

131. Garzon-Ospina D, Lopez C, Forero-Rodriguez J, Patarroyo MA. Genetic diversity and selection in three Plasmodium vivax merozoite surface protein 7 (Pvmsp-7) genes in a Colombian population. *PLoS One.* 2012;7(9):e45962.

132. Songsaigath S, Putaporntip C, Kuamsab N, Jongwutiwes S. Structural diversity, natural selection and intragenic recombination in the Plasmodium vivax merozoite surface protein 9 locus in Thailand. *Infect Genet Evol.* 2020;85:104467.

133. Rodrigues-da-Silva RN, Correa-Moreira D, Soares IF, de-Luca PM, Totino PRR, Morgado FN, et al. Immunogenicity of synthetic peptide constructs based on PvMSP9E795-A808, a linear B-cell epitope of the P. vivax Merozoite Surface Protein-9. *Vaccine.* 2019;37(2):306-13.

134. Soares RR, Nakaie CR, Rodrigues-da-Silva RN, da Silva RL, Lima-Junior JDC, Scopel KKG. Main B-cell epitopes of PvAMA-1 and PvMSP-9 are targeted by naturally acquired antibodies and epitope-specific memory cells in acute and convalescent phases of vivax malaria. *Parasite Immunol.* 2020;42(5):e12705.

135. Schofield L, Grau GE. Immunological processes in malaria pathogenesis. *Nat Rev Immunol.* 2005;5(9):722-35.

136. Chuangchaiya S, Jangpatarapongsa K, Chootong P, Sirichaisinthop J, Sattabongkot J, Pattanapanyasat K, et al. Immune response to Plasmodium vivax has a potential to reduce malaria severity. *Clin Exp Immunol.* 2010;160(2):233-9.

137. Mendonca VR, Queiroz AT, Lopes FM, Andrade BB, Barral-Netto M. Networking the host immune response in Plasmodium vivax malaria. *Malar J.* 2013;12:69.

138. Praba-Egge AD, Montenegro S, Arevalo-Herrera M, Hopper T, Herrera S, James MA. Human cytokine responses to meso-endemic malaria on the Pacific Coast of Colombia. *Ann Trop Med Parasitol.* 2003;97(4):327-37.

139. Lopez C, Yepes-Perez Y, Hincapie-Escobar N, Diaz-Arevalo D, Patarroyo MA. What Is Known about the Immune Response Induced by Plasmodium vivax Malaria Vaccine Candidates? *Front Immunol.* 2017;8:126.

140. Fraser T, Michon P, Barnwell JW, Noe AR, Al-Yaman F, Kaslow DC, et al. Expression and serologic activity of a soluble recombinant Plasmodium vivax Duffy binding protein. *Infect Immun.* 1997;65(7):2772-7.

141. Michon P, Fraser T, Adams JH. Naturally acquired and vaccine-elicited antibodies block erythrocyte cytoadherence of the Plasmodium vivax Duffy binding protein. *Infect Immun.* 2000;68(6):3164-71.

142. Chootong P, McHenry AM, Ntumngia FB, Sattabongkot J, Adams JH. The association of Duffy binding protein region II polymorphisms and its antigenicity in Plasmodium vivax isolates from Thailand. *Parasitol Int.* 2014;63(6):858-64.

143. Michon PA, Arevalo-Herrera M, Fraser T, Herrera S, Adams JH. Serologic responses to recombinant Plasmodium vivax Duffy binding protein in a Colombian village. *Am J Trop Med Hyg.* 1998;59(4):597-9.

144. Ntumngia FB, Adams JH. Design and immunogenicity of a novel synthetic antigen based on the ligand domain of the *Plasmodium vivax* duffy binding protein. *Clin Vaccine Immunol.* 2012;19(1):30-6.
145. VanBuskirk KM, Sevova E, Adams JH. Conserved residues in the *Plasmodium vivax* Duffy-binding protein ligand domain are critical for erythrocyte receptor recognition. *Proc Natl Acad Sci U S A.* 2004;101(44):15754-9.
146. VanBuskirk KM, Cole-Tobian JL, Baisor M, Sevova ES, Bockarie M, King CL, et al. Antigenic drift in the ligand domain of *Plasmodium vivax* duffy binding protein confers resistance to inhibitory antibodies. *J Infect Dis.* 2004;190(9):1556-62.
147. Popovici J, Roesch C, Carias LL, Khim N, Kim S, Vantaux A, et al. Amplification of Duffy binding protein-encoding gene allows *Plasmodium vivax* to evade host anti-DBP humoral immunity. *Nat Commun.* 2020;11(1):953.
148. Lima-Junior JC, Rodrigues-da-Silva RN, Banic DM, Jiang J, Singh B, Fabricio-Silva GM, et al. Influence of HLA-DRB1 and HLA-DQB1 alleles on IgG antibody response to the *P. vivax* MSP-1, MSP-3alpha and MSP-9 in individuals from Brazilian endemic area. *PLoS One.* 2012;7(5):e36419.
149. Cheng Y, Wang Y, Ito D, Kong DH, Ha KS, Chen JH, et al. The *Plasmodium vivax* merozoite surface protein 1 paralog is a novel erythrocyte-binding ligand of *P. vivax*. *Infect Immun.* 2013;81(5):1585-95.
150. Wang Q, Zhao Z, Zhang X, Li X, Zhu M, Li P, et al. Naturally Acquired Antibody Responses to *Plasmodium vivax* and *Plasmodium falciparum* Merozoite Surface Protein 1 (MSP1) C-Terminal 19 kDa Domains in an Area of Unstable Malaria Transmission in Southeast Asia. *PLoS One.* 2016;11(3):e0151900.
151. Lima-Junior JC, Jiang J, Rodrigues-da-Silva RN, Banic DM, Tran TM, Ribeiro RY, et al. B cell epitope mapping and characterization of naturally acquired antibodies to the *Plasmodium vivax* merozoite surface protein-3alpha (PvMSP-3alpha) in malaria exposed individuals from Brazilian Amazon. *Vaccine.* 2011;29(9):1801-11.
152. Stanisic DI, Javati S, Kiniboro B, Lin E, Jiang J, Singh B, et al. Naturally acquired immune responses to *P. vivax* merozoite surface protein 3alpha and merozoite surface protein 9 are associated with reduced risk of *P. vivax* malaria in young Papua New Guinean children. *PLoS Negl Trop Dis.* 2013;7(11):e2498.
153. Lima-Junior JC, Tran TM, Meyer EV, Singh B, De-Simone SG, Santos F, et al. Naturally acquired humoral and cellular immune responses to *Plasmodium vivax* merozoite surface protein 9 in Northwestern Amazon individuals. *Vaccine.* 2008;26(51):6645-54.
154. Chim-Ong A, Surit T, Chainarin S, Roobsoong W, Sattabongkot J, Cui L, et al. The Blood Stage Antigen RBP2-P1 of *Plasmodium vivax* Binds Reticulocytes and Is a Target of Naturally Acquired Immunity. *Infect Immun.* 2020;88(4).
155. Ferreira AR, Singh B, Cabrera-Mora M, Magri De Souza AC, Queiroz Marques MT, Porto LC, et al. Evaluation of naturally acquired IgG antibodies to a chimeric and non-chimeric recombinant species of *Plasmodium vivax* reticulocyte binding protein-1: lack of association with HLA-DRB1\*/DQB1\* in malaria exposed individuals from the Brazilian Amazon. *PLoS One.* 2014;9(8):e105828.
156. Urquiza M, Patarroyo MA, Mari V, Ocampo M, Suarez J, Lopez R, et al. Identification and polymorphism of *Plasmodium vivax* RBP-1 peptides which bind specifically to reticulocytes. *Peptides.* 2002;23(12):2265-77.

157. Arevalo-Herrera M, Soto L, Perlaza BL, Cespedes N, Vera O, Lenis AM, et al. Antibody-mediated and cellular immune responses induced in naive volunteers by vaccination with long synthetic peptides derived from the *Plasmodium vivax* circumsporozoite protein. *Am J Trop Med Hyg.* 2011;84(2 Suppl):35-42.
158. Fernandez-Becerra C, Bernabeu M, Castellanos A, Correa BR, Obadia T, Ramirez M, et al. *Plasmodium vivax* spleen-dependent genes encode antigens associated with cytoadhesion and clinical protection. *Proc Natl Acad Sci U S A.* 2020;117(23):13056-65.
159. Lu F, Li J, Wang B, Cheng Y, Kong DH, Cui L, et al. Profiling the humoral immune responses to *Plasmodium vivax* infection and identification of candidate immunogenic rhoptry-associated membrane antigen (RAMA). *J Proteomics.* 2014;102:66-82.
160. Kim A, Popovici J, Vantaux A, Samreth R, Bin S, Kim S, et al. Characterization of *P. vivax* blood stage transcriptomes from field isolates reveals similarities among infections and complex gene isoforms. *Sci Rep.* 2017;7(1):7761.
161. Bernabeu M, Lopez FJ, Ferrer M, Martin-Jaular L, Razaname A, Corradin G, et al. Functional analysis of *Plasmodium vivax* VIR proteins reveals different subcellular localizations and cytoadherence to the ICAM-1 endothelial receptor. *Cell Microbiol.* 2012;14(3):386-400.
162. Requena P, Rui E, Padilla N, Martinez-Espinosa FE, Castellanos ME, Botto-Menezes C, et al. *Plasmodium vivax* VIR Proteins Are Targets of Naturally-Acquired Antibody and T Cell Immune Responses to Malaria in Pregnant Women. *PLoS Negl Trop Dis.* 2016;10(10):e0005009.
163. Brazeau NF, Whitesell AN, Doctor SM, Keeler C, Mwandagilirwa MK, Tshefu AK, et al. *Plasmodium vivax* Infections in Duffy-Negative Individuals in the Democratic Republic of the Congo. *Am J Trop Med Hyg.* 2018;99(5):1128-33.
164. Mendes C, Dias F, Figueiredo J, Mora VG, Cano J, de Sousa B, et al. Duffy negative antigen is no longer a barrier to *Plasmodium vivax*--molecular evidences from the African West Coast (Angola and Equatorial Guinea). *PLoS Negl Trop Dis.* 2011;5(6):e1192.
165. Motshoge T, Ababio GK, Aleksenko L, Read J, Peloewetse E, Loeto M, et al. Molecular evidence of high rates of asymptomatic *P. vivax* infection and very low *P. falciparum* malaria in Botswana. *BMC Infect Dis.* 2016;16(1):520.
166. Niang M, Sane R, Sow A, Sadio BD, Chy S, Legrand E, et al. Asymptomatic *Plasmodium vivax* infections among Duffy-negative population in Kedougou, Senegal. *Trop Med Health.* 2018;46:45.
167. Niangaly A, Karthigayan G, Amed O, Coulibaly D, Sa JM, Adams M, et al. *Plasmodium vivax* Infections over 3 Years in Duffy Blood Group Negative Malians in Bandiagara, Mali. *Am J Trop Med Hyg.* 2017;97(3):744-52.
168. Oboh MA, Singh US, Ndiaye D, Badiane AS, Ali NA, Bharti PK, et al. Presence of additional *Plasmodium vivax* malaria in Duffy negative individuals from Southwestern Nigeria. *Malar J.* 2020;19(1):229.
169. Russo G, Faggioni G, Paganotti GM, Djeunang Dongho GB, Pomponi A, De Santis R, et al. Molecular evidence of *Plasmodium vivax* infection in Duffy negative symptomatic individuals from Dschang, West Cameroon. *Malar J.* 2017;16(1):74.
170. Gupta ED, Anand G, Singh H, Chaddha K, Bharti PK, Singh N, et al. Naturally Acquired Human Antibodies Against Reticulocyte-Binding Domains of *Plasmodium vivax* Proteins, PvRBP2c and PvRBP1a, Exhibit Binding-Inhibitory Activity. *J Infect Dis.* 2017;215(10):1558-68.

171. Battle KE, Lucas TCD, Nguyen M, Howes RE, Nandi AK, Twohig KA, et al. Mapping the global endemicity and clinical burden of *Plasmodium vivax*, 2000-17: a spatial and temporal modelling study. *Lancet*. 2019;394(10195):332-43.
172. Lo E, Yewhalaw D, Zhong D, Zemene E, Degefa T, Tushune K, et al. Molecular epidemiology of *Plasmodium vivax* and *Plasmodium falciparum* malaria among Duffy-positive and Duffy-negative populations in Ethiopia. *Malar J*. 2015;14:84.
173. Haubold B, Hudson RR. LIAN 3.0: detecting linkage disequilibrium in multilocus data. *Linkage Analysis. Bioinformatics*. 2000;16(9):847-8.
174. Meirmans PG TP. genotype and genodive: two programs for the analysis of genetic diversity of asexual organisms. *Molecular Ecology Notes*. 2004;4(4):792-4.
175. Pritchard JK, Stephens M, Donnelly P. Inference of population structure using multilocus genotype data. *Genetics*. 2000;155(2):945-59.
176. NA R. distruct: a program for the graphical display of population structure. *Molecular Ecology Notes*. 2003;4(1):137-8.
177. Jombart T, Devillard S, Balloux F. Discriminant analysis of principal components: a new method for the analysis of genetically structured populations. *BMC Genet*. 2010;11:94.
178. de Bernardi Schneider A, Ford CT, Hostager R, Williams J, Cioce M, Catalyurek UV, et al. StrainHub: a phylogenetic tool to construct pathogen transmission networks. *Bioinformatics*. 2020;36(3):945-7.
179. Paradis E, Schliep K. ape 5.0: an environment for modern phylogenetics and evolutionary analyses in R. *Bioinformatics*. 2019;35(3):526-8.
180. Taylor AR, Jacob PE, Neafsey DE, Buckee CO. Estimating Relatedness Between Malaria Parasites. *Genetics*. 2019;212(4):1337-51.
181. Dray S, Dufour, A., & Chessel, D. The ade4 Package – II: Two-Table and K-Table Methods. *R News*. 2007;7(2):47-52.
182. Meijer JR HM, Schotten KCGJ, Schipper AM. Global patterns of current and future road infrastructure. *Environmental Research Letters*. 2018;13(6).
183. JPL N. NASA Shuttle Radar Topography Mission Global 1 arc second. NASA EOSDIS Land Processes DAAC. 2013.
184. WE P. ResistanceGA: An R package for the optimization of resistance surfaces using genetic algorithms. *Methods in Ecology and Evolution*. 2018;9(6):1638-47.
185. Kim D, Paggi JM, Park C, Bennett C, Salzberg SL. Graph-based genome alignment and genotyping with HISAT2 and HISAT-genotype. *Nat Biotechnol*. 2019;37(8):907-15.
186. Soneson C. hisat2: R Wrapper for HISAT2 Aligner. R package version 1120,. 2022.
187. Li H, Handsaker B, Wysoker A, Fennell T, Ruan J, Homer N, et al. The Sequence Alignment/Map format and SAMtools. *Bioinformatics*. 2009;25(16):2078-9.
188. Morgan M PH, Obenchain V, Hayden N. Rsamtools: Binary alignment (BAM), FASTA, variant call (BCF), and tabix file import. R package version 2120. 2022.
189. Liao Y, Smyth GK, Shi W. The R package Rsubread is easier, faster, cheaper and better for alignment and quantification of RNA sequencing reads. *Nucleic Acids Res*. 2019;47(8):e47.
190. Newman AM, Steen CB, Liu CL, Gentles AJ, Chaudhuri AA, Scherer F, et al. Determining cell type abundance and expression from bulk tissues with digital cytometry. *Nat Biotechnol*. 2019;37(7):773-82.
191. Tebben K, Dia A, Serre D. Determination of the Stage Composition of *Plasmodium* Infections from Bulk Gene Expression Data. *mSystems*. 2022:e0025822.

192. Kepple D, Pestana K, Tomida J, Abebe A, Golassa L, Lo E. Alternative Invasion Mechanisms and Host Immune Response to *Plasmodium vivax* Malaria: Trends and Future Directions. *Microorganisms*. 2020;9(1).
193. Robinson MD, McCarthy DJ, Smyth GK. edgeR: a Bioconductor package for differential expression analysis of digital gene expression data. *Bioinformatics*. 2010;26(1):139-40.
194. Rangel GW, Clark MA, Kanjee U, Goldberg JM, MacInnis B, Jose Menezes M, et al. *Plasmodium vivax* transcriptional profiling of low input cryopreserved isolates through the intraerythrocytic development cycle. *PLoS Negl Trop Dis*. 2020;14(3):e0008104.
195. Obaldia N, Barahona I, Lasso J, Avila M, Quijada M, Nunez M, et al. Comparison of PvLAP5 and Pvs25 qRT-PCR assays for the detection of *Plasmodium vivax* gametocytes in field samples preserved at ambient temperature from remote malaria endemic regions of Panama. *PLoS Negl Trop Dis*. 2022;16(4):e0010327.
196. Hoffman GE, Roussos P. Dream: powerful differential expression analysis for repeated measures designs. *Bioinformatics*. 2021;37(2):192-201.
197. Hoffman GE, Schadt EE. variancePartition: interpreting drivers of variation in complex gene expression studies. *BMC Bioinformatics*. 2016;17(1):483.
198. Sibley CH. A Solid Beginning to Understanding *Plasmodium vivax* in Africa. *J Infect Dis*. 2019;220(11):1716-8.
199. Albsheer MMA, Pestana K, Ahmed S, Elfaki M, Gamil E, Ahmed SM, et al. Distribution of Duffy Phenotypes among *Plasmodium vivax* Infections in Sudan. *Genes (Basel)*. 2019;10(6).
200. Pakalapati D, Garg S, Middha S, Acharya J, Subudhi AK, Boopathi AP, et al. Development and evaluation of a 28S rRNA gene-based nested PCR assay for *P. falciparum* and *P. vivax*. *Pathog Glob Health*. 2013;107(4):180-8.
201. Hupalo DN, Luo Z, Melnikov A, Sutton PL, Rogov P, Escalante A, et al. Population genomics studies identify signatures of global dispersal and drug resistance in *Plasmodium vivax*. *Nat Genet*. 2016;48(8):953-8.
202. Fola AA, Harrison GLA, Hazairin MH, Barnadas C, Hetzel MW, Iga J, et al. Higher Complexity of Infection and Genetic Diversity of *Plasmodium vivax* Than *Plasmodium falciparum* Across All Malaria Transmission Zones of Papua New Guinea. *Am J Trop Med Hyg*. 2017;96(3):630-41.
203. Orjuela-Sanchez P, Sa JM, Brandi MC, Rodrigues PT, Bastos MS, Amaratunga C, et al. Higher microsatellite diversity in *Plasmodium vivax* than in sympatric *Plasmodium falciparum* populations in Pursat, Western Cambodia. *Exp Parasitol*. 2013;134(3):318-26.
204. Gray KA, Dowd S, Bain L, Bobogare A, Wini L, Shanks GD, et al. Population genetics of *Plasmodium falciparum* and *Plasmodium vivax* and asymptomatic malaria in Temotu Province, Solomon Islands. *Malar J*. 2013;12:429.
205. Jennison C, Arnott A, Tessier N, Tavul L, Koepfli C, Felger I, et al. *Plasmodium vivax* populations are more genetically diverse and less structured than sympatric *Plasmodium falciparum* populations. *PLoS Negl Trop Dis*. 2015;9(4):e0003634.
206. Ferreira MU, Karunaweera ND, da Silva-Nunes M, da Silva NS, Wirth DF, Hartl DL. Population structure and transmission dynamics of *Plasmodium vivax* in rural Amazonia. *J Infect Dis*. 2007;195(8):1218-26.
207. Markus MB. The hypnozoite concept, with particular reference to malaria. *Parasitol Res*. 2011;108(1):247-52.

208. Kasehagen LJ, Mueller I, Kiniboro B, Bockarie MJ, Reeder JC, Kazura JW, et al. Reduced *Plasmodium vivax* erythrocyte infection in PNG Duffy-negative heterozygotes. *PLoS One*. 2007;2(3):e336.
209. Vafa M, Troye-Blomberg M, Anchang J, Garcia A, Migot-Nabias F. Multiplicity of *Plasmodium falciparum* infection in asymptomatic children in Senegal: relation to transmission, age and erythrocyte variants. *Malar J*. 2008;7:17.
210. Chan LJ, Dietrich MH, Nguitragool W, Tham WH. *Plasmodium vivax* Reticulocyte Binding Proteins for invasion into reticulocytes. *Cell Microbiol*. 2020;22(1):e13110.
211. Cheng Y, Lu F, Wang B, Li J, Han JH, Ito D, et al. *Plasmodium vivax* GPI-anchored micronemal antigen (PvGAMA) binds human erythrocytes independent of Duffy antigen status. *Sci Rep*. 2016;6:35581.
212. Robert V, Macintyre K, Keating J, Trape JF, Duchemin JB, Warren M, et al. Malaria transmission in urban sub-Saharan Africa. *Am J Trop Med Hyg*. 2003;68(2):169-76.
213. Talha AA, Pirahmadi S, Mehrizi AA, Djadid ND, Nour BY, Zakeri S. Molecular genetic analysis of *Plasmodium vivax* isolates from Eastern and Central Sudan using pvcsp and pvmsp-3alpha genes as molecular markers. *Infect Genet Evol*. 2015;32:12-22.
214. Legendre P FM, Borcard D. Should the Mantel test be used in spatial analysis? *Methods in Ecology and Evolution*. 2015;6(11):1239-47.
215. Escalante AA, Cepeda AS, Pacheco MA. Why *Plasmodium vivax* and *Plasmodium falciparum* are so different? A tale of two clades and their species diversities. *Malar J*. 2022;21(1):139.
216. Luo Z, Sullivan SA, Carlton JM. The biology of *Plasmodium vivax* explored through genomics. *Ann N Y Acad Sci*. 2015;1342:53-61.
217. Rougeron V, Boundenga L, Arnathau C, Durand P, Prugnolle F. The origin of *Plasmodium vivax*: science or story telling? *FEMS Microbiol Rev*. 2022;46(4).
218. Daron J, Boissiere A, Boundenga L, Ngoubangoye B, Houze S, Arnathau C, et al. Population genomic evidence of *Plasmodium vivax* Southeast Asian origin. *Sci Adv*. 2021;7(18).
219. Auburn S, Bohme U, Steinbiss S, Trimarsanto H, Hostetler J, Sanders M, et al. A new *Plasmodium vivax* reference sequence with improved assembly of the subtelomeres reveals an abundance of pir genes. *Wellcome Open Res*. 2016;1:4.
220. Zhu L, Mok S, Imwong M, Jaidee A, Russell B, Nosten F, et al. New insights into the *Plasmodium vivax* transcriptome using RNA-Seq. *Sci Rep*. 2016;6:20498.
221. Bowyer PW, Stewart LB, Aspeling-Jones H, Mensah-Brown HE, Ahouidi AD, Amambua-Ngwa A, et al. Variation in *Plasmodium falciparum* erythrocyte invasion phenotypes and merozoite ligand gene expression across different populations in areas of malaria endemicity. *Infect Immun*. 2015;83(6):2575-82.
222. Cortes A, Crowley VM, Vaquero A, Voss TS. A view on the role of epigenetics in the biology of malaria parasites. *PLoS Pathog*. 2012;8(12):e1002943.
223. Kepple D, Hubbard A, Ali MM, Abargero BR, Lopez K, Pestana K, et al. *Plasmodium vivax* From Duffy-Negative and Duffy-Positive Individuals Share Similar Gene Pools in East Africa. *J Infect Dis*. 2021;224(8):1422-31.
224. Ragotte RJ, Higgins MK, Draper SJ. The RH5-CyRPA-Ripr Complex as a Malaria Vaccine Target. *Trends Parasitol*. 2020;36(6):545-59.

225. Rougeron V, Elguero E, Arnathau C, Acuna Hidalgo B, Durand P, Houze S, et al. Human *Plasmodium vivax* diversity, population structure and evolutionary origin. *PLoS Negl Trop Dis*. 2020;14(3):e0008072.
226. Kumar M, Skillman K, Duraisingh MT. Linking nutrient sensing and gene expression in *Plasmodium falciparum* blood-stage parasites. *Mol Microbiol*. 2021;115(5):891-900.
227. Alexandre MA, Benzecry SG, Siqueira AM, Vitor-Silva S, Melo GC, Monteiro WM, et al. The association between nutritional status and malaria in children from a rural community in the Amazonian region: a longitudinal study. *PLoS Negl Trop Dis*. 2015;9(4):e0003743.
228. McCurley AT, Callard GV. Characterization of housekeeping genes in zebrafish: male-female differences and effects of tissue type, developmental stage and chemical treatment. *BMC Mol Biol*. 2008;9:102.
229. Yam XY, Brugat T, Siau A, Lawton J, Wong DS, Farah A, et al. Characterization of the *Plasmodium* Interspersed Repeats (PIR) proteins of *Plasmodium chabaudi* indicates functional diversity. *Sci Rep*. 2016;6:23449.
230. Cunningham D, Lawton J, Jarra W, Preiser P, Langhorne J. The *pir* multigene family of *Plasmodium*: antigenic variation and beyond. *Mol Biochem Parasitol*. 2010;170(2):65-73.
231. Little TS, Cunningham DA, Vandomme A, Lopez CT, Amis S, Alder C, et al. Analysis of *pir* gene expression across the *Plasmodium* life cycle. *Malar J*. 2021;20(1):445.
232. del Portillo HA, Fernandez-Becerra C, Bowman S, Oliver K, Preuss M, Sanchez CP, et al. A superfamily of variant genes encoded in the subtelomeric region of *Plasmodium vivax*. *Nature*. 2001;410(6830):839-42.
233. Hollin T, Le Roch KG. From Genes to Transcripts, a Tightly Regulated Journey in *Plasmodium*. *Front Cell Infect Microbiol*. 2020;10:618454.
234. Hoo R, Zhu L, Amaladoss A, Mok S, Natalang O, Lapp SA, et al. Integrated analysis of the *Plasmodium* species transcriptome. *EBioMedicine*. 2016;7:255-66.
235. Kim A, Popovici J, Menard D, Serre D. *Plasmodium vivax* transcriptomes reveal stage-specific chloroquine response and differential regulation of male and female gametocytes. *Nat Commun*. 2019;10(1):371.
236. Sa JM, Cannon MV, Caleon RL, Wellems TE, Serre D. Single-cell transcription analysis of *Plasmodium vivax* blood-stage parasites identifies stage- and species-specific profiles of expression. *PLoS Biol*. 2020;18(5):e3000711.
237. Liu F, Yang F, Wang Y, Hong M, Zheng W, Min H, et al. A conserved malaria parasite antigen Pb22 plays a critical role in male gametogenesis in *Plasmodium berghei*. *Cell Microbiol*. 2021;23(3):e13294.
238. Yuda M, Kaneko I, Murata Y, Iwanaga S, Nishi T. Mechanisms of triggering malaria gametocytogenesis by AP2-G. *Parasitol Int*. 2021;84:102403.
239. Vallejo AF, Garcia J, Amado-Garavito AB, Arevalo-Herrera M, Herrera S. *Plasmodium vivax* gametocyte infectivity in sub-microscopic infections. *Malar J*. 2016;15:48.
240. Kori LD, Valecha N, Anvikar AR. Insights into the early liver stage biology of *Plasmodium*. *J Vector Borne Dis*. 2018;55(1):9-13.
241. Milner DA, Jr. Malaria Pathogenesis. *Cold Spring Harb Perspect Med*. 2018;8(1).
242. Muhseen ZT, Hameed AR, Al-Bhadly O, Ahmad S, Li G. Natural products for treatment of *Plasmodium falciparum* malaria: An integrated computational approach. *Comput Biol Med*. 2021;134:104415.

243. Sterling CR, Seed TM, Aikawa M, Rabbege J. Erythrocyte membrane alterations induced by *Plasmodium simium* infection in *Saimiri sciureus*: relation to Schüffner's dots. *J Parasitol.* 1975;61(2):177-88.
244. Golassa L, Amenga-Etego L, Lo E, Amambua-Ngwa A. The biology of unconventional invasion of Duffy-negative reticulocytes by *Plasmodium vivax* and its implication in malaria epidemiology and public health. *Malar J.* 2020;19(1):299.
245. Meyer EV, Semanya AA, Okenu DM, Dluzewski AR, Bannister LH, Barnwell JW, et al. The reticulocyte binding-like proteins of *P. knowlesi* locate to the micronemes of merozoites and define two new members of this invasion ligand family. *Mol Biochem Parasitol.* 2009;165(2):111-21.
246. Semanya AA, Tran TM, Meyer EV, Barnwell JW, Galinski MR. Two functional reticulocyte binding-like (RBL) invasion ligands of zoonotic *Plasmodium knowlesi* exhibit differential adhesion to monkey and human erythrocytes. *Malar J.* 2012;11:228.
247. Rossati A, Bargiacchi O, Kroumova V, Zaramella M, Caputo A, Garavelli PL. Climate, environment and transmission of malaria. *Infez Med.* 2016;24(2):93-104.
248. Beier JC. Malaria parasite development in mosquitoes. *Annu Rev Entomol.* 1998;43:519-43.
249. Ngotho P, Soares AB, Hentzschel F, Achcar F, Bertuccini L, Marti M. Revisiting gametocyte biology in malaria parasites. *FEMS Microbiol Rev.* 2019;43(4):401-14.
250. Basu S, Sahi PK. Malaria: An Update. *Indian J Pediatr.* 2017;84(7):521-8.
251. Bansal GP, Kumar N. Immune Responses in Malaria Transmission. *Current Clinical Microbiology Reports.* 2018;5(1):38-44.
252. Tadesse FG, van den Hoogen L, Lanke K, Schildkraut J, Tetteh K, Aseffa A, et al. The shape of the iceberg: quantification of submicroscopic *Plasmodium falciparum* and *Plasmodium vivax* parasitaemia and gametocytaemia in five low endemic settings in Ethiopia. *Malar J.* 2017;16(1):99.
253. Wampfler R, Mwingira F, Javati S, Robinson L, Betuela I, Siba P, et al. Strategies for detection of *Plasmodium* species gametocytes. *PLoS One.* 2013;8(9):e76316.
254. Koepfli C, Robinson LJ, Rarau P, Salib M, Sambale N, Wampfler R, et al. Blood-Stage Parasitaemia and Age Determine *Plasmodium falciparum* and *P. vivax* Gametocytaemia in Papua New Guinea. *PLoS One.* 2015;10(5):e0126747.
255. Bharti AR, Chuquiyauri R, Brouwer KC, Stancil J, Lin J, Llanos-Cuentas A, et al. Experimental infection of the neotropical malaria vector *Anopheles darlingi* by human patient-derived *Plasmodium vivax* in the Peruvian Amazon. *Am J Trop Med Hyg.* 2006;75(4):610-6.
256. Bousema T, Drakeley C. Epidemiology and infectivity of *Plasmodium falciparum* and *Plasmodium vivax* gametocytes in relation to malaria control and elimination. *Clin Microbiol Rev.* 2011;24(2):377-410.
257. Lima NF, Bastos MS, Ferreira MU. *Plasmodium vivax*: reverse transcriptase real-time PCR for gametocyte detection and quantitation in clinical samples. *Exp Parasitol.* 2012;132(3):348-54.
258. Nacher M, Carrara VI, McGready R, Ashley E, Nguen JV, Thwai KL, et al. Seasonal fluctuations in the carriage of *Plasmodium vivax* gametocytes in Thailand. *Ann Trop Med Parasitol.* 2004;98(2):115-20.
259. Olliaro PL, Barnwell JW, Barry A, Mendis K, Mueller I, Reeder JC, et al. Implications of *Plasmodium vivax* Biology for Control, Elimination, and Research. *Am J Trop Med Hyg.* 2016;95(6 Suppl):4-14.



260. Dixon MW, Thompson J, Gardiner DL, Trenholme KR. Sex in *Plasmodium*: a sign of commitment. *Trends Parasitol.* 2008;24(4):168-75.
261. Reece SE, Ramiro RS, Nussey DH. Plastic parasites: sophisticated strategies for survival and reproduction? *Evol Appl.* 2009;2(1):11-23.
262. Hofmann NE, Gruenberg M, Nate E, Ura A, Rodriguez-Rodriguez D, Salib M, et al. Assessment of ultra-sensitive malaria diagnosis versus standard molecular diagnostics for malaria elimination: an in-depth molecular community cross-sectional study. *Lancet Infect Dis.* 2018;18(10):1108-16.
263. Tadesse FG, Slater HC, Chali W, Teelen K, Lanke K, Belachew M, et al. The Relative Contribution of Symptomatic and Asymptomatic *Plasmodium vivax* and *Plasmodium falciparum* Infections to the Infectious Reservoir in a Low-Endemic Setting in Ethiopia. *Clin Infect Dis.* 2018;66(12):1883-91.
264. Baker DA. Malaria gametocytogenesis. *Mol Biochem Parasitol.* 2010;172(2):57-65.
265. Drakeley C, Sutherland C, Bousema JT, Sauerwein RW, Targett GA. The epidemiology of *Plasmodium falciparum* gametocytes: weapons of mass dispersion. *Trends Parasitol.* 2006;22(9):424-30.
266. Abdelraheem MH, Bansal D, Idris MA, Mukhtar MM, Hamid MMA, Imam ZS, et al. Genetic diversity and transmissibility of imported *Plasmodium vivax* in Qatar and three countries of origin. *Sci Rep.* 2018;8(1):8870.
267. Bousema T, Okell L, Felger I, Drakeley C. Asymptomatic malaria infections: detectability, transmissibility and public health relevance. *Nat Rev Microbiol.* 2014;12(12):833-40.
268. Ford A, Kepple D, Williams J, Kolesar G, Ford CT, Abebe A, et al. Gene Polymorphisms Among *Plasmodium vivax* Geographical Isolates and the Potential as New Biomarkers for Gametocyte Detection. *Front Cell Infect Microbiol.* 2021;11:789417.

## Appendix: Publications

- (1) Abagero B, Kepple D, Pestana K, Witherspoon L, Hordofa A, Adanew A, Baharu F, Hansel S, Lopez K, Janies D, Lo E, Yewhalaw D. Low density *Plasmodium* infections and G6PD deficiency among malaria suspected febrile individuals in Ethiopia. *Frontiers in Tropical Disease*. 2022. doi: 10.3389/fitd.2022.966930
- (2) Ford A, Kepple D, Williams J, Kolesar G, Ford C, Abebe A, Golassa L, Janies D, Yewhalaw D, Lo E. Gene polymorphisms among *plasmodium vivax* geographical isolates and the potential as new biomarkers for gametocyte detection. *Frontiers in Cellular and Infection Microbiology*. 2021;11:789417. DOI: doi.org/10.3389/fcimb.2021.789417
- (3) Kepple D, Ford A, Little E, Kolesar G, Abagero B, Blackwell A, Indrasekara S, Yewhalaw D, Eugenia Lo E. From Genes to Biomarkers: Understanding the Biology of Malaria Gametocytes and Their Detection. *IntechOpen Genetic Polymorphisms – new insights*. 2021. DOI: 10.5772/intechopen.99364
- (4) Lo E, Russo G, Pestana K, Kepple D, Abagero B, Dongho G, Gunalan K, Miller L, Hamid M, Yewhalaw D, Paganotti G. Contrasting epidemiology and genetic variation of *Plasmodium vivax* Infecting Duffy Negatives across Africa. *International Journal of Infectious Diseases*. 2021;108:63-71. DOI: doi.org/10.1016/j.ijid.2021.05.009
- (5) Kepple D, Hubbard A, Ali MM, Abagero BR, Lopez K, Pestana K, Janies D, Yan G, Hamid M, Yewhalaw D, Lo E. *Plasmodium vivax* from duffy-negative and duffy-positive Individuals shares Similar gene pool in East Africa. *The Journal of Infectious Diseases*. 2021;224(8):1422-1431. DOI: 10.1093/infdis/jiab063
- (6) Kepple D, Pestana K, Tomida J, Abebe A, Golassa L, Lo E. Alternative Invasion Mechanisms and Host Immune Response to *Plasmodium vivax* Malaria: Trends and Future

Directions. Microorganisms. 2020;9(1):15. DOI: [10.3390/microorganisms9010015](https://doi.org/10.3390/microorganisms9010015)

- (7) Ford A\*, Kepple D\*, Raya B, Connors J, Pearson R, Auburn S, Getachew S, Ford C, Gunalan K, Miller L, Janies D, Rayner J, Yan G, Yewhalaw D, Lo E. Whole Genome Sequencing of *Plasmodium vivax* Isolates Reveals Frequent Sequence and Structural Polymorphisms in Erythrocyte Binding Genes. PLOS Neglected Tropical Diseases 2020; 14:e0008234. \*co-first authors. DOI: [doi.org/10.1371/journal.pone.0238186](https://doi.org/10.1371/journal.pone.0238186)
- (8) Lo E, Hostetler JB, Yewhalaw D, Pearson RD, Hamid MMA, Gunalan K, Kepple D, Ford A, Janies D, Rayner J, Miller L, Yan G. Frequent expansion of *Plasmodium vivax* Duffy Binding Protein in Ethiopia and its epidemiological significance. PLOS Neglected Tropical Diseases. 2019;13:e0007222. DOI: [10.1371/journal.pntd.0007222](https://doi.org/10.1371/journal.pntd.0007222)